The role of cytochrome P450 derived arachidonic acid metabolites against Angiotensin II-induced cardiac hypertrophy in Sprague Dawley rats and the RL-14 cell line

by

Samya Elkhatali

A thesis submitted in partial fulfillment of the requirements for the degree of

Master of Science

in
Pharmaceutical Sciences

Faculty of Pharmacy and Pharmaceutical Sciences
University of Alberta

Abstract

Several cytochrome P450 (CYP) enzymes and their arachidonic acid (AA) metabolites play essential roles in the maintenance of cardiovascular health, and their alteration gives rise to a number of cardiovascular diseases, including cardiac hypertrophy and heart failure. Recent data demonstrated that 19-hydroxyeicosatetraenoic acid (19-HETE) is the major subterminal-HETE in the heart tissue and its formation is decreased during cardiac hypertrophy, while in contrast that of mid-chain HETEs increased. Therefore, our aims were; 1) to examine whether 19-HETE confers cardioprotection against angiotensin II (Ang II)-induced cardiac hypertrophy at *in vitro* and *in vivo* levels in which isoniazid (INH) was used to increase 19-HETE formation *in vivo*, and 2) to study the cardioprotective effect of inhibiting the formation of midchain HETEs [using 2,3',4,5'-tetramethoxystilbene (TMS)] against Ang II-induced cardiac hypertrophy also at *in vitro* and *in vivo* levels. Our results demonstrated that 19-HETE conferred a cardioprotective effect against Ang II-induced cellular hypertrophy, as indicated by the significant reduction in the β/α-MHC ratio. Echocardiographic analysis showed that INH improved heart dimensions, in addition to reversing the increase in heart weight to tibial length ratio caused by Ang II. The cardioprotective effect of INH was associated with an increased level of cardiac 19-HETE. Additionally, INH significantly reduced levels of the cardiotoxic AA metabolite 20-HETE-induced by Ang II treatment. Likewise, we demonstrated that TMS protected against Ang II-induced cardiac hypertrophy as indicated by echocardiography and heart weight to tibia length ratio. TMS significantly reduced the β/α-MHC ratio. In addition, this cardioprotective effect of TMS was associated with decreased levels of cardiac mid-chain and 20-HETE as well as significantly reducing AA levels. TMS decreased oxidative stress, inhibiting the phosphorylation

of ERK1/2, p38 MAPK and the binding of p65 NF-κB. In conclusion, our results demonstrate that both INH and TMS partially protect against Ang II-induced cardiac hypertrophy through manipulating the levels of AA metabolites. This further confirms the role of CYPs, and their associated AA metabolites, in the development of cardiac hypertrophy.

This work is dedicated to my beloved husband, parents and children, for their patience and support.

Thank you

Acknowledgements

My deep gratitude goes first to my supervisor, Dr. Ayman El-Kadi for his consistent support, guidance and mentorship.

I am grateful to my supervisory committee member, Dr. Dion Brocks for his insightful remarks and valuable advice.

I would like to thank my lab members for their invaluable help and advice throughout my study.

I am grateful to the Libyan ministry of higher education and research for providing me with financial support and I would like to thank the Canadian Institutes of Health Research (CIHR) for funding the research project.

Table of Contents

List of Tables

List of Figures

List of Abbreviations

3MC	3-methylcholanthrene
AA	Arachidonic acid
AC	Adenylyl cyclase
AhR	Aryl hydrocarbon receptor
AhRE	Aryl hydrocarbon responsive element
ANP	Atrial natriuretic peptide
ARNT	AhR nuclear translocator
ATP	Adenosine-5'-triphosphate
BNP	Brain natriuretic peptide
cAMP	cyclic adenosine monophosphate
CAR	Constitutive androstane receptor
COX	Cyclooxygenase
CYP	Cytochrome P450
DBD	DNA-binding domain
DDMS	N-methylsulfonyl-12,12-dibromododec-11-enamide
DUSP	Dual-specificity phosphatases
EC	Endothelial cells

EDHF	Endothelium-derived hyperpolarizing factor
EETs	Epoxyeicosatrienoic acids
ER	Endoplasmic reticulum
ERK	Extracellular signal-regulated kinases
GPCRs	G-protein coupled receptors
GSK-3	Glycogen synthase kinase 3
HETEs	Hydroxyeicosatetraenoic acids
INH	Isoniazid
Inpp5f	Inositol polyphosphate-5-phosphatase F JAK/
IP3	Inositol 1,4,5- triphosphate
JAK	Janus kinase
JNK	Jun N-terminal kinase
LBD	Ligand-binding domain
LOX	Lipoxygenase
MAPK	Mitogen-activated protein kinase
MCIP	Modulatory calcineurin-interacting proteins
MHC	Myosin heavy chain
MI	Myocardial infarction

NADH	Nicotinamide adenine dinucleotide
NFAT	Nuclear factor of activated T cells
NF-κB	Nuclear factor-kappaB
PKA	Protein kinase A
PI3K	Phosphoinositide 3-kinases
PXR	Pregnane X Receptor
ROS	Reactive oxygen species
RXR	Retinioid X receptor
SHR	Spontaneously hypertensive rats
SMCs	Smooth muscle cells
STAT	Signal transducer and activator of transcription
SXR	Steroid and xenobiotic sensing nuclear receptor
TCDD	2,3,7,8-tetrachloro-dibenzodioxin
TMS	2,3',4,5'-tetramethoxystilbene
VSMCs	Vascular smooth muscle cells

Chapter 1 :

INTRODUCTION

1.1. Cardiac Hypertrophy

The heart is a muscular organ that pumps blood throughout the body. Under normal conditions it supplies a steady blood volume. Normally the balance between supply and demand is maintained. If this balance is disrupted and there is an increase in demand or stress, either physiological (pregnancy, exercise) or pathological (hypertension, aortic stenosis), the heart responds by increasing stroke rate and volume. In cases where the change in demand is short term, this response is acute and is not accompanied by any alteration in the myocardial structure. However as the demand is prolonged, irreversible changes in the myocardial structure occur (Wakatsuki et al., 2004).

Cardiac hypertrophy is defined as the thickening of the myocardium resulting in a decrease in the chamber size of the heart, including the left and right ventricles. Initially hypertrophy is an adaptive mechanism by which the heart maintains its function and continues to pump blood; however this cannot be maintained for extended periods of time and eventually the hearts' ability to pump blood is weakened. Cardiac hypertrophy can be classified either according to heart geometry into eccentric or concentric or according to aetiology into physiological and pathological.

1.1.1. Eccentric and concentric hypertrophy

The main difference between the two classes of hypertrophy is that eccentric hypertrophy is characterized by cell elongation while concentric hypertrophy is due to myocyte thickening. During eccentric hypertrophy volume overload causes new sarcomeres to be added in-series to existing sarcomeres, leading to an increase in myocyte cell length and ventricular dilation (Mihl

et al., 2008) while during concentric hypertrophy the heart responds to pressure overload by the inclusion of new sarcomeres in-parallel to those present, leading to an increase in wall thickness (Mihl et al., 2008). Additionally, eccentric hypertrophy results from increased systolic stress while concentric hypertrophy results from an increase in diastolic stretch (Katz, 2002).

1.1.2. Pathological and Physiological hypertrophy

Heart mass, function, fibrosis and gene expression are the four distinct features of cardiac hypertrophy. Heart mass increases in a similar manner in both physiological and pathological hypertrophy; however homogeneous growth is seen in physiological hypertrophy with an equivalent increase in both the myocyte and non-myocyte components of the cardiac muscle, i.e tissue homogeneity is preserved. Conversely, pathological hypertrophy is non-homogeneous with an increase in apoptotic and necrotic cell death. The dead myocytes are then replaced with a disproportionate contribution of cardiac fibroblasts, producing exorbitant amounts of interstitial fibrillar collagen, causing fibrosis and ultimately leading to a decrease in heart function, while physiological hypertrophy is characterized by normal or enhanced contractile function and normal architecture and organization of cardiac structure. In addition, the change occurring in physiological hypertrophy is reversible while that of pathological hypertrophy is not.

Physiological hypertrophy stimuli include aerobic exercise training, pregnancy and postnatal growth while pathological hypertrophy stimuli include pressure or volume overload and cardiomyopathy comprising different etiologies such as familial, viral, diabetic, and metabolic causes.

Furthermore, there is a change in the fetal gene expression. Myosin heavy chain (MHC) present in the cardiac ventricle consists of two isoforms: α- and β-MHCs. The α-MHC is the

main isoform in adult rat hearts (Lompre et al., 1984) accompanied by an increase in actin-activated ATPase activity while β-MHC is the main isoform in fetal hearts (Lompre et al., 1984), with reduced ATPase activity. It should be noted that the ATPase activity of myosin is inversely proportional to the muscle contraction time (Barany, 1967). Hence, alterations in the ratio of β-MHC (fetal phenotype) to α-MHC (adult phenotype) in the cardiac ventricle significantly alter the contractile properties of the heart. In addition, natriuretic peptides including atrial natriuretic peptide (ANP) and brain natriuretic peptide (BNP) are up-regulated in cardiac hypertrophy.

Physiological hypertrophy involves signaling pathways distinct from those of pathological hypertrophy. Physiological hypertrophy signaling pathways include the extracellular-signal-regulated kinases ERK1 and ERK2 and protein kinase B (Akt). Conversely, pathological hypertrophy includes p38 and Jun N-terminal kinase (JNK) in addition to ERK1/2 (Wakatsuki et al., 2004)

Pathological hypertrophy can be brought about by several factors including either systemic or pulmonary hypertension, metabolic cardiomyopathy, genetic defects in the sarcomeric protein genes, congenital defects, myocardial infarction, coronary artery disease and valvular insufficiency. Several changes occur during pathological hypertrophy including fibrosis, an increased rate of myocyte death, and decreased systolic and diastolic function, ultimately leading to congestive heart failure, arrhythmia or sudden death. In contrast, physiological hypertrophy is induced by pregnancy and exercise. The changes that occur are reversible and the cardiac structure is normal. Additionally, cardiac function in physiological hypertrophy is either normal or improved.

Cardiac hypertrophy for research purposes has been induced by several methods, and the model we used in our experiments is Ang II-induced cardiac hypertrophy which will be explained below.

1.1.3. Angiotensin II induced hypertrophy

Angiotensin II (Ang II) is an octapeptide hormone. It is a well-known sympathetic agent that plays a fundamental role in cardiovascular homeostasis. Ang II causes vasoconstriction, sympathetic nervous stimulation and a rise in aldosterone biosynthesis, ultimately causing an elevation in blood pressure (Fyhrquist et al., 1995). Both circulating Ang II and aldosterone participate in the fibrosis and resultant heterogeneity in tissue structure (Weber and Brilla, 1991). In addition, Ang II-induced vascular hypertrophy is in part independent of its vasopressor effect (Griffin et al., 1991). AT1 receptors mediate the increase in blood pressure by Ang II (Crowley et al., 2004). In addition, it was also found that the AT2 receptor was important in the development of left ventricular hypertrophy and cardiac fibrosis. Mice with an AT2 gene deletion rarely developed LVH and cardiac fibrosis (Ichihara et al., 2001). Mounting evidence suggests that cardiac hypertrophy induced by Ag II involves increased ROS production as a result of inducing vascular NADH oxidase (Cave et al., 2005).

Ang II has been found to activate a number of signaling pathways including the MAPKs, PI3K/Akt, and JAK/STAT pathways, suggesting that Ang II performs an array of functions other than promoting contraction or inducing cellular hypertrophy (Taubman, 2003).

1.1.4. Molecular pathways involved in pathological cardiac hypertrophy

Numerous molecular pathways are activated during cardiac hypertrophy. These pathways are complex and integrated, and they include G-protein coupled receptors, calcineurin/nuclear factor of activated T-cells (NFAT) signaling, phosphoinositide 3-kinase (PI3K), mitogen activated protein kinases (MAPKs), and nuclear factor kappa B (NF-κB). A schematic diagram of the major intracellular signaling pathways involved in cardiac hypertrophic response is shown in Figure 1.1.

1.1.4.1. G-protein Coupled receptors (GPCRs):

GPCRs are the largest group of plasma membrane receptors and are a target for around 40% of all prescription medications. The principal GPCRs are either α or β adrenergic or muscarinic. Signal transduction mainly involves the cyclic adenosine monophosphate (cAMP) signaling pathway and the phosphatidylinositol signaling pathway, as illustrated in Figure 1.1. These receptors couple to GTP-binding heterotrimeric G proteins that exchange GDP for GTP. Three classes of G proteins exist: Gi, Gs and Gq/G11, consisting of Gα, Gβγ subunits. At rest they are assembled into a complex (Gαβγ) attached to the cytoplasmic side of the plasma membrane. When this complex dissociates, each subunit will activate intracellular signalling pathways through downstream effectors. Adenylyl cyclase (AC) activity is modulated by Gαs and Gαi. AC generates cAMP and thereafter activates cAMP-dependent protein kinase A (PKA). On the other hand Gαq activates phospholipase C, generating diacylglycerol (DAG) and inositol 1,4,5- triphosphate (IP3) that work to activate protein kinase C. Mitogen-activated protein kinase

(MAPK) signaling cascade, phosphatidyl inositol 3-kinase activity, and Ras signaling pathways are directly activated through Gβγ.

PKA also acts on the phosphorylation of contractile and regulatory proteins including cardiac troponin I that enhances muscle relaxation (Baryshnikova et al., 2008) and ryanodine receptor Ca^{2+} release channels that are the main pathway for Ca^{2+} release during cardiac excitation–contraction coupling (Coronado et al., 1994). PKA activates L-type Ca^{2+} channels, allowing the influx of Ca^{2+} (I_{Ca}) contributing to the increased cardiac contraction (positive inotropic response). Phospholamban is an endogenous inhibitor of the SR Ca^{2+}-ATPase, therefore enhancing the rate of cardiac myocyte relaxation (Bers, 2002). The modulation of these contractile and regulatory proteins plays a role in the pathophysiology of heart failure (Scoote and Williams, 2002, Schmitt et al., 2003).

1.1.4.2. Calcineurin-NFAT signaling

Calcineurin, a protein phosphatase, acts on nuclear factor of activated T cells (NFAT). Once activated by increased calcium, calcineurin facilitates the hypertrophic response through its downstream transcriptional effector NFAT, as illustrated in Figure 1.1. Calcineurin directly dephosphorylates NFAT, resulting in nuclear translocation. It has been found that calcineurin overexpression results in prominent cardiac hypertrophy in mice (Heineke and Molkentin, 2006) while its inhibition prevents cardiac hypertrophy in the isoproterenol model (De Windt et al., 2001) and the Ang II model of cardiac hypertrophy (Molkentin et al., 1998, Wilkins and Molkentin, 2004, Heineke and Molkentin, 2006). There are three modulatory calcineurin-interacting proteins (MCIP) identified to date, one of which is MCIP1. MCIP1 is an endogenous calcineurin inhibitor that works in both a competitive manner by working as a substrate for

calcineurin and through non-competitive means through multiple MCIP1 domains that bind and inhibit calcineurin (Vega et al., 2002).

The overexpression of MCIP was able to reduce isoproterenol- and even exercise-induced increases in cardiac mass (Rothermel et al., 2001), suggesting that calcineurin plays a role in both pathological and physiological hypertrophy.

1.1.4.3. PI3K/Akt/GSK-3-Dependent Signaling

Phosphoinositide 3-kinases are a family of lipid kinases affecting cell movement, growth, and survival (Cantley, 2002). PI3Ks are classified into three groups, classes I, II, and III. Class I are heterodimers and are further subdivided into IA and IB. Class IA PI3Ks consist of a p110 catalytic subunit α, β or δ and a p85 or p55 regulatory subunit. The only Class IB PI3K is p110γ, which is regulated by the p101 regulatory subunit (Vanhaesebroeck et al., 1997). p110α and p110γ are abundantly expressed in the heart and it was found that the overexpression of a constitutively active p110α mutant leads to an enlarged heart size while inversely dominant-negative mutants produced a reduced heart size (Shioi et al., 2000).

A major target of PI3K signaling is the serine/threonine kinase Akt, which upon activation is translocated to the membrane then further phosphorylated by phosphatidylinositol 3,4,5-trisphosphate (PIP_3). Inositol polyphosphate-5-phosphatase F (Inpp5f), one of the polyphosphoinositide phosphatases, can degrade PIP_3 and thus modulates the PI3K/Akt pathway. Its overexpression reduces its response to isoproterenol-induced hypertrophic stimulation in Inpp5f transgenic mice (Zhu et al., 2009). Glycogen synthase kinase 3 (GSK-3) is a serine/threonine protein kinase and is a downstream target of Akt inhibiting its activity. The

overexpression of cardiac GSK-3β reduces the hypertrophic response to chronic isoproterenol administration and pressure overload (Frey and Olson, 2003). This pathway is illustrated in Figure 1.1.

1.1.4.4. Mitogen Activated Protein Kinases (MAPK)

MAPKs are serine/threonine kinases that mediate intracellular signal transduction in response to a variety of stimuli. The MAPK family includes the extracellular-regulated kinases (ERK1/2) Jun kinase (JNK/SAPK) and p38 MAPK (Zhang and Liu, 2002), as illustrated in Figure 1.1. ERK is mainly involved in cellular growth and differentiation, while p38 and JNK act as mediators of cellular stresses such as inflammation and apoptosis. Upon activation, ERKs, JNKs and p38 phosphorylate intracellular targets, which involve an array of transcription factors that reprogram cardiac gene expression. MAPKs are activated by GPCR ligands or reactive oxidative species (Hancock, 2010). In their inactive form, MAPKs are found in the cytoplasm. Once activated, they are translocated into the nucleus, leading to the phosphorylation and activation of transcription factors that will in turn cause an increase in their rate of transcription.

ERK1/2s are deemed essential for promoting cardiac growth due to the fact that they are activated in response to nearly every stress- and agonist-induced hypertrophic stimulus (Kehat and Molkentin, 2010). However, recent evidence has found that the chronic inhibition of ERK1/2 did not reduce pathologic or physiologic stimulus-induced cardiac growth in vivo (Purcell et al., 2007); this could be explained by the pleiotropic effects of ERK1/2 (Kehat and Molkentin, 2010).

p38 is found to be activated in pressure-overload hypertrophy as well as heart failure (Wang et al., 1998) and the pharmacological inhibition of p38 is found to enhance contractile performance and reduce ischemic injury (Marber et al., 2011). The M3 muscarinic acetylcholine receptor agonist, choline, was found to prevent Ang II-induced cardiac hypertrophy by inhibiting ROS-mediated p38 MAPK activation and by regulating the Ca2+-mediated calcineurin signal transduction pathway (Wang et al., 2012).

The role of JNK in cardiac hypertrophy is less clear and its action differs according to the stimuli (Rose et al., 2010). JNK is activated rapidly in rats after the application of pressure overload by transverse aortic constriction (Nadruz et al., 2004). Reduction of JNK activity by cardiac-specific deletion of MKK4, a member of the MAPKK family that directly activates JNK, enhanced cardiac hypertrophy (Liang et al., 2003).

MAPK deactivation occurs by dephosphorylation by means of phosphatases through dual-specificity phosphatases (DUSPs) and non-specific phosphatases including PP2A and CD45 (Liu and Hofmann, 2004, Tonks, 2006, Cobb, 1999, Sohaskey and Ferrell, 1999). A member of the DUSP family DUSP5, was found to play a role in the regulation of myocyte growth. Class I HDAC inhibitors suppressed the expression of DUSP5 by inhibiting nuclear ERK1/2 signaling, ultimately protecting against cardiac hypertrophy (Ferguson et al., 2013). In addition, Ang (1–7), which generally has contrasting effects to that of Ang II, was found to increase DUSP1 in rats and attenuate Ang II induced cardiac hypertrophy regardless of the co-treatment with Ang II, suggesting that Ang (1–7) up-regulates DUSP-1 to reduce Ang II-stimulated ERK activation (McCollum et al., 2012). In addition, it has been found that Dusp1 and Dusp4 diminish p38

MAPK signaling, suggesting that both DUSP1 and DUSP4 have cardioprotective roles (Auger-Messier et al., 2013).

1.1.4.5. Nuclear factor-kappaB (NF-κB)

NF-κB is a family of rapidly acting transcription factors and consists of the members RelA (p65), RelB, c-Rel, p50, and p52. The activation of NF-κB is directed by two signaling pathways, including the classical (or the canonical pathway) and the alternative (or non-canonical pathway), forming both homo- and heterodimers. The principal NF-κB complex is the p50/p65 heterodimer, which in its inactive form binds to inhibitory (IκB) that masks the nuclear localization signals and is present in the cytosol. Upon activation, IκB is phosphorylated by IκB kinase (IKK), resulting in its dissociation from the NF-κB complex. NF-κB then translocates to the nucleus. The NF-κB family of transcription factors had initially been discovered and intensely studied in the immune system, controlling the expression of a number of cytokines and growth factors (Ghosh et al., 1998); however, it is now known to be involved in an array of physiological processes including embryonic development, cell survival and inflammation in numerous cell types including cardiomyocytes. Note that NF-κB has the ability to induce either pro- or anti-apoptotic genes depending on the cell type and stimulus (Luo et al., 2005).

The exact role of NF-κB in cardiac hypertrophy and heart failure is not yet fully identified. However, it has been found that Nf-kB is required for adaptive cardiac hypertrophy and that the genetic NF-κB inhibition attenuates Ang II-induced hypertrophy (Zelarayan et al., 2009). In addition, chronic p65 activation promotes adverse remodeling and stimulates maladaptive endoplasmic reticulum (ER) stress (Hamid et al., 2011).

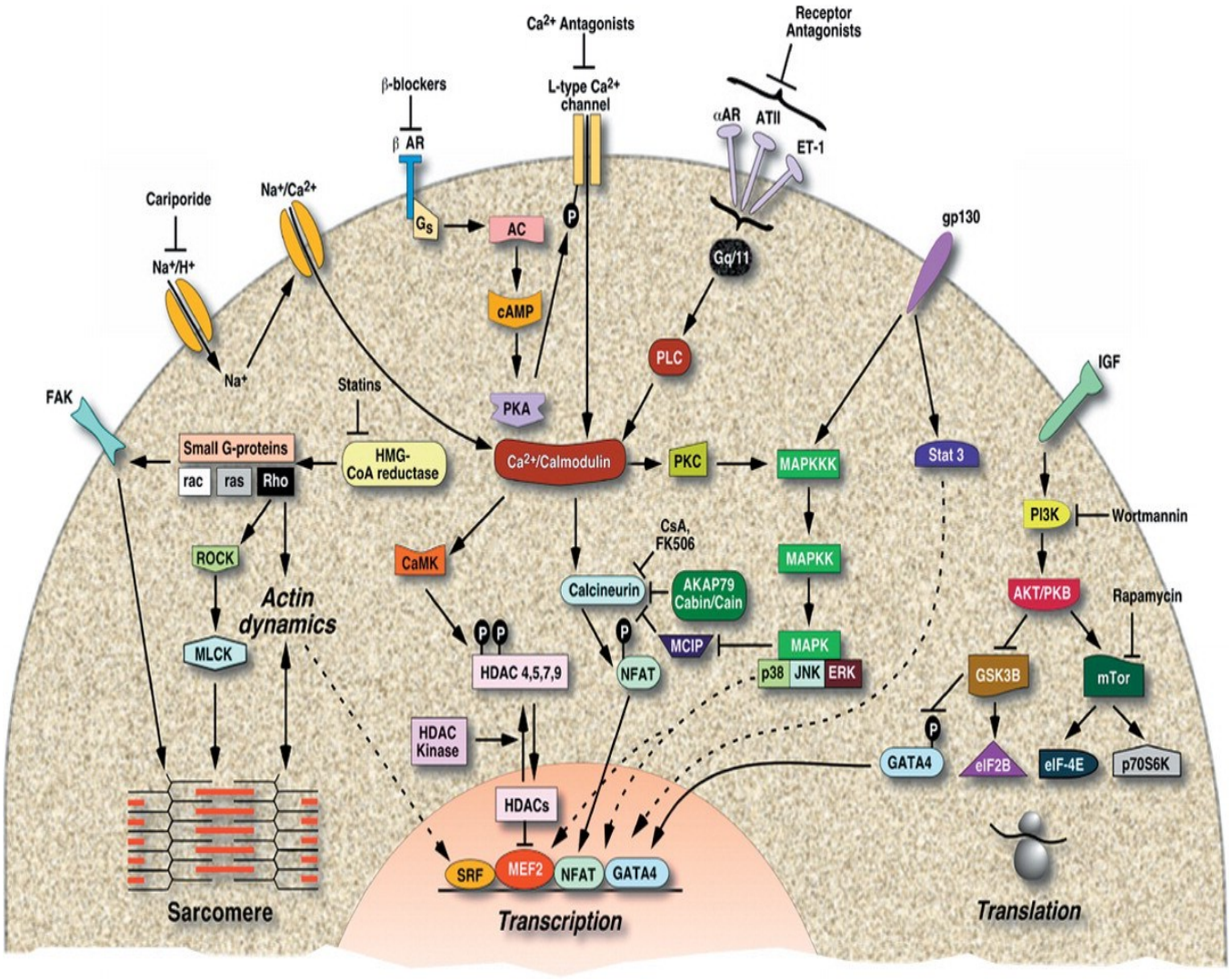

Figure 1.1 Signalling pathways involved in cardiomyocyte hypertrophy. Taken from (Frey and Olson, 2003)

1.2. Arachidonic Acid

Arachidonic acid (AA) is a polyunsaturated omega 6 fatty acid comprised of a 20-carbon atom chain and four double bonds. AA is bound to plasma membrane and is released by the activity of phospholipases, most prominently cPLA2 (Tacconelli and Patrignani, 2014) which is released by several stimuli including Ang II, norepinephrine and bradykinin (Zafari et al., 1999, Mukherjee et al., 1994). Once AA is released from the membrane, free AA can then be metabolized into a number of biologically active eicosanoid metabolites (Choudhary et al., 2004) through three different pathways (i) cyclooxygenase (COX) pathway that produces prostanoids, (ii) lipoxygenase (LOX) pathway that produces leukotrienes, lipoxins and mid-chain hydroxyeicosatetraenoic acids (HETEs) or (iii) cytochrome P450 (CYP) pathway that mediates the metabolism of AA to epoxyeicosatrienoic acids (EETs) and HETEs. The type of stimuli, the cofactors available and the tissue in which it occurs all dictate what pathway AA adopts (Omata et al., 1992).

AA metabolites have been long known to exhibit potent biological activities. In fact, the association between alterations in AA metabolism and the onset, duration and severity of several heart diseases has been observed and reported (Roman, 2002). In addition to the indirect mechanism of AA mechanism of activity on cardiomyocytes through its metabolites, AA also has a direct effect. It affects the electrophysiology of cardiac myocytes through altering the voltage-dependent T-type Ca^{2+} channels (Talavera et al., 2004). AA also increases ROS production (Cocco et al., 1999) and reduces heart rate through altering the availability of intracellular calcium, suppressing membrane electrical excitability (Kang et al., 1995, Kang and Leaf, 1994). However, under normal conditions, AA is present in low amounts in cardiac tissue (Van der Vusse et al., 1997).

1.3. Cytochrome P450 (CYP)

CYP enzymes are a superfamily of heme-thiolate enzymes involved in the metabolism of endogenous and exogenous compounds. CYPs are part of phase I drug metabolizing enzymes (Ioannides, 2008) and are present in all biological kingdoms; the differences between those found in humans to those found in bacteria are minimal (Ioannides, 2008). There are 57 identified individual P450s and 58 pseudogenes classified in humans to date (Lewis, 2004). Around 35 CYP isoenzymes are of clinical relevance (Martignoni et al., 2006). They are classified into different families and subfamilies according to their amino acid sequences. Members of the same family share more than 40% amino acid sequence identity while members of the same subfamily have greater than 55% amino acid sequence identity. The prefix CYP precedes an arabic number representing the family, followed by a capital letter to specify the subfamily. Then finally there is an additional arabic number representing the specific enzyme (Nelson, 2006, Sim and Ingelman-Sundberg, 2006). Usually the name is italicized when referring to the gene (for example, *CYP1A1*) whereas small letters are used to describe mouse enzymes (for example, Cyp1a1).

CYPs are responsible for the biotransformation of xenobiotics in addition to steroid, prostanoid, eicosanoid and fatty acid metabolism (Lewis, 2004). CYP11, CYP17, CYP19, and CYP21 are involved in the synthesis of endogenous substrates such as steroids, fatty acids, and prostaglandins while CYP1, CYP2, CYP3 and CYP4 are mostly involved in drug metabolism. CYP-mediated AA metabolism and the metabolic fate of CYP-mediated AA metabolites is represented in Figure 1.2. The expression of CYP enzymes in cardiovascular tissues will be reviewed in the following sections.

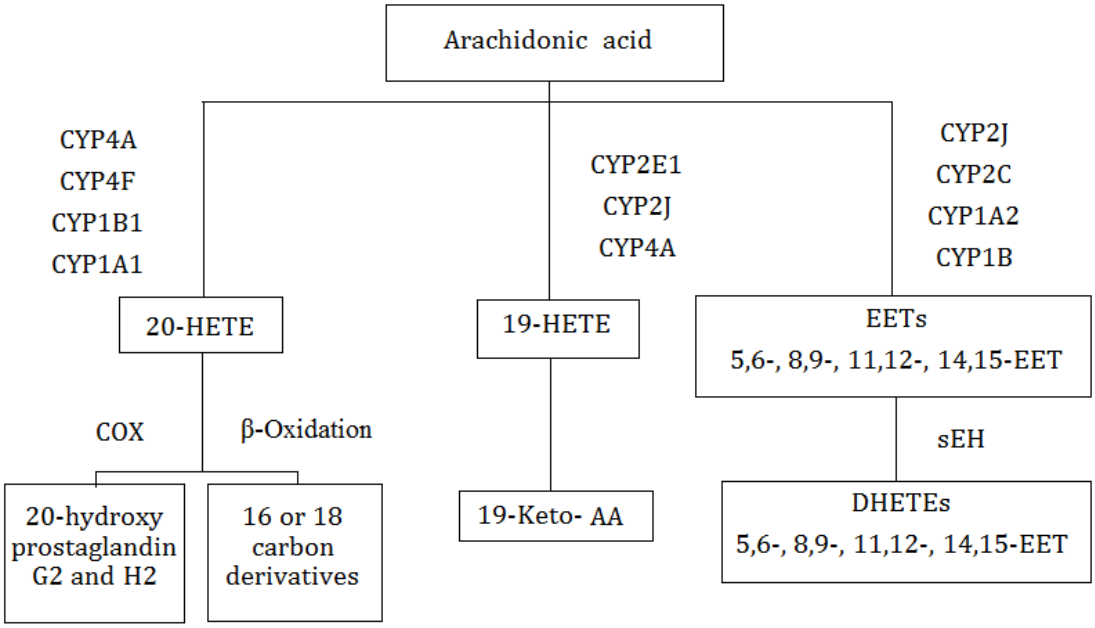

Figure 1.2 CYP-mediated AA metabolism and the metabolic fate of CYP-mediated AA metabolites

1.3.1. Cardiac expression of cytochrome P450

CYPs are present in a number of different organs and although their presence is most abundant in hepatic tissue, growing evidence demonstrates that their existence in extra-hepatic tissue and the ability to metabolize endogenous substrates is of critical importance (Roman, 2002).

1.3.1.1. CYP1 family

The currently identified members of the human CYP1 family are CYP1A1, CYP1A2 and CYP1B1. CYP1A1 is an extra-hepatic enzyme and is only expressed minutely in the liver (Monostory et al., 2009); however, it is found in the heart, more specifically the left ventricle of explanted human hearts (Michaud et al., 2010) in addition to being present in the right ventricle and the left atrium of patients with dilated cardiomyopathy (Thum and Borlak, 2000a). CYP1A1 is also found in other organs such as the lung, gastrointestinal tract, kidney, breast, and skin (Ding and Kaminsky, 2003). Conversely, CYP1A2 is essentially a hepatic enzyme but is also expressed in the endothelium of the endocardium and coronary vessels (Minamiyama et al., 1999). CYP1B1 is an extra-hepatic enzyme that is highly expressed in the cardiovascular tissue (Bieche et al., 2007). CYP1B1 is expressed in vascular smooth muscle cells (VSMCs) (Kerzee and Ramos, 2001) as well as being detected in endothelial cells (ECs) and aortic SMCs of mice (Bertrand-Thiebault et al., 2004). CYP1B1 has been shown to be the second most abundantly expressed CYP gene in human hearts (Bieche et al., 2007).

The CYP1A subfamily is highly inducible through aryl hydrocarbon receptor-mediated gene transcription by polyaromatic hydrocarbons and halogenated aromatic hydrocarbons

including cigarette smoke (Ma and Lu, 2007). Classical inducers of CYP1A1 include 2,3,7,8-tetrachloro-dibenzodioxin (TCDD) and 3-methylcholanthrene (3MC) (Monostory et al., 2009). Benzo(a)pyrene (BaP) is able to induce both CYP1A1 and CYP1B1 in rat heart (Aboutabl et al., 2009). In addition to receptor-mediated xenobiotic induction, CYP1A hormonal regulation also plays a role in its expression (Monostory et al., 2009). CYP1A1 contributes to 19-HETE formation (El-Sherbeni and El-Kadi, 2014b) while CYP1A2 catalyzes the formation of EETs as well as 7-, 10-, and 13-HETE (Roman, 2002). CYP1B1 metabolizes AA into HETEs, mainly mid-chain HETEs (Choudhary et al., 2004). Both CYP1A and CYP1B subfamilies are also involved in the generation of 20-HETE within the vascular system (Choudhary et al., 2004).

1.3.1.2. CYP2 family

The CYP2 family includes five subfamilies: CYP2A, CYP2B, CYP2C, CYP2D and CYP2E. The CYP2 family is widely expressed in the cardiovascular system, and the main CYP2 cardiac expoxygenase enzymes are CYP2C8, CYP2C9, and CYP2J2. The most abundant isoform in all human heart left ventricules is CYP2J2 mRNA while low levels of CYP2B6 and CYP2C9 mRNAs are expressed (Michaud et al., 2010). In addition, CYP2D6 was detected in the right ventricle, while CYP2E1 was found in the atria and ventricles in addition to the ventricular septum (Thum and Borlak, 2000b). It has been found that during cardiac ischemia, induced by left anterior descending coronary artery ligation, CYP2C6, CYP2E1 and CYP2J3 protein levels increased in the ischemic region without an effect on mRNA (Ishihara et al., 2012).

1.3.1.3. CYP3 family

The CYP3 subfamily consists of CYP3A4, CYP3A5, CYP3A7 and CYP3A43, of which CYP3A4 is the most predominantly expressed and is responsible for 60% of the hepatic CYP-mediated metabolism of drugs in humans (Martinez-Jimenez et al., 2007). The expression of CYP3A4 in cardiovascular tissue has been detected in the endothelium, endocardium and coronary vessels (Minamiyama et al., 1999).

1.3.1.4. CYP4 family

This family consists mainly of the CYP4A, 4B, and 4F subfamilies and is responsible for fatty acid ω-hydroxylation. The CYP4 family is highly expressed in cardiovascular tissue (Elbekai and El-Kadi, 2006). CYP4A1, CYP4A2 and CYP4F were detected in canine heart tissues (Nithipatikom et al., 2004). CYP4F2 is associated with hypertension and cardioembolic stroke (independent of hypertension) in southern India (Munshi et al., 2012). Furthermore CYP4F2 polymorphisms were associated with coronary heart disease in a Chinese population (Yu et al., 2014).

1.3.2. The role of arachidonic acid in cardiovascular disease

1.3.2.1. 20- Hydroxyeicosatetraenoic acids (20-HETE)

20-HETE is the major metabolic product of arachidonic acid by CYP ω-hydroxylases. It is a potent vasoconstrictor mainly synthesized in the vasculature, kidney and lung. 20-HETEs' vasoconstrictive effect is by blocking calcium-activated K^+ channels, consequently leading to the

depolarization of the VSMCs, and leading to an increase of intracellular K^+ levels with subsequent activation of voltage-gated Ca^{2+} channels. In patients with coronary artery disease, the level of 20-HETE is inversely associated with brachial artery flow-mediated dilation (Schuck et al., 2013). In addition, 20-HETE plays a role during ischemic reperfusion injury as the levels of 20-HETE are found to increase and the inhibition of CYP ω-hydroxylases causes a reduction in infarct size (Gross et al., 2004). Chronic selective blockade of 20-HETE and soluble epoxide hydrolase production provided protection against the development of hypertension and its associated cardiac hypertrophy in young pre-hypertensive Ren-2 renin transgenic rats as well as reducing the augmented vascular responsiveness to Ang II in adult Ren-2 renin transgenic rats (Certikova Chabova et al., 2010).

In cases of acute and chronic elevations in circulating Ang II levels, an increased level of 20-HETE formation was observed in the kidneys and peripheral vasculature potentiating vasopressor effects of Ang II (Alonso-Galicia et al., 2002). In addition, 20-HETE was found to be the main AA metabolite released into the renal effluent of sham-operated rats stimulated with Ang II (Bautista et al., 2001).

1.3.2.2. 19- Hydroxyeicosatetraenoic acids (19-HETE)

19-HETE is the metabolic product of a number of CYPs, including CYP1As, CYP2E1 and CYP4As (Poloyac et al., 2004, El-Sherbeni and El-Kadi, 2014b, Capdevila et al., 2000). 19-HETE stimulates the rat renal cortical Na^+/K^+ ATPase activity in vascular smooth muscle (Escalante et al., 1990) and stimulates proximal tubule volume transport (Quigley et al., 2000), in addition to its vasodilatary effect in the renal arcuate arteries (Ma et al., 1993). 19-HETE blocks the vasoconstrictor actions of 20-HETE in renal and cerebral arteries (Roman, 2002) by acting as

an antagonist to 20-HETE (Alonso-Galicia et al., 1999). It is also thought that 19-HETE may affect the sensitizing action of endogenous 20-HETE (Zhang et al., 2005). 19-HETE prevented exogenous 20-HETE from sensitizing arteries treated with N-methylsulfonyl-12,12-dibromododec-11-enamide (DDMS), a CYP4A inhibitor, of spontaneously hypertensive rats (SHR) to phenylephrine and vasopressin. In addition, 19-HETE is also found to inhibit recombinant P/Q-type Ca^{2+}channel activity expressed in Purkinje cells (Qu et al., 2001).

1.3.3. Cytochrome P450 modulation

Modulation by CYPs includes either inhibition or induction. Inhibition can be reversible, irreversible or quasi-irreversible, with reversible being the most common form. Irreversible inhibition is also termed ‘‘mechanism-based inhibition’’ or ‘‘suicide inhibition’’ in which the drug that is metabolized by a certain cytochrome then binds covalently to the active site, either the heme and/or protein of the enzyme, and renders the enzyme inactive. Whereas in quasi-irreversible inhibition a non-covalent tight metabolic intermediate CYP complex is formed. Competitive inhibition is frequently encountered due to the fact that the same enzyme metabolizes diverse substrates.

The onset of enzyme induction is usually slower than that of inhibition. A classic example is the development of tolerance to the hypnotic effect of barbiturates upon prolonged treatment through cytochrome induction (Kurata et al., 1989). Human CYP1A1, CYP1A2, CYP2B6, CYP2C8, CYP2C9, CYP2C19 and CYP3A4 are known to be inducible, whereas CYP2D6 is not (Martignoni et al., 2006). This induction occurs by two main pathways, either through ligand activation of transcription factors or stabilization of translation or inhibition of the

protein degradation pathway. Transcription factors include aryl hydrocarbon receptor, pregnane X Receptor, and constitutive androstane receptor.

Aryl hydrocarbon receptor (AhR), is a ligand-activated basic helix-loop-helix transcription factor that regulates CYPs through dimerizing with its DNA binding partner AhR nuclear translocator, ARNT. Upon exposure, the CYP inducer binds to the AhR in the cytosol that in return is bound to heat shock proteins. Once ligand activation occurs, AhR then translocates into the nucleus and forms the AhR-ARNT heterodimer that binds to the aryl hydrocarbon responsive element (AhRE) and activates transcription of the specific CYP gene. AhR plays a role in the cardiovascular system and it has been found that genetic deletion of the AhR leads to cardiac hypertrophy (Thackaberry et al., 2002). Furthermore a correlation was found between cardiac hypertrophy in aryl hydrocarbon receptor null mice and elevated Ang II, endothelin-1, and mean arterial blood pressure (Lund et al., 2003).

Pregnane X Receptor (PXR), also known as the steroid and xenobiotic sensing nuclear receptor (SXR). Structurally, it consists of a ligand-binding domain (LBD) at the C-terminus and DNA-binding domain (DBD) at the N-terminus. Once binding of a substrate inducer occurs, PXR forms a heterodimer with retinioid X receptor (RXR). It binds with the response element at the premotor of the target gene (Smutny et al., 2013). In addition to ligand binding, PXR is also modulated through post-translational modification including posphorylation, acetylation, ubiquitination and SUMOylation (Smutny et al., 2013). A number of CYP isoforms are known to be induced through PXR activation, including CYP3A4, CYP2B6 and CYP2C (Synold et al., 2001, Gerbal-Chaloin et al., 2001, Goodwin et al., 2001).

Constitutive Androstane Receptor (CAR), upon activation translocates from the cytoplasm to the nucleus where it then similarly to PXR forms a heterodimer with RXR binding

to DNA response element. CAR is found to a play a role in the regulation of mostly CYP2B, in addition to CYP2C and CYP3A subfamilies (Ueda et al., 2002).

1.3.3.1. Inter-individual variability in CYP450 inhibition and induction

It has been very difficult to predict the extent of enzyme induction or inhibition due to marked inter-individual variability. Many factors play a role in this variability including genetic and environmental factors. Genetic factors are responsible for 20 to 95% of patient variability in response to individual drugs (Kalow et al., 1998). A number of CYPs are polymorphic; 75 allelic variants have been identified for *CYP2D6,* and studies indicate that people with the variants CYP2D6*3, CYP2D6*4, CYP2D6*5, CYP2D6*6 and CYP2D6*17 are slow metabolizers; since CYP2D6 is responsible for the metabolism of a number of drugs including codeine's conversion to morphine, people with these variants have poor analgesic response (Belle and Singh, 2008).

CYP polymorphisms play a role in individual susceptibility to cardiovascular diseases. A study in Germany revealed a correlation between CYP2J2*7 and coronary heart disease (Spiecker et al., 2004) in addition to another Taiwanese study that correlates CYP2J2*7 polymorphism and premature MI. In contrast, it was correlated with a lower risk of coronary heart disease in African-Americans in the ARIC study (Lee et al., 2007). Moreover, genetic disparities in CYP2C8 were associated with higher risk of coronary heart disease in smokers (Lee et al., 2007). However, polymorphisms in CYP2C8 and CYP2C9 did not show any correlation with ischemic stroke or myocardial ischemia (Marciante et al., 2008). In addition, epigenetic factors including environmental factors play a role in CYP variation. These may include the use of medications, dietary factors, pollutants, smoking and alcohol. Moreover, several reports have showed that the same chemical agent may have organ-specific effects on

CYP expression (Zordoky et al., 2008, Anwar-mohamed et al., 2010, Anwar-Mohamed et al., 2013, Poloyac et al., 2004). The characteristic of CYP induction and inhibition has been used as a treatment target. Chloramphenicol, a CYP2C19 and CYP3A4 inhibitor (Park et al., 2003) and sulfaphenazole (SPZ), a CYP2C6 inhibitor (Kobayashi et al., 2003), were found to decrease global ischemia induced myocardial infarct size (Granville et al., 2004). Examples of inducers and inhibitors used in this project include isoniazid and 2,3',4,5'-tetramethoxystilbene.

1.3.3.2. Isoniazid (INH)

INH was the first line treatment for the management of tuberculosis for decades and was first approved by the FDA in 1952. Its mechanism of action is through inhibiting the synthesis of mycoloic acid, which is an essential component of the bacterial cell wall. Upon absorption INH is distributed in all body tissues and fluids. It undergoes hepatic metabolism by acetylation and dehydrazination. The half-life differs among the population and can be divided according to acetylation phenotype into fast acetylators with a half-life of 30 to 100 minutes while the half-life for low acetylators is 2 to 5 hours; this may be further lengthened with hepatic or severe renal injury.

Pretreatment with INH enhances the activity of CYP2E1 in several species including humans (Zand et al., 1993). The mechanism by which INH confers this induction is complex and can occur through numerous methods, including transcriptional activation (Umeno et al., 1988), increased translational efficiency of mRNA (Kim et al., 1990) or its stabilization (Song et al., 1987), in addition to the stabilization of the protein (Song et al., 1989). However INH is also found to have a biphasic effect (i.e induction and competitive inhibition) on CYP2E1, since INH can induce the enzyme through stabilization of the protein by binding to the active site protecting

the enzyme from degradation, this also results in competitive inhibition of substrate clearance (Chien et al., 1997). In addition, INH is found to competitively inhibit the activity of CYP2C19 and CYP3A (Desta et al., 2001).

1.3.3.3. 2,3',4,5'-tetramethoxystilbene (TMS)

TMS is a potent and selective inhibitor of CYP1B1. TMS interferes in the proximity of the heme region of CYP1B1 with high affinity as suggested by binding studies with purified CYP1B1 (Divi et al., 2012). The inhibitory effects of TMS on ethoxyresorufin *O*-deethylation (EROD) was quantified and found to have an IC50 of 6 ± 2 nM (Kim et al., 2002). TMS was found to have anticancer activity in a number of human cancer cell lines therefore is considered to be a potential cancer preventive agent but to this point has not been approved for clinical use. In general *trans*-stilbene compounds have a long terminal elimination half-life and slow clearance (Lin et al., 2010).

1.4. Rationale, Hypotheses, and Objectives

1.4.1. Rationale

Cardiac hypertrophy is considered a major risk factor for several serious heart diseases, most importantly heart failure (Hawkins et al., 2007, Felix-Redondo et al., 2012). Currently, there are about 6.6 million people in US with heart failure, and the number is expected to rise to about 9.6 million by 2030 (Roger et al., 2012). In Canada, 500,000 patients are living with heart failure and 50,000 new patients are diagnosed each year. This results in a significant burden on

health care system (Graham et al., 2006). The prognosis of heart failure is poor, and only 35% of patients survive 5 years after the first diagnosis (Bleumink et al., 2004). Besides heart failure, it is well known that left ventricular hypertrophy increases the incidence of myocardial infarction, arrhythmia and premature death (Schunkert et al., 1997). The term cardiac hypertrophy was coined to describe the distinctive alteration in heart wall thicknesses and heart chambers volumes, in response to biomechanical stresses, such as hypertension (Frey and Olson, 2003). Accordingly, cardiac hypertrophy has been under extensive study in order to identify new targets for its prevention and control.

AA metabolites have been long known to exhibit potent biological activities. In fact, the association between alterations in AA metabolism and the onset, duration and severity of several heart diseases has been observed and reported (Roman, 2002). AA is bound to plasma membrane and is released by the activity of phospholipases, most prominently cPLA2 (Tacconelli and Patrignani, 2014). Once released, free AA can be metabolized into a number of biologically active eicosanoid metabolites.

There are three pathways for AA metabolism, cyclooxygenase (COX), lipoxygenase (LOX) and cytochrome P450 (CYP) (Capdevila et al., 1981). CYP exclusively mediates the metabolism of AA to epoxyeicosatrienoic acids (EETs) and hydroxyeicosatetraenoic acids (HETEs). EETs and HETEs play critical roles in the regulation of renal, pulmonary and cardiac functions and vascular tone (Roman, 2002, Chu et al., 2000). Evidence suggests that CYP-derived HETEs and EETs influence vascular tone and their importance in the progression of hypertension in different animal models (Roman, 2002, Chu et al., 2000). EETs have been suggested to be the endothelium-derived hyperpolarizing factor (EDHF), providing a cardioprotective effect, while 20-HETE is a potent vasoconstrictor and considered as a

cardiotoxic metabolite (Elbekai and El-Kadi, 2006, Elshenawy et al., 2013). Interestingly, 19-HETE was found to act as an antagonist to 20-HETE (Alonso-Galicia et al., 1999). 19-HETE inhibits 20-HETE mediated vasoconstriction and antagonizes 20-HETE induced endothelial dysfunction. (Alonso-Galicia et al., 1999, Cheng et al., 2008b). Recently data from our laboratory demonstrated that a decrease in 19-HETE was associated with cardiac hypertrophy (El-Sherbeni and El-Kadi, 2014a). A number of studies have demonstrated the role of 19-HETE in counterbalancing the cardiotoxic effect of 20-HETE. However none has shown its potential cardioprotective role in cardiac hypertrophy. Multiple CYP enzymes have been reported to mediate 19-HETE formation, such as CYP1As, CYP2E1 and CYP4As (Poloyac et al., 2004, El-Sherbeni and El-Kadi, 2014b, Capdevila et al., 2000). Therefore it will be important to examine the role of these enzymes in cardiac hypertrophy.

CYP1B1 is a member of the CYP enzymes and is highly expressed in the cardiovascular tissue (Bieche et al., 2007). CYP1B1 metabolizes AA into HETEs, mainly mid-chain HETE and 20-HETE (Choudhary et al., 2004). Even though in previous years CYP1B1 metabolism has been extensively studied, the main focus of CYP1B1 research has been in the field of cancer and its capacity for the bioactivation of carcinogens, due to CYP1B1 overexpression in a variety of human tumors. However, recently, its role in cardiovascular disorders is being investigated and is shown to be a promising therapeutic target (Jennings et al., 2012b, Sahan-Firat et al., 2010). TMS is a resveratrol analogue, and a potent and selective inhibitor of CYP1B1.

In studying the role of CYPs and their expression in cardiovascular tissue several in vivo models have been used (Imaoka et al., 2005, Thum and Borlak, 2002, Zordoky et al., 2008, Alsaad et al., 2012, Aboutabl et al., 2011, El-Sherbeni and El-Kadi, 2014a). In the current study, Ang II is used as an inducer of cardiac hypertrophy. Ang II is the primary effector of the renin-angiotensin

system, and its elevated levels have been reported in the hypertrophied and failing heart (Rosenbaugh et al., 2013). The direct hypertrophic and hypertensive effects of Ang II is well-documented and underscores its important role in the development of cardiac hypertrophy and heart failure. Induction of cardiac hypertrophy by Ang II may have an advantage over other models of cardiac hypertrophy. Other exogenous agents used previously to induce cardiac hypertrophy may have their own effect on CYP-mediated AA metabolism. In addition, unlike surgical procedures, the factor of variability is easier to control, giving more consistent results.

For studying the cellular mechanisms and signaling pathways in the heart, human fetal ventricular cardiomyocyte RL-14 cells were used. RL-14 cells are derived from non-proliferating primary cultures from human fetal heart tissue. RL-14 cells have been found to express CYP isoenzymes at comparable levels to those expressed in the primary cell line and therefore can be used as a reliable model for studying drug metabolizing enzymes in the heart (Maayah et al., 2015).

1.4.2. Hypotheses

Hypothesis 1: Administration of 19-HETE exerts a protective effect against Ang II-induced cellular hypertrophy.

Hypothesis 2: Inducing CYP2E1 using INH will increase the level of cardioprotective 19-HETE.

Hypothesis 3: INH will protect against Ang II-induced cardiac hypertrophy.

Hypothesis 4: Inhibiting CYP1B1 will decrease the levels of 5-, 12-, and 15-HETE and 20-HETE, which will protect against Ang II-induced cardiac hypertrophy.

1.4.3. Objectives

The specific objectives of the present work are:

1) To examine the effect of 19-HETE against Ang II-induced cellular hypertrophy.

2) To determine the effect of INH on cardiac CYP gene and protein expression and activity and thereafter investigate the consequent alteration caused by INH in the cardiac levels of EETs and HETEs.

3) To determine the effect of INH on Ang II-induced cardiac hypertrophy

4) To determine the effect of TMS on Ang II-induced cardiac hypertrophy and its effect on the cardiac levels of 5-, 12-, 15-, and 20-HETE *in-vivo* and subsequently to investigate the underlying molecular mechanisms involved *in-vitro*.

Chapter 2 : MATERIALS & METHODS

2.1. Materials and Methods

2.1.1. Materials

TRIzol reagent and UltraPure distilled water, fetal bovine serum, L-glutamine, and penicillin–streptomycin were purchased from Invitrogen (Carlsbad, CA). Reagents used for liquid chromatography (LC)-electron spray ionization (ESI)-mass spectrometry (MS) were of HPLC grade. Acetonitrile and water (HPLC grade) were purchased from EM Scientific (Gibbstown, NJ). Ang II, INH and Dulbecco's Modified Eagle's Medium/F-12 (DMEM/F-12) were purchased from Sigma-Aldrich (St. Louis, MO). TMS and the AA metabolite standards 5,6-EET, 8,9-EET, 11,12-EET, 14,15-EET, 5,6-DHET, 8,9-DHET, 11,12-DHET, 14,15-DHET, 19-HETE and 20-HETE were obtained from Cayman Chemical (Ann Arbor, MI). For real time-polymerase chain reaction (PCR), a High-Capacity cDNA Reverse Transcription Kit, SYBR Green SuperMix, and 96-well optical reaction plates with optical adhesive films were purchased from Applied Biosystems (Foster City, CA, USA). Real time-PCR primers were synthesized by Integrated DNA Technologies Inc. (Coralville, IA, USA) according to previously published sequences. Acrylamide, N'N'-bis-methylene-acrylamide, ammonium persulphate, β-mercaptoethanol, glycine, nitrocellulose membrane (0.45μm) and N,N,N',N'-tetramethylethylenediamine (TEMED) were purchased from Bio-Rad Laboratories (Hercules, CA).

Chemiluminescence Western blotting detection reagents were purchased from GE Healthcare Life Sciences (Piscataway, NJ). CYP2E1 rabbit polyclonal primary antibody and the MAPKs kit were purchased from Abcam (Cambridge, UK). CYP1B1 mouse polyclonal primary antibody, GAPDH mouse monoclonal primary antibody and Goat anti-rabbit IgG with horseradish

peroxidase secondary antibody were purchased from Santa Cruz Biotechnology, Inc. (Santa Cruz, CA, USA). Anti-mouse IgG peroxidase secondary antibody was purchased from R&D Systems, Inc. (Minneapolis, MN, USA). Amphotericin B was purchased from ICN Biomedicals Canada (Montreal, QC, Canada).

The NF-κB Family EZ-TFA Transcription Factor Assay Chemiluminescent Kit was purchased from Millipore (Millipore, Schwalbach/ Ts., Germany, #70-660). All other chemicals were purchased from Thermo Fisher Scientific (Waltham, MA).

2.1.2. Methods

2.1.2.1. Cell culture and treatments

Human ventricular cardiomyocyte RL-14 cells (American Type Cell Culture, Manassas, VA) were grown in 75 cm^2 tissue culture flasks at 37 °C under a 5% CO_2 humidified environment. Cell culture was maintained in DMEM/F-12, with phenol red supplemented with 12.5% fetal bovine serum, 20 μM l-glutamine, 100 IU/ml penicillin G and 100 μg/ml streptomycin. Cells were cultivated in a six-well tissue culture plate in F12/DMEM culture media. Upon confluence (60-80%), the appropriate treatment was initialized.

For the 19-HETE study, cells were exposed for 24 h to vehicle or Ang II (10 μM) with or without 19-HETE (20 μM) in serum-free media. As for the TMS study, cells were treated for 24 h with vehicle or Ang II (10 μM) with or without TMS (0.5 μM) in serum-free media.

2.1.2.2. Animal Model

2.1.2.2.1 Hypertrophy Model

All animal experimental procedures were approved by the University of Alberta Health Sciences Animal Policy and Welfare Committee. Male Sprague Dawley (SD) rats weighing 190-210 g were obtained from Charles River Canada (Montreal, QC, Canada). They were allowed free access to food and water throughout the experiment period and were maintained on a 12-h light/dark cycle. Ang II was used as a hypertrophic agent. For the INH study, two experiments were performed: In the first experiment, 6 male Sprague-Dawley rats were injected intraperitoneally (i.p.) with 200 mg/kg/day of INH dissolved in saline for 14 days, and 6 weight matched controls received the same volume of saline. In the second experiment, 18 rats were segregated into 3 groups. In the first group, 6 rats were given saline i.p. plus saline via miniosmotic pump for 14 days (control group). In the second group, 6 rats were given saline i.p. plus 450 ng/kg/minute of Ang II in saline via miniosmotic pump for 14 days (Ang II treated group). In the third group, 6 rats were given 200 mg/kg/day of INH in saline i.p. plus 450 ng/kg/minute of Ang II in saline via miniosmotic pump for 14 days (INH-Ang II treated group).Thereafter, animals were sacrificed under isoflurane anaesthesia. Hearts were immediately frozen in liquid nitrogen and stored at −80 °C. The tibial length was measured by micro-CT (SkyScan NV, Kontich, Belgium).

For the TMS study, male Sprague-Dawley rats (200–250 g) were segregated into 3 groups. The first group (n=6) received saline (i.p.) plus saline via miniosmotic pump (control group). The second group (n=6) rats were given saline i.p. plus 450 ng/kg/minute of Ang II in saline via miniosmotic pump for 14 days (Ang II treated group). The third group, (n=6) rats were given

300 μg/kg every 3rd day of TMS in DMSO i.p. plus 450 ng/kg/minute of Ang II in saline via miniosmotic pump for 14 days (TMS-Ang II treated group). Thereafter, animals were euthanized under isoflurane anesthesia 24 h after the last injection during the morning. Hearts were immediately frozen in liquid nitrogen and stored at −80 °C. The tibial length was measure by micro-CT (SkyScan NV, Kontich, Belgium).

2.1.2.3. Echocardiography

After 14 days, SD rats were weighed and mildly anesthetized using 1.5% isoflurane. Subsequently, transthoracic echocardiography was performed using a Vevo 770 Imaging System (VisualSonics, Toronto, ON). Heart dimensions, LVIDs: left ventricular internal diameter in systole; LVPWs: left ventricular posterior wall thickness in systole; and LVPWd: left ventricular posterior wall thickness in diastole in addition to the ejection fraction were determined using M-mode measurements taken from parasternal long and short axis views at the mid-papillary level. Measurements were averaged from 3 to 6 cardiac cycles according to the American Society of Echocardiography (Barbieri et al., 2012, Byrd et al., 2015), and digitally transferred online to a computer, and subsequently analyzed by an analyst blinded to the treatment groups. Echocardiography was performed by a trained technician; Donna Beker, from the Cardiovascular Research Centre, University of Alberta.

2.1.2.4. Blood pressure Measurement

Measuring blood pressures was conducted using iiTC NIBP 12-multichannel blood pressure tail cuff system (Life Science; Woodland Hills, CA). Rats were conditioned to the restrainers for 3

consecutive days prior to readings. After the 3-day training period, rats were typically calm and co-operative when placed in the restrainers for testing. The warming chamber was kept at 30°C while a darkened nose cone aided in calming the animal. Three consecutive readings were taken during a typical run using the automated inflation-deflation cycles of the tail cuff. Analysis was performed on the readings using system software. Systolic blood pressure was used for assessment of the three groups. Blood pressure measurement was performed by trained personnel; Amy Barr, from the Cardiovascular Research Centre, University of Alberta.

2.1.2.5. Measurement of cell viability

The effect of the tested chemical on cell viability was determined by the MTT assay in which the capacity of reducing enzymes present in viable cells to convert 3-[4,5-dimethylthiazol-2-yl]-2,5-diphenyltetrazolium bromide (MTT) to formazan crystals was measured. Tested chemical was incubating in RL-14 cells for 24 hours in a 96-well plate at 37°C under a 5% CO_2 humidified incubator. The medium was replaced with 100 µl of serum-free medium containing 1.2 mM of MTT dissolved in PBS, pH 7.2. The plate was then incubated at 37°C in a 5% CO_2 humidified incubator for 2 h. The medium was then decanted off by inverting the plate, and 100 µl of isopropyl alcohol was added to each well with shaking for 1 h to dissolve the formazan crystals. The color intensity in each well was measured at wavelength of 550 ηm using a Synergy H1 hybrid multi-mode microplate reader (Biotek Instruments Inc., VT, USA). The percentage of cell viability was calculated relative to control wells designated as 100% viable cells.

2.1.2.6. RNA Isolation

Total RNA was isolated from tissue or cells using TRIzol (Invitrogen) reagent following the manufacturer's instructions. In brief, 1 ml of TRIzol was used per 100 mg of tissue to homogenize the frozen tissue or 600 µl per well using a 6 well plate. TRIzol should be used in sufficient amounts; failure to do results in DNA contamination of the isolated RNA. The lysate was then poured into a 1.5 mL microcentrifuge tube and mixed with 120 µL chloroform, then centrifuged at 12,000 x g for 15 min at 4°C. The lysate separated into layers, RNA is found in the aqueous upper layer, and this was collected and relocated to a new microcentrifuge tube. Thereafter, isopropanol was added to each tube at a 1:2 ratio of isopropanol to TRIzol and then the samples were frozen at -20°C overnight. After the RNA was precipitated, it was then collected by centrifugation at 12,000 x g for 10 min at 4°C. Subsequently, the supernatant was removed leaving only the RNA pellet which was washed by 75% ethanol in diethyl pyrocarbonate (DEPC)-treated water. The RNA pellet was then washed by lightly vortexing the tubes. The tubes were centrifuged again at 12,000 x g for 5 min at 4°C to let the pellet settle down. The solution was aspirated out, the pellet was dried, and then dissolved in 50 µl DEPC-treated water. The tubes were placed in a water bath at 60°C for 15 min. Total RNA was quantified by measuring the absorbance at 260 nm. RNA quality was determined by measuring the 260/280 ratio.

2.1.2.7. cDNA Synthesis

After RNA isolation, first strand cDNA synthesis was performed by using the High-Capacity cDNA reverse transcription kit (Applied Biosystems) according to the manufacturer's

instructions. Briefly, 1.5 µg of total RNA from each sample was added to a mix of 2.0 µl of 10x reverse transcriptase buffer, 0.8 µl of 25x dNTP mix (100 mM), 2.0 µl of 10x reverse transcriptase random primers, 1.0 µl of MultiScribe reverse transcriptase, and 4.2 µl of nuclease-free water. The final reaction mix was kept at 25°C for 10 min, heated to 37°C for 120 min, heated for 85°C for 5 min, and finally cooled to 4°C.

2.1.2.8. Quantification by Real time PCR

The expression of specific mRNA was quantitatively analyzed by real time-PCR, by subjecting the particular cDNA to PCR amplification using 96-well optical reaction plates in the ABI Prism 7500 System (Applied Biosystems) according to the manufacturer's instructions. The 25 µl reaction mix contained 0.1 µl of 10 µM forward primer, 0.1 µl of 10 µM reverse primer (40 nM final concentration of each primer), 12.5 µl of SYBR Green Universal Mastermix, 11.05 µl of nuclease-free water, and 1.25 µl of cDNA sample. The primers were chosen from previously published studies and are listed in Table 2.1. Assay controls were incorporated onto the same plate, namely, no-template controls to test for the contamination of any assay reagents. After sealing the plate with an optical adhesive cover, the thermocycling conditions were initiated at 95°C for 10 min, followed by 40 PCR cycles of denaturation at 95°C for 15 s, and annealing/extension at 60°C for 1 min. To confirm the specificity of the primers and the purity of the final PCR product, the dissociation curves were performed by the end of each cycle.

The real time-PCR data were analyzed using the relative gene expression, also known as the ΔΔCT method as described in Applied Biosystems User Bulletin No.2. Briefly, the fold change in gene expression was normalized to the endogenous reference gene glyceraldehyde-3-phophate dehydrogenase (GAPDH) relative to the untreated control.

Table 2.1 Rat primer sequences used for real-time PCR reactions.

Gene	Forward Primer	Reverse Primer
CYP1A1	CCAAACGAGTTCCGGCCT	TGCCCAAACCAAAGAGAATGA
CYP2B1	AACCCTTGATGACCGCAGTAAA	TGTGGTACTCCAATAGGGACAAGATC
CYP2C11	CACCAGCTATCAGTGGATTTGG	GTCTGCCCTTTGCACAGGAA
CYP2E1	AAAGCGTGTGTGTGTTGGAGAA	AGAGACTTCAGGTTAAAATGCTGCA
CYP2J3	CATTGAGCTCACAAGTGGCTTT	CAATTCCTAGGCTGTGATGTCG
CYP4F5	AGGATGCCGTGGCTAACTG	GGCTCCAAGCAGCAGAAGA
CYP4A3	CTCGCCATAGCCATGCTTATC	CCTTCAGCTCATTCATGGCAATC
CYP1B1	CAGAAGCTGCTGGAGCTGATAAG	TGTAGGGCCTTGGTCCTTTG
GAPDH	CAAGGTCATCCATGACAACTTTG	GGGCCATCCACAGTCTTCTG

Table 2.2 Human primer sequences used for real-time PCR reactions

Gene	Forward Primer	Reverse Primer
α-MHC	CCAAACGAGTTCCGGCCT	TGCCCAAACCAAAGAGAATGA
β-MHC	GAATGGCTTCTAGTCCCA	TCATCTTCTCACTAAGGGCT
β-actin	CCAGATCATGTTTGAGACCTTCAA	GTGGTACGACCAGAGGCATACA

2.1.2.9. Microsomal Protein Extraction and Western Blot Analysis

Microsomal fractions were prepared by differential centrifugation of homogenized tissues as described previously (Barakat et al., 2001). Briefly, organs were washed in ice-cold potassium chloride (1.15%, w/v), successively cut into pieces, and homogenized in ice-cold 0.25 M sucrose solution sucrose (17%, w/v). After homogenization the tissues were separated by differential ultracentrifugation. The final pellet was re-suspended in cold sucrose and stored at −80 °C. The protein concentration was calculated using the Lowry method (Lowry et al., 1951).

Western blot analysis was performed, 50 μg of the protein was first dissolved in 2X sample buffer, boiled for 5 min, then separated by 10% sodium dodecyl sulphate-polyacrylamide gel (SDS-PAGE) and electrophoretically transferred to a nitrocellulose membrane. Protein blots were blocked in blocking buffer containing 5% skim milk powder, 2% bovine serum albumin and 0.05% (v/v) Tween-20 in Tris-buffered saline solution, overnight at 4 °C. Thereafter, the blots were washed then incubated with the relevant primary antibodies CYP2E1 rabbit polyclonal primary antibody, CYP1B1 mouse polyclonal primary antibody, GAPDH mouse monoclonal primary antibody, and β-actin rabbit primary antibody overnight at 4 °C. The primary antibodies were prepared in TBS solution containing 0.05% (v/v) Tween-20 and 0.02% sodium azide. Incubation with a peroxidase-conjugated antibody was carried out for another 2 h at room temperature. The bands were visualized using an enhanced chemiluminescence method according to the manufacturer's instructions (GE Healthcare Life Sciences, Piscataway, NJ, USA). The intensities of the protein bands were quantified relative to the signals obtained for actin, using ImageJ software (National Institutes of Health, Bethesda, MD, http://rsb.info.nih.gov/ij).

2.1.2.10. Metabolite Activity

Microsomal protein (1 mg/mL) was incubated for 30 min with AA (50 μM) in the incubation buffer (3 mM magnesium chloride hexahydrate dissolved in 100 mM potassium phosphate buffer, pH 7.4) in a shaking water bath at a temperature of 37 °C at 90rpm, a period of 5 minutes pre-equilibration was allowed. The reaction was initiated by the addition of the cofactor NADPH (final concentration 2 mM) and terminated by the addition of 600 μL ice-cold acidified acetonitrile. Samples were then evaporated to dryness, reconstituted with 50 μL acetonitrile and CYP-derived AA metabolites were analyzed simultaneously using liquid chromatography-electrospray ionization-mass spectrometry as explained in section (2.1.2.13).

2.1.2.11. Endogenous Metabolite Measurement

Homogenization of heart tissue (350 mg) was performed on ice with 350 uL of methanol containing internal standards. Centrifugation of the homogenates was done at 10,000 g for 30 min at 0℃. AA metabolites were extracted from the resultant supernatant using solid-phase cartridges (Oasis1HLB). Conditioning and equilibration of solid-phase cartridges were performed with methanol, ethyl acetate, 0.2% formic acid (v/v), and 10% methanol, in sequence. After sample application, cartridges were washed by 0.2% formic acid (v/v), and 10% methanol in 0.2% formic acid (v/v), in sequence. AA metabolites were then eluted by 1% formic acid in acetonitrile (v/v) followed by ethyl acetate. Samples were then evaporated to dryness, reconstituted with 50 μL acetonitrile. AA and CYP-derived AA metabolites were analyzed simultaneously using liquid chromatography-electrospray ionization-mass spectrometry as

explained in section (2.1.2.13). Epoxy-metabolites were measured as the sum of each EET and its corresponding dihydroxyeicosatrienoic acid.

2.1.2.12. Direct effect of INH on metabolite activity

Heart microsomes (100 μg) separated from control rats were incubated with 0 and 50 μM of INH for 10 min on ice (all samples contained a fixed concentration of 0.1% dimethylsulfoxide). AA (50 μM) was added, and the reaction was initiated by the addition of NADPH and terminated by the addition of acetonitrile. Ethyl acetate (1 ml) was used for the double extraction of the incubation mixtures; the organic extracts were then combined, evaporated to dryness and reconstituted in 50μL acetonitrile containing 0.01% formic acid. CYP-derived AA metabolites were analyzed simultaneously using liquid chromatography-electrospray ionization-mass spectrometry as explained in section (2.1.2.13).

2.1.2.13. Apparatus and chromatographic conditions

AA and CYP-derived AA metabolites were analyzed simultaneously using liquid chromatography-electrospray ionization-mass spectrometry (LC-ESI-MS) (Waters Micromass ZQ 4000 spectrometer). The mass spectrometer was run in negative ionization mode with single ion monitoring. For EETs, the most abundant ions were at m/z = 319. For DHETs, the most abundant ions were at m/z = 337. For 19- and 20-HETE, the most abundant ions were at m/ z = 319. The nebulizer gas was acquired from an in house high purity nitrogen source. The temperature of the source was set at 150 °C, and the capillary and cone voltages were 3.51 kV and 25 V, respectively. A gradient separation was performed on a reverse phase C18 column

(Alltima HP, 250 × 2.1 mm) at 35°C. Mobile phase A consisted of water with 0.01% formic acid and 0.005% triethylamine (v/v), while mobile phase B consisted of 8% methanol, 8% isopropanol and 84% acetonitrile with 0.01% formic acid and 0.005% triethylamine (v/v). Samples were subjected to linear gradient elution at a flow rate of 200 µL/min, as follows: 60 to 48% in 4 min, held isocratically at 48% for 24 min, 48 to 35% in 11 min, 35 to 0% in 11 min, and finally held isocratically at 0% for 7 min of mobile phase A.

Three standard samples were prepared by spiking protein preparation with known amounts of tested compounds, as well as internal standards. The final concentrations of the tested compounds were 0.01, 0.1, and 1 µg/ml for AA metabolites and 0.24, 2.4, and 24 µg/ml for AA, whereas the final concentration of internal standards was 0.25 µg/ml. Standard samples were subjected to the same extraction procedure as test samples to be analyzed at the beginning and at the end of the run. The concentrations of the AA metabolites were determined from standard curves using analyte to internal standard peak area (response ratio). The lower limit of quantification is 0.005 µg/ml.

2.1.2.14. Determination of Reactive Oxygen Species

A fluorometric assay was utilized in order to determine ROS formation caused by Ang II and TMS. The DCF test was used in which diacetate H2DCFDA enters into the cells through the cell membrane where esterases cleave the acetate groups. Thereafter, the intracellular oxidation of H2DCF by ROS converts the molecule to 2',7'dichlorodihydrofluorescein (DCF), which is highly fluorescent. RL14 cells were grown on 6 well plates and treated with either Ang II, TMS or their combination for 24 hours. Thereafter the cells were treated with 0.5µM AA for three hours followed by incubation with DCF-DA. The fluorescence was directly measured using

excitation and emission wavelengths of 485 and 535 nm, respectively using a Synergy H1 hybrid multi-mode microplate reader (Biotek Instruments Inc., VT, USA).

2.1.2.15. Preparation of nuclear extract

Nuclear extracts from RL-14 cells were prepared according to a previously described procedure with minor modifications (Andrews and Faller, 1991) Briefly, RL-14 cells were grown on 100-mm petri dishes and treated with vehicle or Ang II alone or in combination with TMS for 8 h. The group being treated with Ang II + TMS was pretreated with TMS alone for 24 h. Thereafter, cells were washed twice with cold PBS, pelleted and suspended in cold buffer A [10 mM Hepes–KOH, 1.5 mm MgCl2, 10 mM KC1, 0.5 mM dithiothreitol and 0.5 mM phenylmethylsulfonyl fluoride (PMSF)] pH 7.9, at 4 °C. After 15 min on ice, the cells were centrifuged at 6500*g* and the pellets were suspended again in high salt concentration cold buffer C (20 mM Hepes–KOH, pH 7.9, 25 % glycerol, 420 mM NaCl, 1.5 mM MgCl2, 0.2 mM EDTA, 0.5 mM dithiothreitol and 0.5 mM PMSF) to extract nuclear proteins. The cells were then incubated on ice with vigorous agitation for 60 min followed by centrifugation for 10 min at 12000*g* at 4 °C. The nuclear extracts were stored at −80 °C till further use.

2.1.2.16. Determination of NF-κB binding activity

The NF-κB Family EZ-TFA Transcription Factor Assay Chemiluminescent Kit (Millipore, Schwalbach/Ts., Germany, #70-660) was used according to the manufacturer's protocol. Briefly, RL-14 cells were treated for 8 h with either Ang II (10 μM) alone or in combination with TMS (0.5 μM). The group being treated with Ang II + TMS was pretreated with TMS alone for 24 h.

Nuclear extract was mixed with the NFκB Capture Probe in the Transcription Factor Assay Buffer provided. The complete mixture was then directly transferred to the coated plate. The active NFκB protein was immobilized on the capture probe bound to the plate well, while any inactive, unbound material was washed away. The bound NFκB transcription factor subunits were detected with their specific primary antibodies. A horseradish peroxidase-conjugated secondary antibody was then used for detection which was then measured using a Synergy H1 hybrid multi-mode microplate reader (Biotek Instruments Inc., VT, USA).

2.1.2.17. Determination of MAPKs signaling pathway

MAPK pathway activation was measured by ELISA using the PhosphoTracer ERK1/2 [pT202/Y204+p38 MAPK (pT180/Y182)+JNK1/2/3 (pT183/Y185) ELISA kit (Abcam, Cambridge, UK). The phosphorylation was determined in cytoplasmic protein extracts according to the manufacturer's instructions. Briefly, RL-14 cells were treated for 8 h with either Ang II (10 μM) alone or in combination with TMS (0.5 μM). The group being treated with Ang II + TMS was pretreated with TMS alone for 24 h. Cell lysates were prepared, protein content was measured by the Lowry assay. 50 μg of the protein was transferred to the Phosphotracer microplate. Lysis mix was added to wells followed by the addition of the antibody mix; the mixture was then covered and incubated for 1 hour on a microplate shaker. Freshly prepared substrate mix was then added, and again it was covered with foil and left on the shaker for 10 minutes. The degree of phosphorylation was then measured using a Synergy H1 hybrid multi-mode microplate reader (Biotek Instruments Inc., VT, USA).

2.1.2.18. Statistical Analysis:

Data are presented as mean ± standard error of mean (SEM). Student's t test or one-way analysis of variance, followed by a Student–Newman–Keuls post hoc test, was used. A result was considered statistically significant where $p < 0.05$. Analysis was performed using SigmaPlot® for Windows (Systat Software, Inc, CA).

Chapter 3 : RESULTS

3.1 Effect of 19-HETE on Ang II-induced cellular hypertrophy in RL-14 cells:

3.1.1 Effect of 19-HETE on cell viability

To determine the cytotoxic effect of 19-HETE, RL-14 cells were incubated with increasing concentrations of 19-HETE (1, 2.5, 5, 10, 20 μM) for 24 h. Thereafter, cell viability was evaluated by the MTT assay as described in materials and methods. The MTT assay showed that 19-HETE concentrations ranging from 1-20 μM did not significantly affect cell viability as compared to controls (Fig. 3.1). Therefore, the observed changes in the gene expression are not due to the decreased cell viability caused by toxicity.

3.1.2 Effect of 19-HETE on cardiac hypertrophy markers

The effect of 19-HETE on the development of cellular hypertrophy in RL-14 cells was determined. Cellular hypertrophy in human cardiomyocytes, RL-14, was induced by Ang II. We found that exposing RL-14 cells to 10 μM Ang II for 24 h led to cellular hypertrophy as confirmed by the significant increase in β/α-MHC ratio by 207%, as well as brain natriuretic peptide by 61% in Ang II-treated cells, compared with controls (Fig. 3.2.A and B). Interestingly, pretreatment with 19-HETE was able to protect RL-14 cells from the hypertrophic effect of Ang II as assessed by β/α-MHC ratio. 19-HETE was able to significantly reduce β/α-MHC ratio by 72.9% to return to its normal level in comparison to Ang II. On the other hand, the elevated level of brain natriuretic peptide by Ang II was not affected by 19-HETE exposure in RL-14 (Fig. 3.2.B).

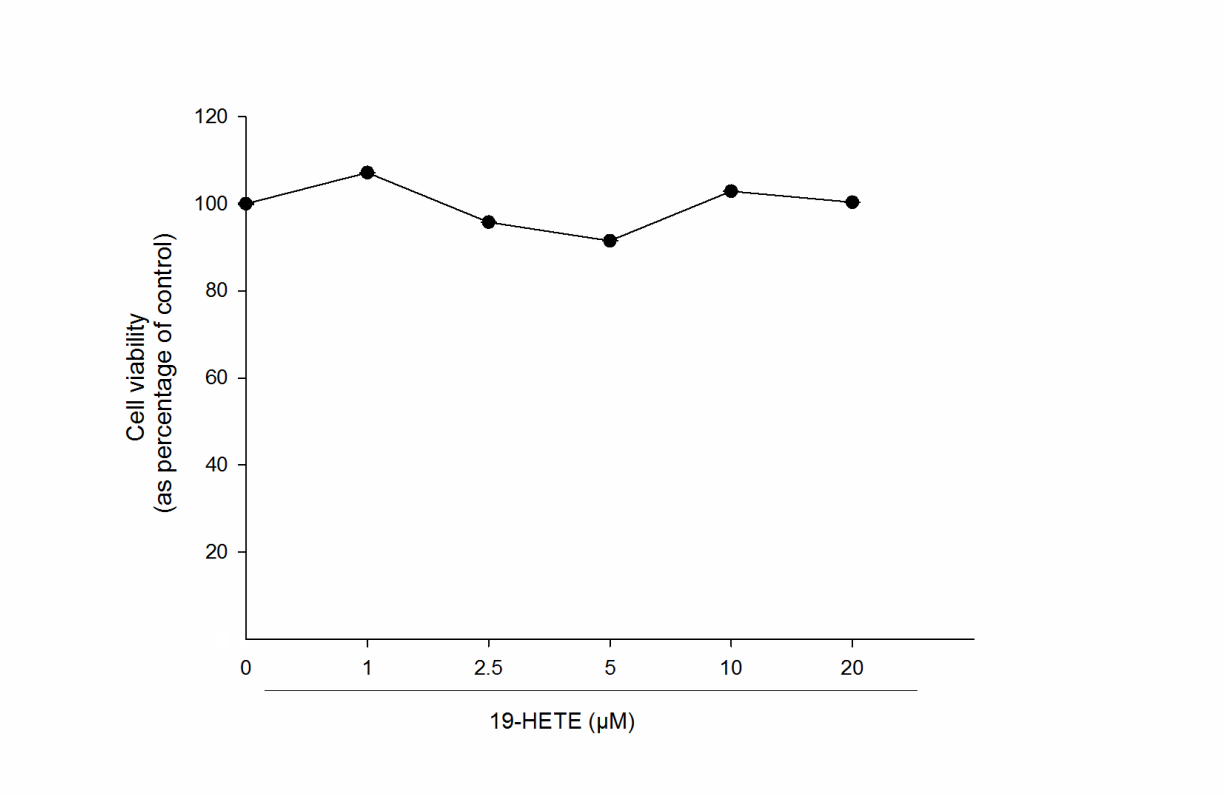

Figure 3.1 Effect of 19-HETE on cell viability.

RL-14 cells were incubated with increasing concentrations of 19-HETE (0, 1, 2.5, 5, 10 and 20 μM) for 24 h. The cell viability was measured by the MTT assay as described in materials and methods. Data are presented as a percentage of control (mean + S.E.M, n=8). * $p < 0.05$ compared to control.

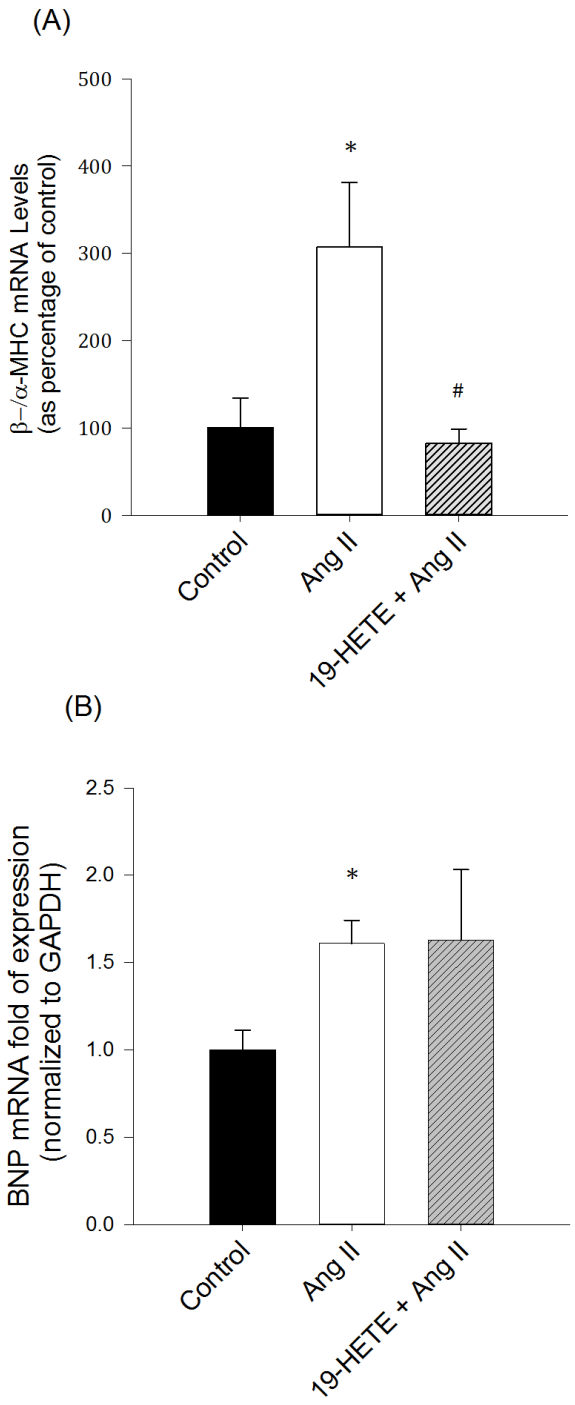

Figure 3.2 Effect of 19-HETE on cardiac hypertrophic markers.

RL-14 cells were treated for 24 h with Ang II in the absence or presence of 20μM 19-HETE. Thereafter, total RNA was isolated using TRIzol reagent, and the mRNA level of β-MHC/α-MHC (A) and brain natriuretic peptide (B) was quantified using real-time PCR and normalized to β-actin. The results are presented as ± S.E.M. (n = 6). *P < 0.05 compared to control #P <0.05 compared to Ang II alone.

3.2 Effect of INH on CYP-mediated metabolism

3.2.1 Effect of INH on the cardiac levels of CYP-derived AA metabolites

The ability of INH to increase the formation of 19-HETE needs to be validated. INH is known to induce CYP2E1 expression in the liver, and CYP2E1 catalyzes the formation of 19-HETE. However, no information is available regarding the effect of INH on 19-HETE levels in the heart. Therefore, we treated SD rats with INH (200 mg/kg/day) for 14 days, and then AA-derived metabolites in heart tissue were extracted and measured in control and INH-treated SD rats. The levels of several CYP-derived AA metabolites in heart tissue were found to be significantly increased by INH. After 2-week INH treatment, the cardiac level of 19-HETE was significantly increased by 2043% in the INH group in comparison to controls. Whereas there was a 98% decrease in the cardiac level of 20-HETE compared with the control group (Fig. 3.3.A). Also, there was a significant decrease in the cardiac levels of 11,12-and 14,15- EETs by 69% and 71%, respectively, in the INH group compared with the control group 5,6- and 8,9-EET levels were not significantly altered by INH treatment (Fig. 3.3.B). Interestingly, the cardiac level of AA was significantly decreased by 51% in the INH group compared with the control group (Fig. 3.4).

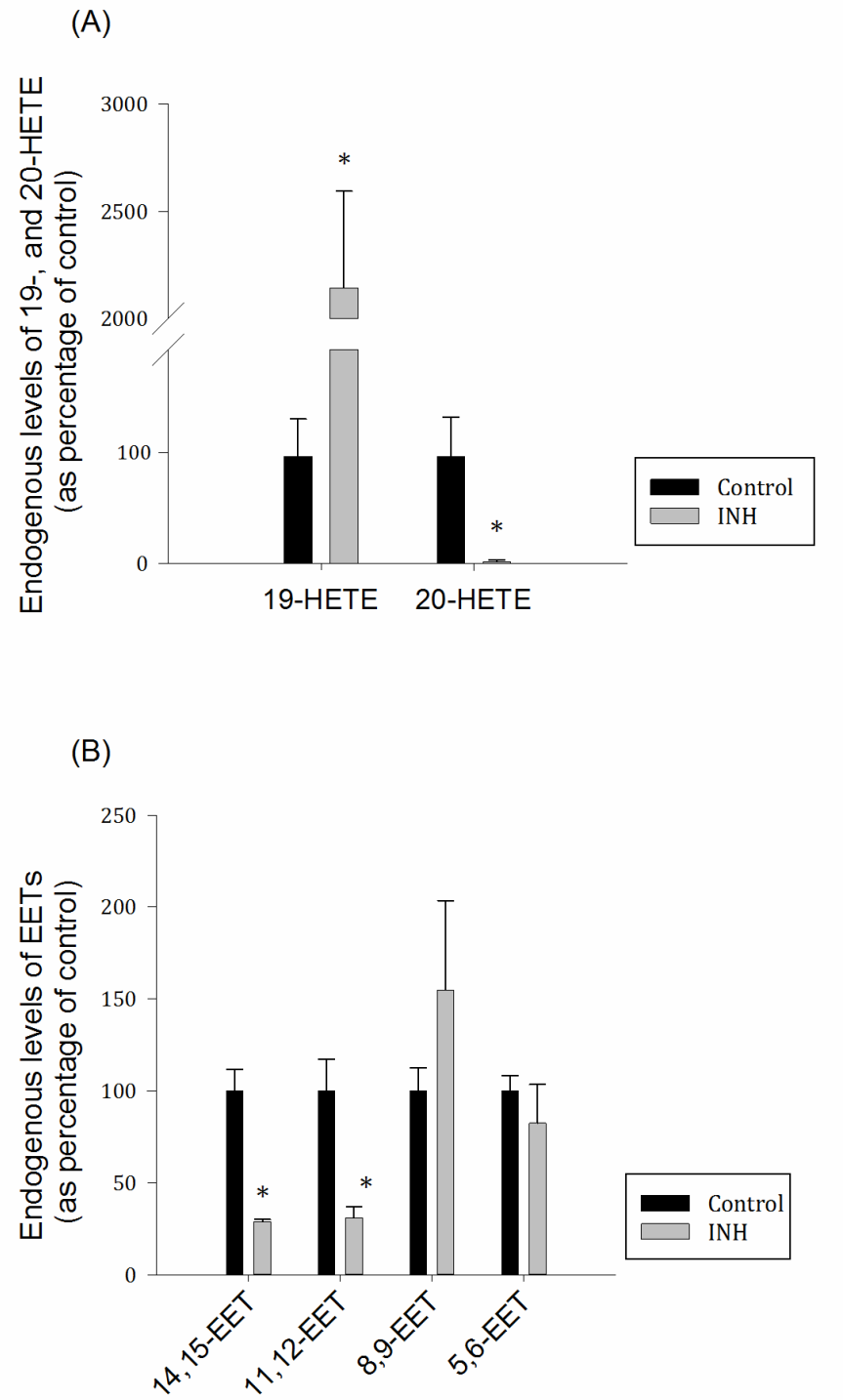

Figure 3.3 Effect of INH on cardiac AA metabolite levels.

Sprague-Dawley rats were injected daily with INH (200 mg/kg/day i.p) dissolved in saline for 14 days, and 6 weight matched controls received the same volume of saline. Heart tissue (350 mg) was homogenized on ice with 350 uL of methanol containing internal standards. The homogenates were centrifuged at 10 000 g for 30 min at 0℃. AA metabolites were extracted from the resultant supernatant by solid-phase cartridges (Oasis1HLB). Samples were evaporated to dryness then reconstituted. (A) 19-, 20-HETE and (B) EETs were measured using LC–ESI-MS. The results are presented as the means of six independent experiments ± S.E.M. (n = 6). *P < 0.05 compared to control.

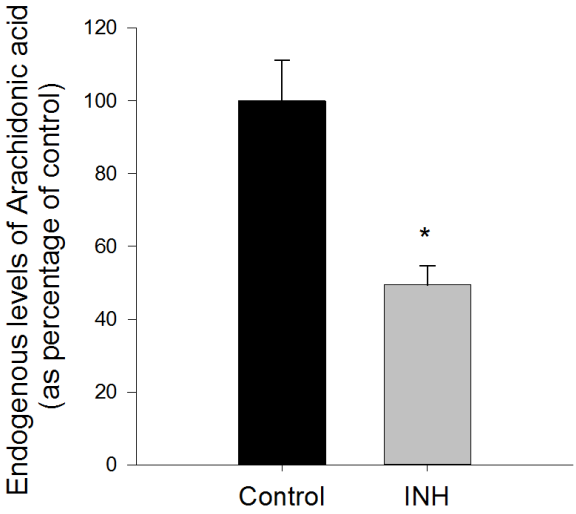

Figure 3.4 Effect of INH on Cardiac AA Levels.

Sprague-Dawley rats were injected daily with INH (200 mg/kg/day i.p) dissolved in saline for 14 days, and 6 weight matched controls received the same volume of saline. Heart tissue (350 mg) was homogenized on ice with 350 uL of methanol containing internal standards. The homogenates were centrifuged at 10 000 g for 30 min at 0℃. AA metabolites were extracted from the resultant supernatant by solid-phase cartridges (Oasis1HLB). Samples were evaporated to dryness then reconstituted. AA was measured using LC–ESI-MS. The results are presented as the means of six independent experiments ± S.E.M. (n = 6). *P < 0.05 compared to control.

3.2.2 Effect of INH on the gene and protein expression of CYP2E1 in the liver and heart.

In order to confirm the effect of INH on CYP2E1 expression in the liver, INH was given at 200 mg/kg/day for 14 days. We found that it was able to induce the expression of CYP2E1 in liver by an extent comparable to what has been previously published. CYP2E1 gene and protein expression in liver was significantly higher in the INH group by 110% and 101.3%, respectively, compared with control group (Fig 3.5.A and B).

Although CYP2E1 expression has been previously investigated in the liver and kidney, it has never been studied in the heart. Interestingly, cardiac CYP2E1 gene was not significantly altered by INH treatment, while CYP2E1 protein expression was significantly reduced by 42.5% in the INH group compared with the control group, in contrast to hepatic CYP2E1 (Fig 3.6. A and B).

3.2.3 Effect of isoniazid on the changes of gene expression of CYPs in the heart.

To study the effect of INH on the expression of CYPs, INH was given at 200 mg/kg/day for 14 days. Thereafter, the mRNA expression of different CYPs was analyzed using real-time PCR. The expression of CYP1A1, CYP2B1, CYP2C11, CYP2J3, CYP4A3 or CYP4F5 did not show any significant alteration by INH treatment (Fig 3.7).

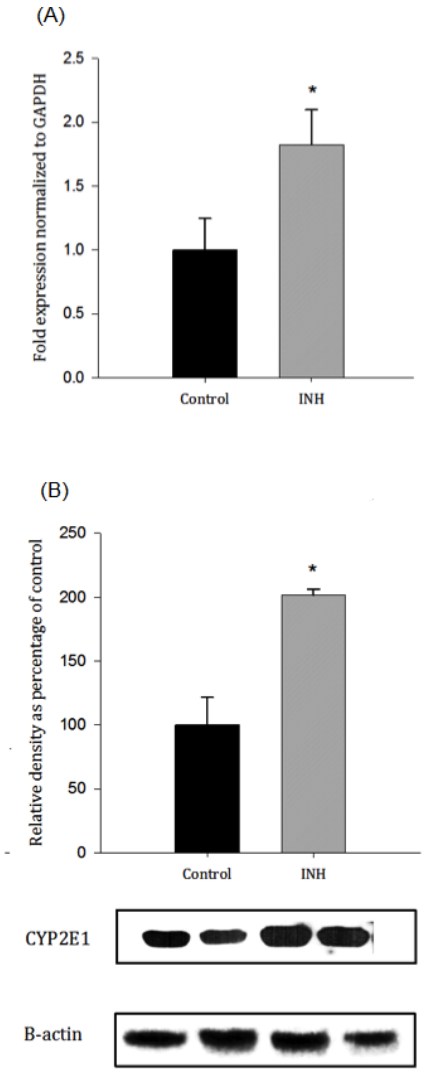

Figure 3.5 Effect of INH on Hepatic CYP2E1 Expression.

CYP2E1 mRNA expression in the liver (A); CYP2E1 protein expression in the liver (B). Sprague-Dawley rats were injected daily with INH (200 mg/kg/day i.p) for 14 days, and 6 weight matched controls received the same volume of saline. Total RNA was isolated from the liver of both control and INH-treated rats and the relative gene expression of CYP was determined by real-time PCR. Duplicate reactions were performed for each experiment, and the results are presented as the means of six independent experiments ± S.E.M. (n = 6). *P < 0.05 compared to control. Hepatic microsomal protein was isolated from both control and INH-treated rats. Thereafter, protein was separated by gel electrophoresis and detected using the enhanced chemiluminescence method. The graph represents the relative amount of protein normalized to β-actin signals (mean ± SEM, n = 4), and the results are expressed as percentage of the control values taken as 100%. *P <0.05 compared to control. Duplicate reactions were performed for each experiment, and the results are presented as the means of six independent experiments ± S.E.M. (n = 6). *P < 0.05 compared to control.

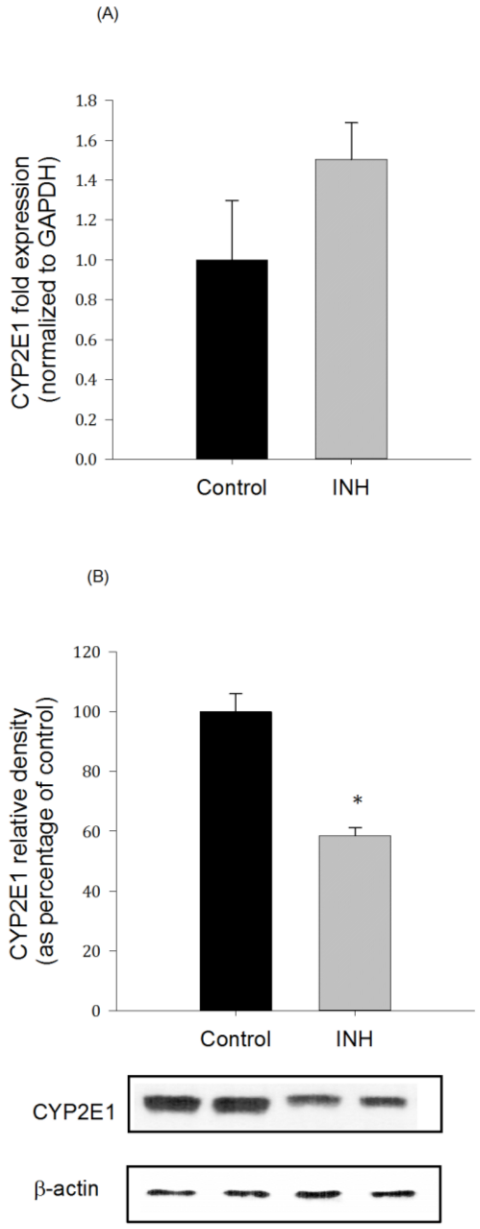

Figure 3.6 Effect of INH on Cardiac CYP Expression.

CYP2E1 mRNA expression in the heart (A); CYP2E1 protein expression in the heart (B). Sprague-Dawley rats were injected daily with INH (200 mg/kg/day i.p) for 14 days, and 6 weight matched controls received the same volume of saline. Total RNA was isolated from the heart of both control and INH-treated rats and the relative gene expression of CYP was determined by real-time PCR. Duplicate reactions were performed for each experiment, and the results are presented as the means of six independent experiments ± S.E.M. (n = 6). *P < 0.05 compared to control. Cardiac microsomal protein was isolated from both control and INH-treated rats. Thereafter, protein was separated by gel electrophoresis. CYP2E1 protein was detected using the enhanced chemiluminescence method. The graph represents the relative amount of protein normalized to β-actin signals (mean ± SEM, n = 4), and the results are expressed as percentage of the control values taken as 100%. *P <0.05 compared to control. Duplicate reactions were performed for each experiment, and the results are presented as the means of six independent experiments ± S.E.M. (n = 6). *P < 0.05 compared to control.

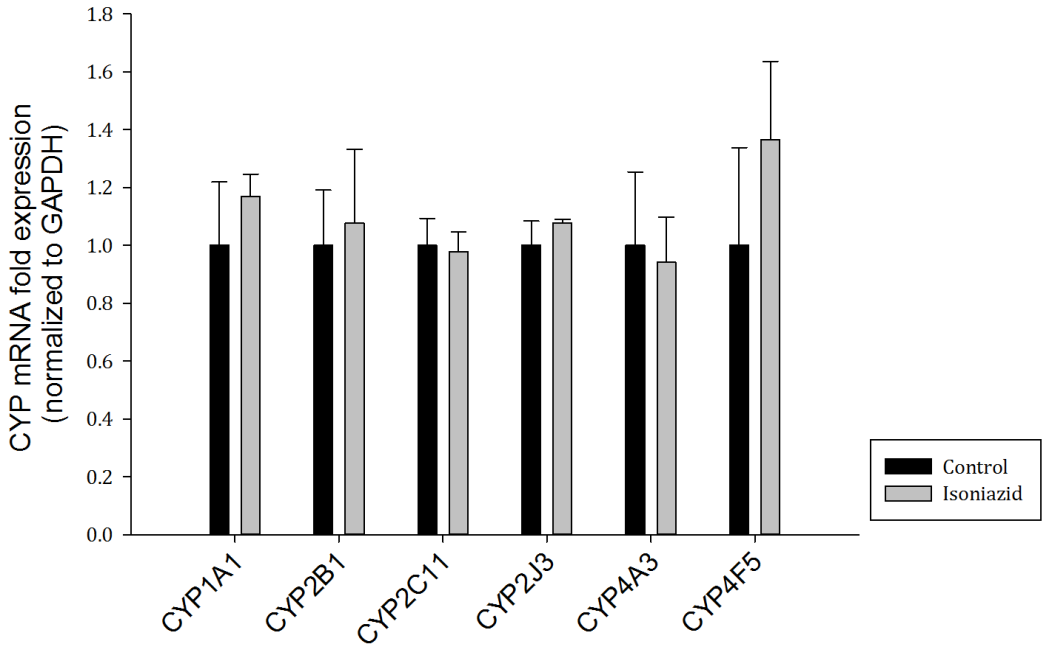

Figure 3.7 Effect of INH on Cardiac CYP mRNA Expression.

Sprague-Dawley rats were injected daily with INH (200 mg/kg/day i.p) dissolved in saline for 14 days, and 6 weight-matched controls received the same volume of saline. Total RNA was isolated from the heart of both control and INH-treated rats and the relative gene expression of CYP1A1, CYP2B1, CYP2C11, CYP2J3, CYP4A3 and CYP4F5 was determined by real-time PCR. Duplicate reactions were performed for each experiment, and the results are presented as the means of six independent experiments ± S.E.M. (n = 6). *P < 0.05 compared to control.

3.2.4 Effect of INH on the CYP-mediated AA metabolites in the heart

With respect to INH-dependent alteration in CYP activity in the heart, we measured the formation rate of CYP-derived AA metabolites mediated by heart microsomes. It has been reported that INH, besides its effect on CYP expression, exhibits direct inhibitory effects on CYP-mediated reactions. Therefore, two experiments were conducted; First, AA incubation was conducted using microsomes isolated from INH-treated and control SD rats to determine the effect of INH-dependent modulation of CYP expression on CYP-mediated AA metabolism. Second, INH was added to AA-microsome incubation mixtures to assess the effect of the direct inhibitory effect of INH on CYP-mediated AA metabolism.

In the liver, INH-dependent induction of hepatic CYP2E1 resulted in a corresponding increase in 19-HETE formation rate and a decrease in 20-HETE formation rate. On the other hand, heart microsomes separated from INH-treated rats showed a significant increase in the formation rate of 11,12- and 14,15-EET by 19% and 22% respectively (Fig. 3.8.A). In line with the aforementioned CYP expression results, 19-HETE was not significantly altered compared with the control group (Fig. 3.8.B). Noteworthy, the measurements of formation rates in this case only correlated with the alterations in expression levels of CYP in the heart. On the other hand, the direct addition of INH to heart microsomes separated from control rats caused diverse alterations in CYP-mediated AA metabolism in which there was a decrease in formation rate of EETs by 17%, 13%, 6.4% and 11% for 5,6-. 8,9-, 11,12- and 14,15-EET, respectively (Fig. 3.9.A). However, there was a significant increase in 19-HETE formation rate by 19%, and a significant decrease in 20-HETE by 58% by heart microsomes with the addition of INH (Fig 3.9.B).

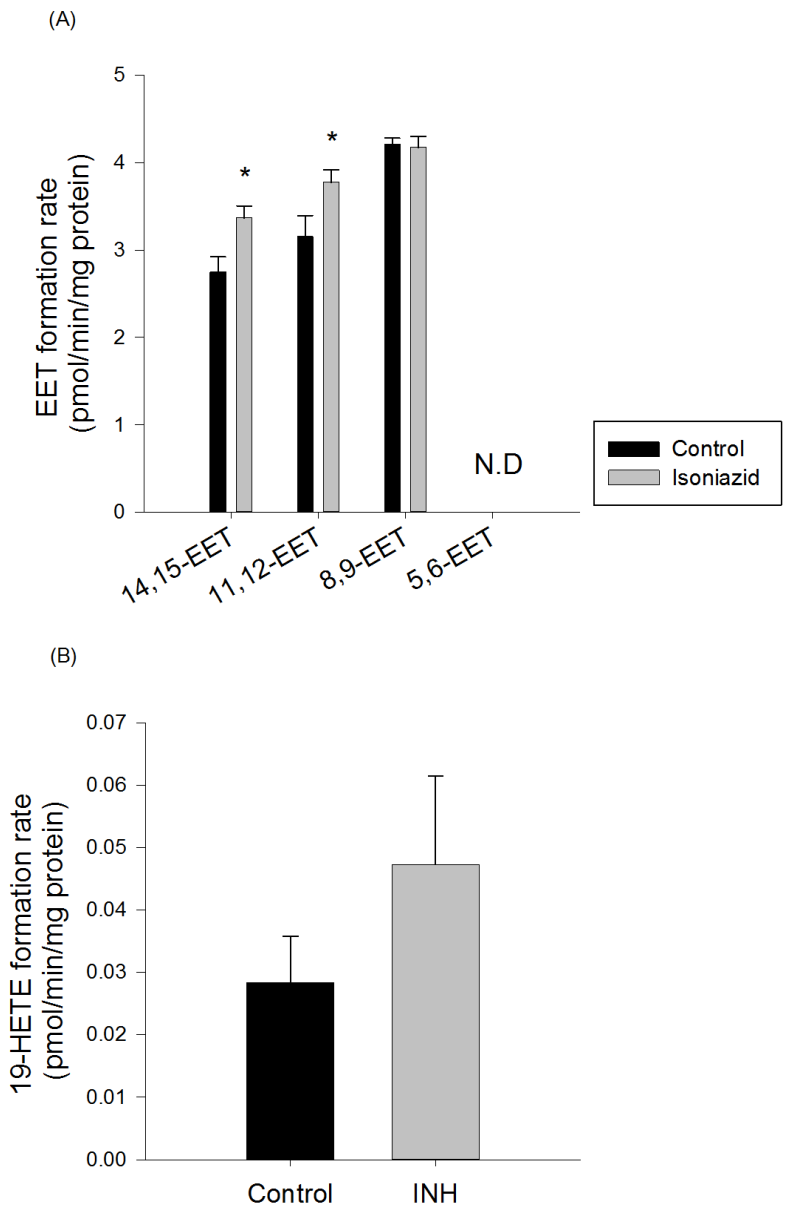

Figure 3.8 Effect of INH on P450-Mediated Arachidonic Acid Metabolism.

Sprague-Dawley rats were injected daily with INH (200 mg/kg/day i.p) dissolved in saline for 14 days, and 6 weight-matched controls received the same volume of saline. Heart microsomes of control and INH treated rats were incubated with 50µM AA. The reaction was started by the addition of 1 mM NADPH and lasted for 30 min. The reaction was terminated by the addition of ice-cold acetonitrile. (A) EETs, and (B) 19-HETE were extracted twice by 1 ml of ethyl acetate and dried using speed vacuum. Reconstituted metabolites were injected into LC-ESI-MS for metabolite determination. Duplicate reactions were performed for each experiment, and the results are presented as the means of six independent experiments ± S.E.M. (n = 6). *P < 0.05 compared to control.

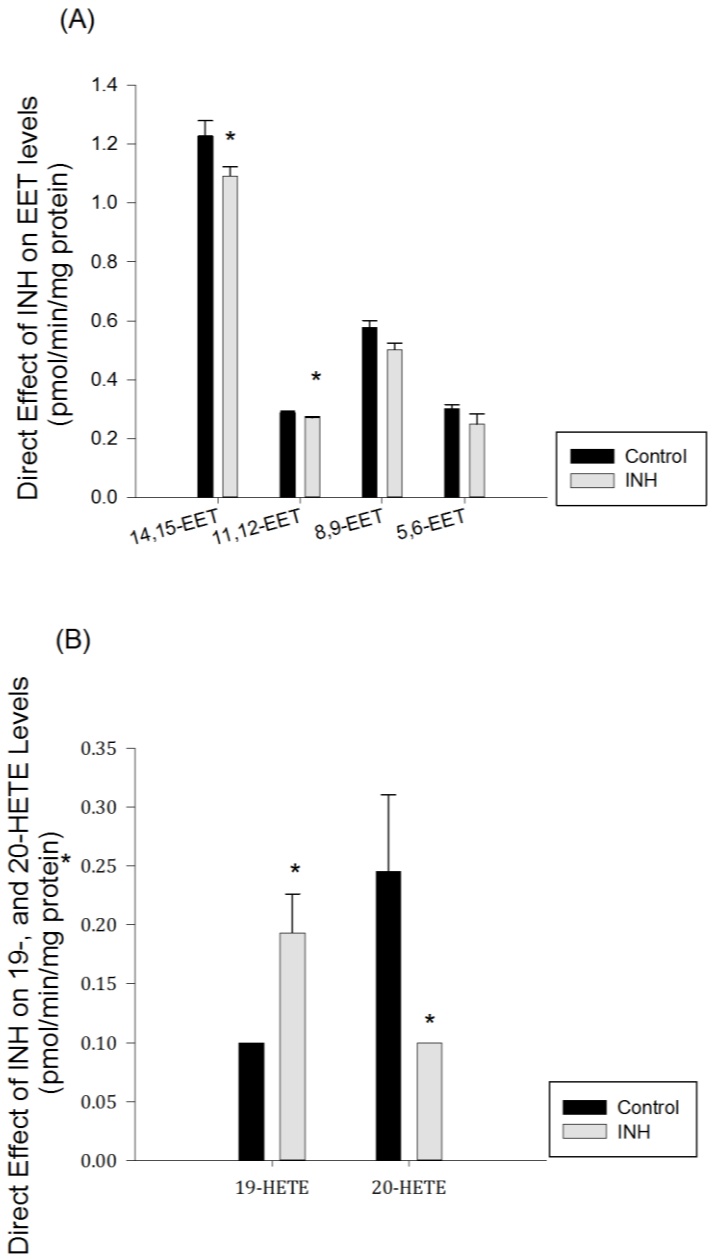

Figure 3.9 Effect of the direct addition of INH to heart microsomes on levels of CYP-derived AA metabolites.

100µg protein of heart microsomes separated from control rats were incubated with 0 and 50 µM of INH for 10 min on ice (all samples contained a fixed concentration of 0.1% dimethylsulfoxide). AA (50 µM) was added, and the reaction was initiated by the addition of NADPH and terminated by the addition of acetonitrile as described above. The incubation mixtures were double extracted with 1 ml ethyl acetate; thereafter the organic extracts were combined, evaporated and (A) EETs, and (B) 19-, 20-HETE were extracted twice by 1 ml of ethyl acetate and dried using speed vacuum. Reconstituted metabolites were injected into LC-ESI-MS for metabolite determination. Duplicate reactions were performed for each experiment, and the results are presented as the means of three independent experiments ± S.E.M. (n = 3). *P < 0.05 compared to control.

3.3 Effect of INH on Ang II-induced cardiac hypertrophy in SD rats

3.3.1 Isoniazid protects against Ang II-induced cardiac hypertrophy

To investigate the cardioprotective effect of INH during Ang II induced cardiac hypertrophy, Sprague-Dawley rats were injected with saline, Ang II (450 ng/kg/minute via miniosmotic pump) or INH (200 mg/kg/day i.p) plus Ang II (450 ng/kg/minute via miniosmotic pump) for 14 days. After 14 days of treatment, rats were weighed and mildly anaesthetized using isoflurane. Echocardiographic parameters were measured; thereafter the heart weight to tibia length was measured upon sacrifice.

Looking into the echocardiographic changes inflicted by Ang II infusion, with respect to echocardiographic parameters, ejection fraction (EF) was not altered (Fig 3.10.A). However, Ang II did induce a significant decrease in left ventricular internal dimension during systole (LVIDs) by 33%, compared with control group (Fig 3.10.B). On the other hand, Ang II induced a significant increase in left ventricular posterior wall thickness during systole (LVPWs) and diastole (LVPWd) by 30% and 31% respectively, as well as interventricular septal thickness at end diastole (IVSd) by 28.8%, compared with control group (Fig 3.10.C,D,E). Ang II treatment did not alter interventricular septal thickness at end systole (IVSs) (Fig 3.10.F).

The concurrent treatment of INH completely restored the Ang II-mediated alterations in these echocardiographic parameters, as compared with control and Ang II groups (Fig 3.10).

Heart weight to tibia length ratio was significantly higher in the Ang II group by 29% compared with the control group. The concurrent treatment of INH completely restored the Ang II-mediated increase in the heart weight to tibia length ratio (Fig. 3.11).

3.3.2 Effect of INH on Blood Pressure

Ang II is known to induce cardiac hypertrophy through a direct hypertrophic effect and by increasing blood pressure. In order to confirm that the observed protective effect of INH was not due to an INH-mediated effect on blood pressure, blood pressure of the animals was measured during different treatments. It was found that blood pressure in Ang II group was significantly higher by 40.7% compared with control group. The concurrent treatment of INH did not significantly affect blood pressure in the Ang II group, which gives an indication that the mechanism by which INH causes a protective cardiac effect is not through means of blood pressure (Fig 3.12).

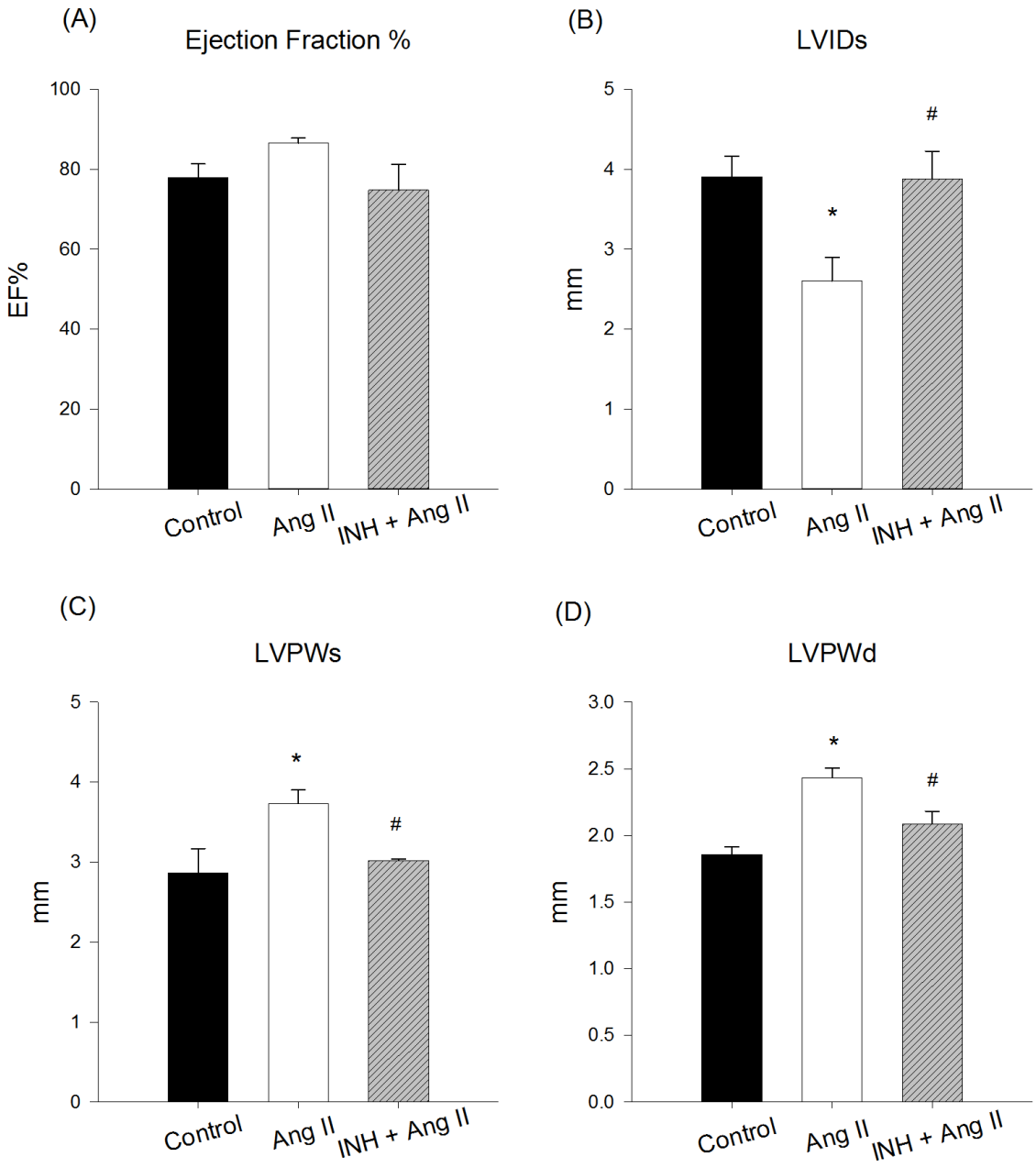
(A)
Ejection Fraction %
EF%
100
80
60
40
20
0
Control
Ang II
INH + Ang II
(B)
LVIDs
mm
5
4
3
2
1
0
*
#
Control
Ang II
INH + Ang II
(C)
LVPWs
mm
5
4
3
2
1
0
*
#
Control
Ang II
INH + Ang II
(D)
LVPWd
mm
3.0
2.5
2.0
1.5
1.0
0.5
0.0
*
#
Control
Ang II
INH + Ang II

Continued,

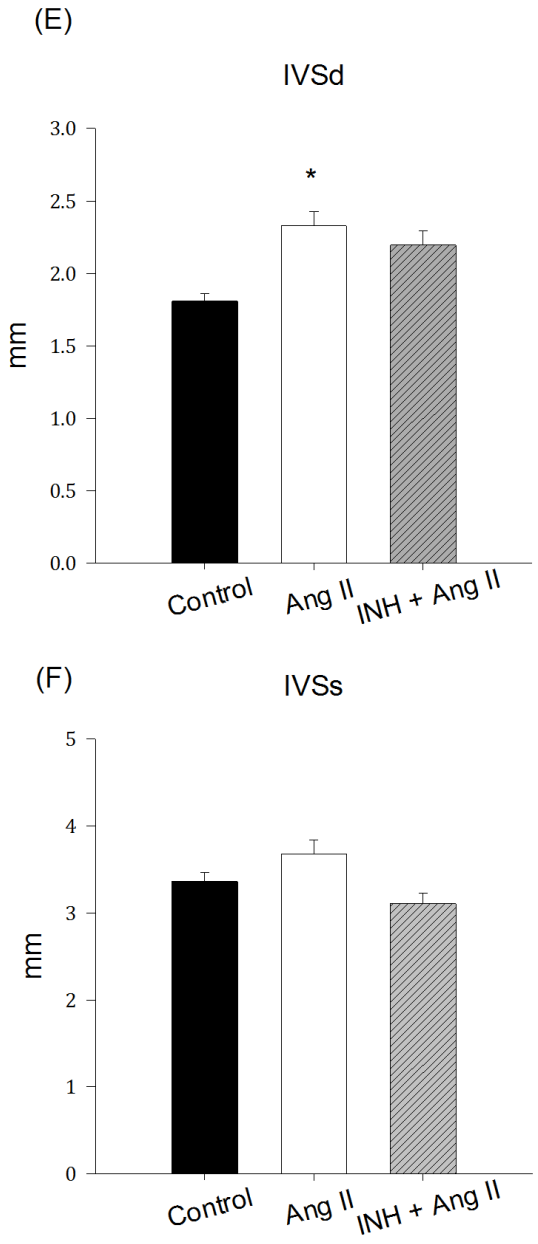

Figure 3.10 Assessment of cardiac hypertrophy through echocardiography.
Sprague-Dawley rats were administered saline, Ang II (450 ng/kg/minute via miniosmotic pump) or INH (200 mg/kg/day i.p) plus Ang II (450 ng/kg/minute via miniosmotic pump) for 14 days. After 14 days of treatment, rats were weighed and mildly anesthetized for echocardiography to measure heart dimension parameters (A) Ejection Fraction (B) Left ventricular internal dimension during systole (C) Left ventricular posterior wall thickness during systole and during diastole (D), (E) Interventricular septal thickness at end diastole and at end systole (F). Results are presented as mean ± S.E.M. *p< 0.05 compared with control. #p < 0.05 compared with Ang II.

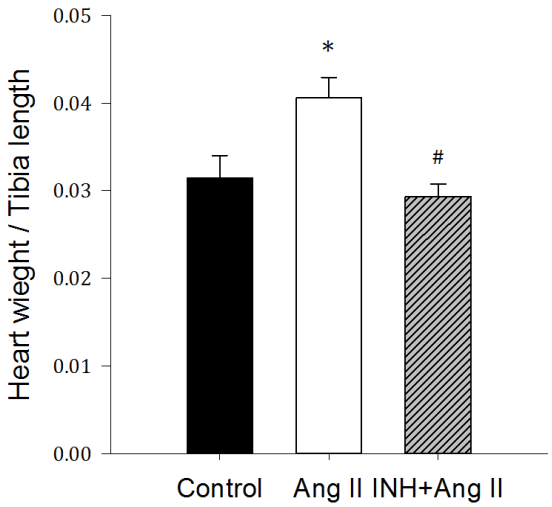

Figure 3.11 Effect of INH on Ang II-induced heart weight to tibia length ratio.

Sprague-Dawley rats were administered saline, Ang II (450 ng/kg/minute via miniosmotic pump) or INH (200 mg/ kg/ day, i.p) plus Ang II (450 ng/ kg/ minute via miniosmotic pump) for 14 days. Heart weight to tibia ratio was determined for each animal after 14 days of treatment.

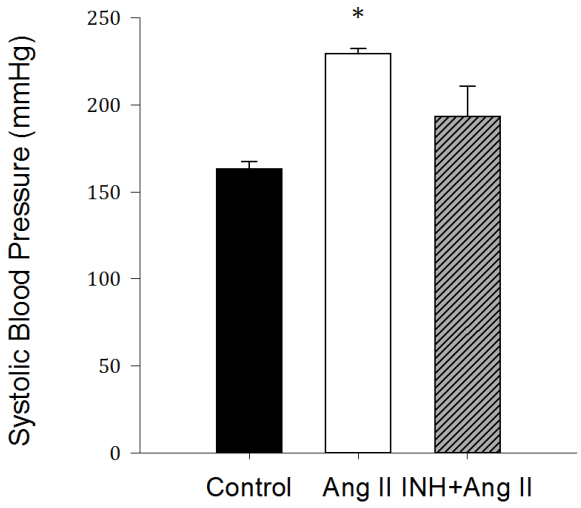

Figure 3.12 Effect of INH on Blood Pressure.

Sprague-Dawley rats were administered saline, Ang II (450 ng/kg/minute via miniosmotic pump) or INH (200 mg/kg/day i.p) plus Ang II (450 ng/kg/minute via miniosmotic pump) for 14 days. Systolic blood pressure (SBP) was measured by tail cuff after 14 days of treatment. The results are presented as the means of six independent experiments ± S.E.M. (n = 6). *P < 0.05 compared to control. #P< 0.05 compared with Ang II.

3.3.3 INH modulates the Ang II-induced alterations in cardiac levels of CYP-derived AA metabolites

The alterations observed in CYP-mediated AA metabolism during Ang II-induced cardiac hypertrophy were prevented by the co-treatment with INH, confirming the protective effect of INH. During Ang II-induced cardiac hypertrophy, there were significant alterations in CYP-mediated AA metabolism in the heart. In the Ang II group, the cardiac levels of 8,9-, 11,12- and 14,15-EETs were significantly decreased by 34%, 45% and 47% respectively, compared with the control group; however, there was no alteration in 5,6-EETs (Fig 3.13.A). Moreover, there was an increase in the cardiac level of 20-HETE in the group receiving Ang II by 819% in comparison to control, but the cardiac level of 19-HETE did not alter significantly compared with the control group (Fig. 3.13.B). In addition, there was an increase in the cardiac levels of AA in the Ang II group by 31.4% compared with the control group (Fig. 3.14).

The co-treatment with INH prevented the observed alterations in AA metabolism during Ang II-induced cardiac hypertrophy. In the group receiving both INH and Ang II, INH led to a significant decrease in the cardiac levels of 5,6- and 14,15-EET by 81% and 33%, respectively in comparison to the group treated with Ang II alone whereas it did not affect the cardiac levels of other EETs compared with Ang II group (Fig.3.13.A). On the other hand, INH significantly increased the cardiac levels of 19-HETE by 1025% compared with the Ang II group (Fig. 3.13.B). Furthermore, INH significantly reduced the significant increase in the cardiac levels of 20-HETE (Figure 3.13 B) and AA (Figure 3.14) induced by Ang II.

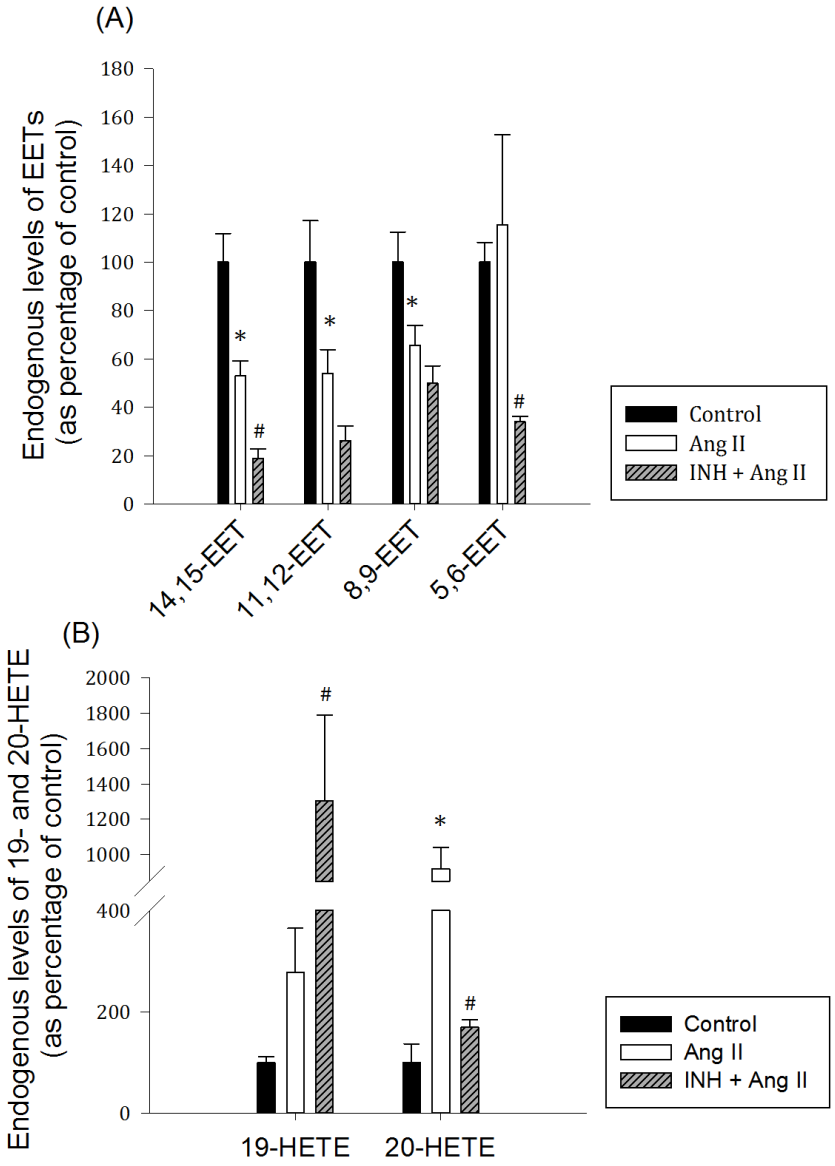

Figure 3.13 Effect of INH on Cardiac CYP-derived AA Metabolite Levels.

Sprague-Dawley rats were administered saline, Ang II (450 ng/kg/minute via miniosmotic pump) or INH (200 mg/ kg/day, i.p) plus Ang II (450 ng/kg/minute via miniosmotic pump) for 14 days. Heart tissue (350 mg) was homogenized on ice with 350 uL of methanol containing internal standards. The homogenates were centrifuged at 10 000 g for 30 min at 0℃. AA metabolites were extracted from the resultant supernatant by solid-phase cartridges (Oasis1HLB). Samples were evaporated to dryness then reconstituted. EETs (A), 19-, 20-HETE and (B) were measured using LC–ESI-MS. The results are presented as the means of six independent experiments ± S.E.M. (n = 6). *P < 0.05 compared to control. #P< 0.05 compared with Ang II.

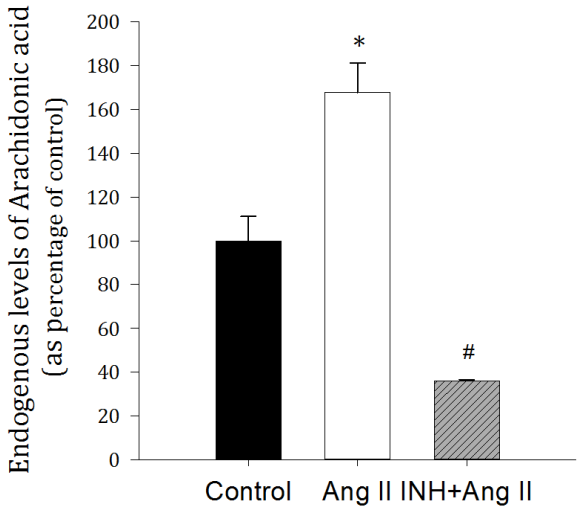

Figure 3.14 Effect of INH on Cardiac CYP-derived AA Metabolites Levels.

Sprague-Dawley rats were administered saline, Ang II (450 ng/kg/minute via miniosmotic pump) or INH (200 mg/ kg/day, i.p) plus Ang II (450 ng/kg/minute via miniosmotic pump) for 14 days. Heart tissue (350 mg) was homogenized on ice with 350 uL of methanol containing internal standards. The homogenates were centrifuged at 10 000 g for 30 min at 0℃. AA metabolites were extracted from the resultant supernatant by solid-phase cartridges (Oasis1HLB). Samples were evaporated to dryness then reconstituted. AA was measured using LC–ESI-MS. The results are presented as the means of six independent experiments ± S.E.M. (n = 6). *P < 0.05 compared to control. #P< 0.05 compared with Ang II.

3.4 Effect of TMS on Ang II-induced cellular hypertrophy in RL-14 cells:

3.4.1 Effect of Ang II on CYP1B1 mRNA and protein expression in the heart *in vivo*.

Ang II-induced alterations in CYP1B1 expression in the heart were investigated. Ang II was administered for 2 weeks via a mini-osmotic pump; thereafter the level of mRNA and protein expression of CYP1B1 was measured. Ang II did not affect the levels of mRNA (Fig. 3.15.A) while it caused a significant rise in the level of CYP1B1 protein expression by 100% (Fig. 3.15.B).

3.4.2 Effect of TMS on Ang II-induced cardiac hypertrophy

The effect of TMS on Ang II-induced cardiac hypertrophy in rats was assessed by heart weight to tibia length ratio and echocardiography. Ang II was administered for 14 days either alone or in combination with TMS. TMS was found to reverse the change in echocardiographic parameters caused by Ang II treatment. Heart weight to tibia length ratio was significantly increased in the Ang II group by 29% compared with the control group (Fig 3.16). The concurrent treatment with TMS completely restored the Ang II-mediated increase in the heart weight to tibia length ratio.

In agreement with the characteristic changes that accompany concentric cardiac hypertrophy we found that Ang II did not alter the ejection fraction (EF) (Fig 3.17.A), while it caused a significant increase in the heart wall thickness represented by the left ventricular posterior wall thickness during systole (LVPWs) and during diastole (LVPWd) which increased by 30% and

31% respectively in comparison to controls while TMS was able to reverse this apparent increase (Fig. 3.17.B and C). In addition, concentric hypertrophy was accompanied by a decrease in the internal diameter of the ventricles that was apparent in our results, as Ang II induced a significant decrease in left ventricular internal dimension during both systole (LVIDs) and diastole (LVIDd) by 33% and 24% respectively, compared with the control group (Fig. 3.17. D and E). Regarding interventricular septal thickness, TMS caused a significant increase in interventricular septal thickness at end diastole (IVSd) which increased by 28% in comparison to control (Fig. 3.17 F). However, it did not alter interventricular septal thickness at end systole (IVSs) (Fig. 3.17.G). Again, the concurrent treatment with TMS restored the Ang II-mediated alterations in these echocardiographic parameters, as compared with control and Ang II groups (Fig. 3.17).

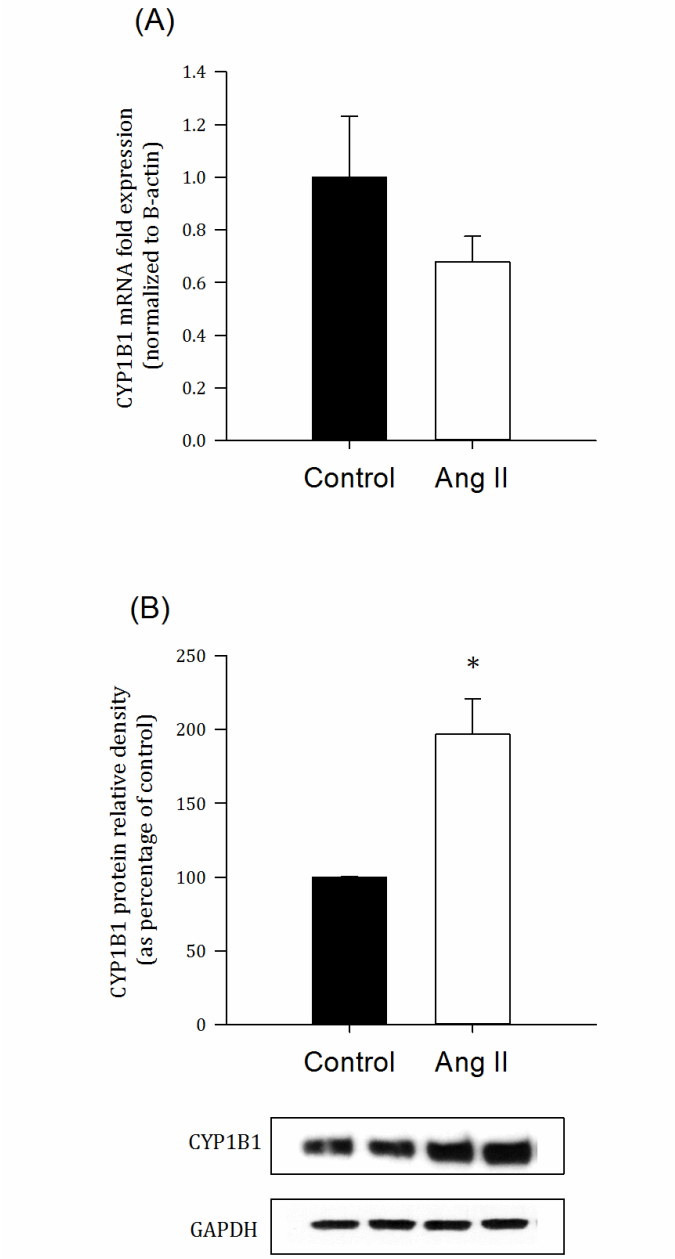

Figure 3.15 Effect of Ang II on CYP1B1 Expression.

CYP1B1 gene expression in the heart (A); CYP1B1 protein expression in the heart (B). Sprague-Dawley rats were administered saline, Ang II (450 ng/kg/minute via miniosmotic pump) for 14 days and 6 weight matched controls received the same volume of saline. Total RNA was isolated from the heart both control and Ang II treated rats and the relative gene expression of CYP was determined by real-time PCR. Duplicate reactions were performed for each experiment, and the results are presented as ± S.E.M. (n = 6). * $p < 0.05$ compared to control. Cardiac microsomal protein was isolated thereafter separated by gel electrophoresis. CYP1B1 protein was detected using the enhanced chemiluminescence method. The graph represents the relative amount of protein normalized to GAPDH signals (mean ± SEM, n = 4), and the results are expressed as percentage of the control values taken as 100%. * $p < 0.05$ compared to control.

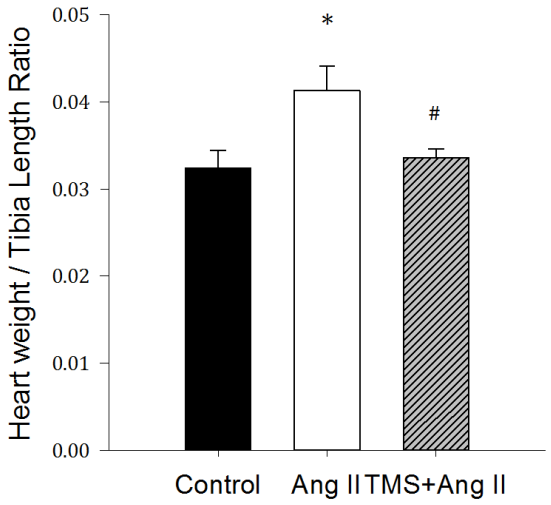

Figure 3.16 Effect of TMS on Ang II-induced heart weight to tibia length ratio.

Sprague-Dawley rats were administered saline, Ang II (450 ng/kg/minute via miniosmotic pump) or TMS (300 µg/kg every 3rd day i.p) plus Ang II (450 ng/kg/minute via miniosmotic pump) for 14 days. Heart weight to tibia ratio was determined for each animal after 14 days of treatment.

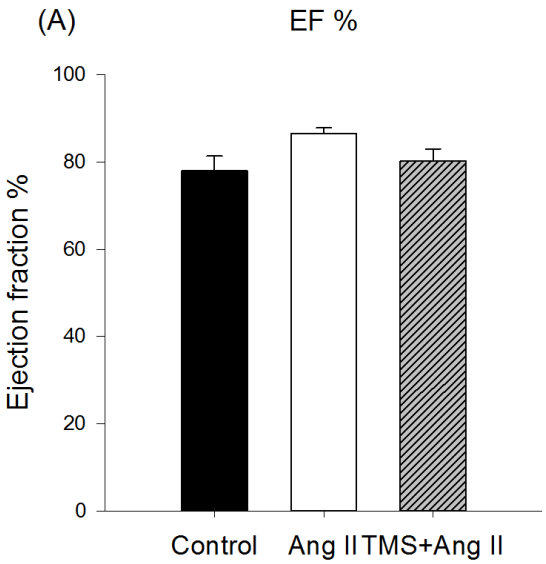
(A)
EF %
Ejection fraction %
100
80
60
40
20
0
Control
Ang II
TMS+Ang II

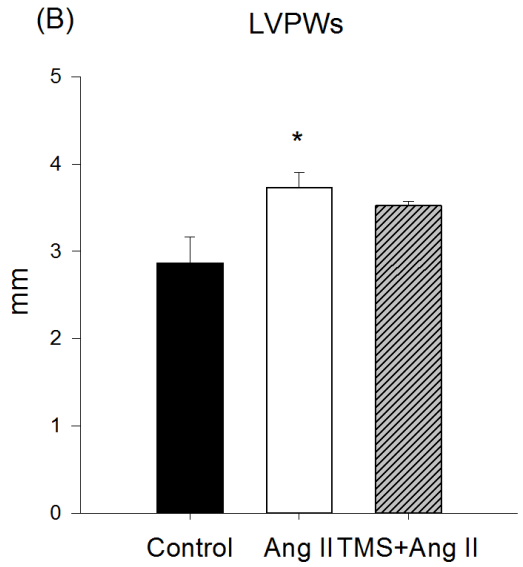
(B)
LVPWs
mm
5
4
3
2
1
0
*
Control
Ang II
TMS+Ang II

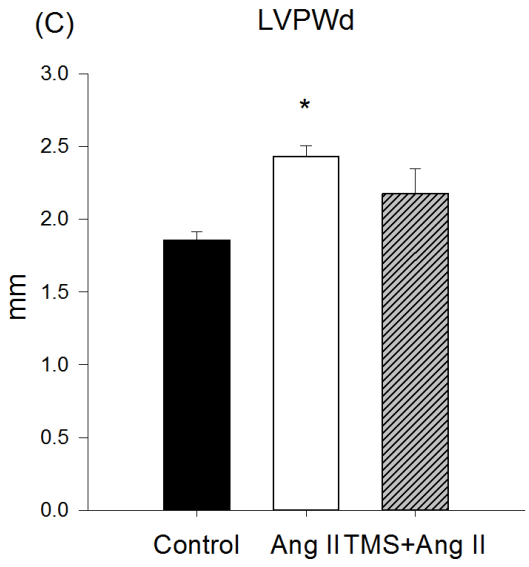
(C)
LVPWd
mm
3.0
2.5
2.0
1.5
1.0
0.5
0.0
*
Control
Ang II
TMS+Ang II

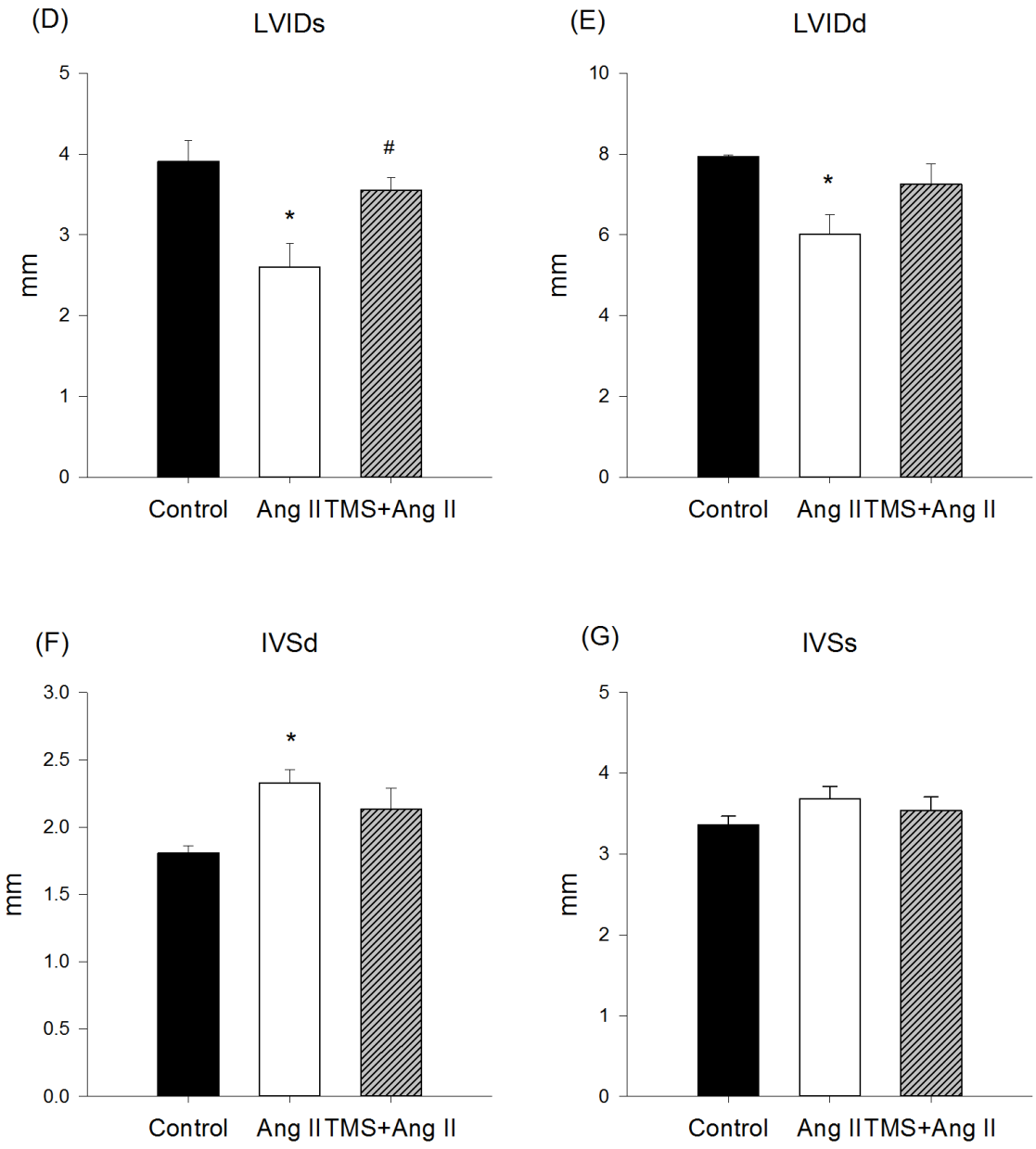

Figure 3.17 Effect of TMS on Ang II-induced cardiac hypertrophy.

Sprague-Dawley rats were administered saline, Ang II (450 ng/kg/minute via miniosmotic pump) or TMS (300 µg/kg every 3rd day i.p) plus Ang II (450 ng/kg/minute via miniosmotic pump) and 6 weight matched controls received the same volume of saline for 14 days. Rats were weighed and mildly anesthetized for echocardiography to measure heart dimensions parameters: ejection fraction (A), left ventricular posterior wall thickness during systole (B) and during diastole (C), interventricular septal thickness at end diastole (D), left ventricular internal dimension during systole (E), and diastole (F) and interventricular septal thickness at end systole (G). The results are presented as the means of six independent experiments ± S.E.M. (n = 6). * $p < 0.05$ compared to control. # $p < 0.05$ compared with Ang II.

3.4.3 Effect of TMS on cardiac levels of Mid-chain HETEs and 20-HETE

To confirm the inhibitory effect of TMS, the level of CYP1B1 metabolites in the heart were measured. SD rats were treated with TMS (300 μg/kg every 3rd day i.p) for 14 days, and then AA-derived AA metabolites in heart tissue were extracted and measured in control, Ang II treated and TMS plus Ang II-treated SD rats (Fig. 3.18).

The cardiac level of 5-, 12- and 15-HETE combined was significantly increased by 50% in the Ang II group in comparison to controls (Fig. 3.18.A) whereas, there was a 62.8% decrease in the group receiving both TMS and Ang II in comparison to the Ang II group (Fig. 3.18.A).

Additionally, the levels of 20-HETE in heart tissue had significantly increased by 819% in the group receiving Ang II alone in comparison to controls. TMS was able to significantly decrease the observed rise in the level of 20-HETE by 389% in comparison to Ang II (Fig. 3.18.B).

Moreover, the cardiac level of AA was significantly increased by 67.7% in the Ang II group in comparison to controls (Fig. 3.19). Whereas, there was a 50.9% decrease in the group receiving TMS alone in comparison to controls and a 93.1% decrease in the group receiving both TMS and Ang II in comparison to the Ang II group (Fig. 3.19).

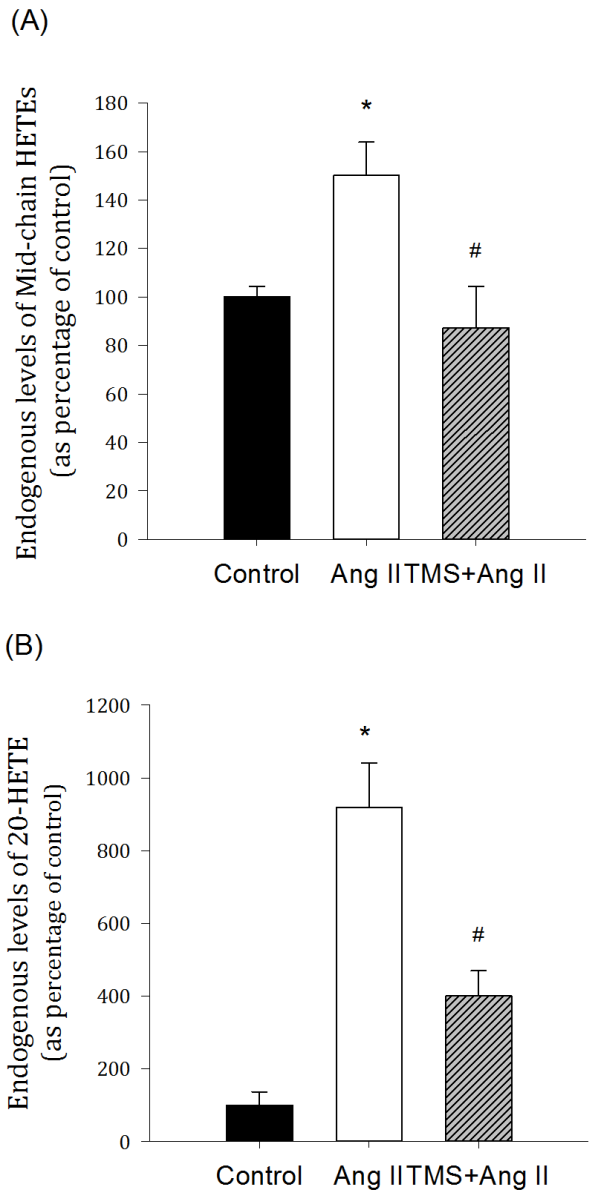

Figure 3.18 Effect of TMS on Cardiac CYP-derived AA Metabolite Levels.

Sprague-Dawley rats were administered saline, Ang II (450 ng/kg/minute via miniosmotic pump) or TMS (300 µg/kg every 3rd day i.p) plus Ang II (450 ng/ kg/minute via miniosmotic pump) and 6 weight matched controls received the same volume of saline for 14 days. Heart tissue (350 mg) was homogenized on ice with 350 uL of methanol containing internal standards, butylated hydroxytoluene and ethylenediaminetetraacetic acid. The homogenates were centrifuged at 10 000 g for 30 min at 0℃. AA metabolites were extracted from the resultant supernatant by solid-phase cartridges (Oasis1HLB). Samples were evaporated to dryness then reconstituted. Mid-chain HETEs (A) and 20-HETE (B) were measured using LC–ESI-MS. The results are presented as the means of six independent experiments ± S.E.M. (n = 6). * $p < 0.05$ compared to control. # $p < 0.05$ compared with Ang II.

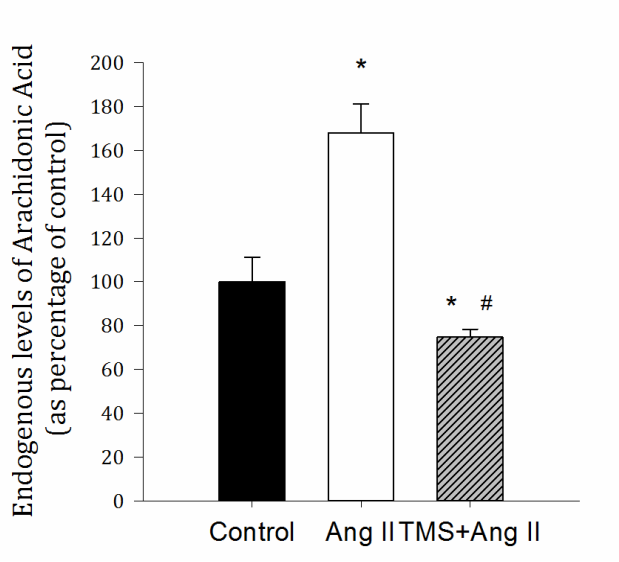

Figure 3.19 Effect of TMS on Cardiac CYP-derived AA Metabolites Levels.

Sprague-Dawley rats were administered saline, Ang II (450 ng/kg/minute via miniosmotic pump) or TMS (300 µg/kg every 3rd day i.p) plus Ang II (450 ng/ kg/minute via miniosmotic pump) and 6 weight matched controls received the same volume of saline for 14 days. Heart tissue (350 mg) was homogenized on ice with 350 uL of methanol containing internal standards, butylated hydroxytoluene and ethylenediaminetetraacetic acid. The homogenates were centrifuged at 10 000 g for 30 min at 0℃. AA metabolites were extracted from the resultant supernatant by solid-phase cartridges (Oasis1HLB). Samples were evaporated to dryness then reconstituted. AA was measured using LC–ESI-MS. The results are presented as the means of six independent experiments ± S.E.M. (n = 6). * $p < 0.05$ compared to control. # $p < 0.05$ compared with Ang II.

3.4.4 Effect of TMS on Ang II-induced cellular hypertrophy in RL-14 cells.

We confirmed the protective effect of TMS on the development of Ang II-induced cardiac hypertrophy in human ventricular cardiomyocytes, RL-14 cells. RL-14 cells were treated for 24 h with Ang II (10 μM), leading to cellular hypertrophy causing a significant increase in β/α-MHC ratio by 163.7% (Fig. 3.20). Pretreatment with TMS was able to protect from Ang II-induced cellular hypertrophy and a reduction in the β/α-MHC ratio was seen. TMS significantly reduced the β/α-MHC ratio, returning it to its normal level.

3.4.5 Effect of TMS on ROS production

Ang II-induced cellular hypertrophy in RL14 cells significantly increased the ROS production in RL14 cells by 41.8% in comparison to control. Concurrent treatment with TMS was able to significantly decrease the ROS production by 40.1% in comparison to Ang II (Fig 3.21).

3.4.6 Effect of TMS and Ang II on MAPK signaling pathway

To ability of TMS to activate MAPK in RL14 cells was examined. RL-14 cells were treated for 8 h with either Ang II (10 μM) alone or in combination with TMS (0.5 μM). The group being treated with Ang II + TMS was pretreated with TMS alone for 24 h. The degree of phosphorylation was then measured. Our results show that Ang II significantly induced ERK1/2 and P38 by 28% and 94.5%, respectively in comparison to controls while TMS significantly inhibited the phosphorylation of ERK1/2 and p38 caused by Ang II by 49.2% and 77.5% respectively. However JNK did not show any significant change either by Ang II nor TMS (Fig 3.22.A).

3.4.7 Effect of TMS and Ang II on NF-κB signaling pathway

The ability of TMS to activate NF-κB was explored. RL-14 cells were treated for 8 h with either Ang II (10 μM) alone or in combination with TMS (0.5 μM). The group being treated with Ang II + TMS was pretreated with TMS alone for 24 h. In the group receiving Ang II alone the DNA binding activity for P65 was significantly increased by 110% in comparison to controls while it did not significantly alter P50 binding activity. However, TMS had the ability to significantly reduce the observed rise in P65 binding activity induced by Ang II treatment by 149% in comparison to Ang II; P50 was not altered (Fig. 3.22.B).

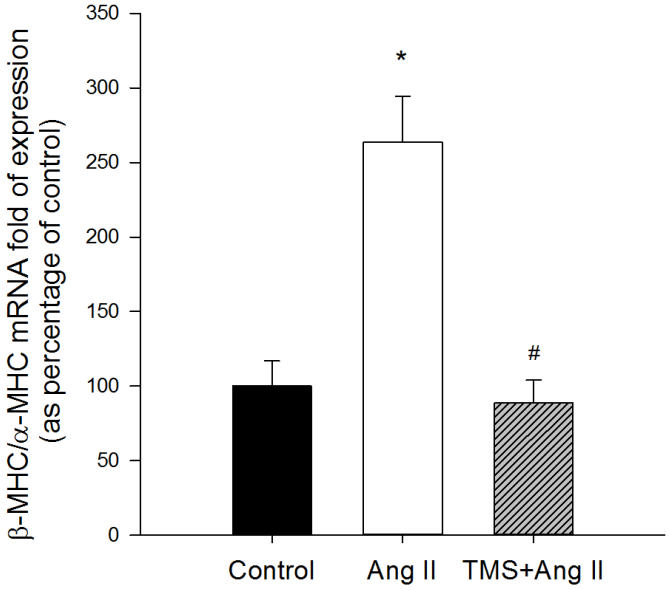

Figure 3.20 The effect of TMS on cardiac hypertrophic markers.

RL-14 cells were treated for 24 h with Ang II in the absence or presence of 0.5 μM TMS. Thereafter, total RNA was isolated using TRIzol reagent, and the mRNA level of β-MHC/α-MHC was quantified using real-time PCR and normalized to β-actin. The results are presented as ± S.E.M. (n = 6). * $p < 0.05$ compared to control # $p < 0.05$ compared to Ang II alone.

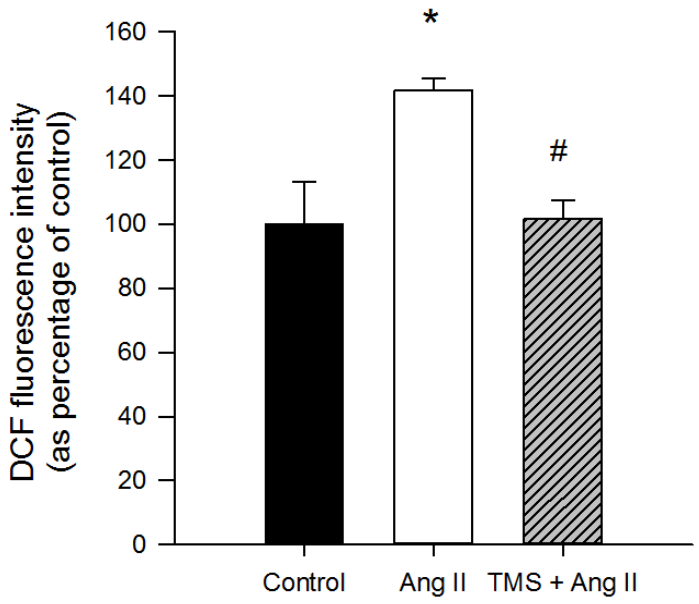

Figure 3.21 The effect of TMS on ROS.

RL-14 cells were treated for 24 h with Ang II in the absence or presence of 0.5 μM TMS. ROS production. The results are presented as ± S.E.M. (n = 6). *$p < 0.05$ compared to control # $p < 0.05$ compared to Ang II alone.

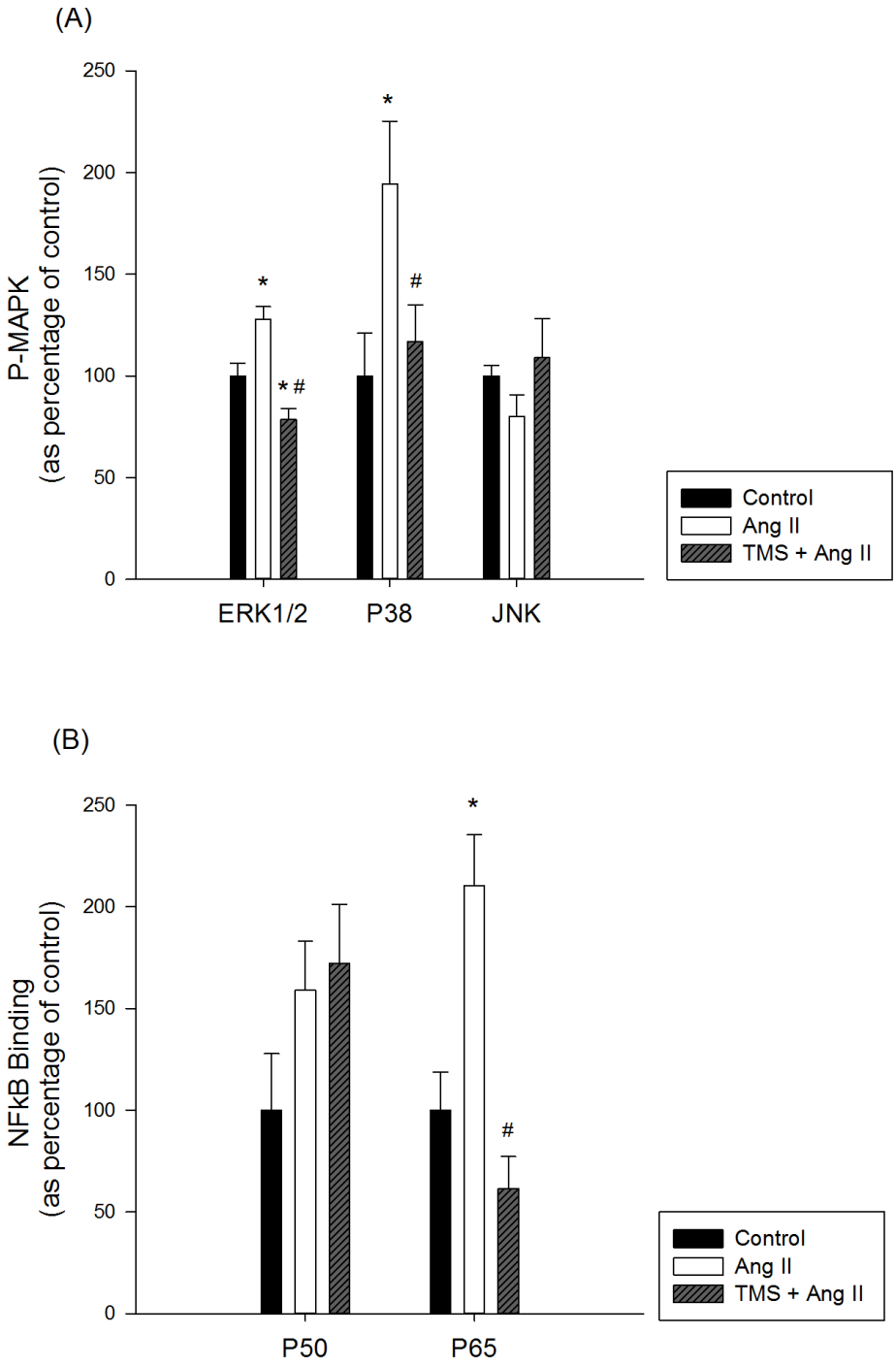

Figure 3.22 The effect of TMS on MAPK and NF-κB.

RL-14 cells were treated for 24 h with Ang II in the absence or presence of 0.5 μM TMS. MAPK protein phosphorylation (A) and NF-κB binding activity were determined (B). The results are presented as ± S.E.M. (n = 6). *p < 0.05 compared to control # p <0.05 compared to Ang II alone.

Chapter 4 : DISCUSSION

4.1. Isoniazid protects against Ang II-induced cardiac hypertrophy

The effect of INH treatment on CYP expression and activity in the hearts of SD rats was investigated. Due to the finding that INH triggered substantial alterations in CYP expression and its associated AA metabolism in the heart, it was important to examine the biological effects of these alterations against one of the most serious risk factors for cardiovascular morbidity and mortality, cardiac hypertrophy.

With regard to INH-induced alteration in CYP expression, we showed, for the first time, that CYP2E1 expression in the heart was down-regulated by INH (Figure 3.6). Conversely, in the liver, INH is a well-known CYP2E1 inducer, and this is consistent with our results of the induction of hepatic CYP2E1 (Poloyac et al., 2004). This completely opposite effect of INH on cardiac CYP2E1 underscores the unsuitability of hepatic data, of known CYP modulators, for making conclusions on their effects on cardiac CYP expression. In agreement with our results, several reports have showed that the same chemical agent may have organ-specific effects on CYP expression (Zordoky et al., 2008, Anwar-mohamed et al., 2010, Anwar-Mohamed et al., 2013, Poloyac et al., 2004). Interestingly, the effect of INH treatment was confined to CYP2E1, i.e. the expression of other cardiac CYPs was not affected (Figure 3.7). The regulation of CYP2E1 expression is unique among other CYPs for its complexity; it includes transcriptional, posttranscriptional, translational, posttranslational and epigenetic regulatory mechanisms. CYP2E1 induction is complicated and differs according to the inducing agent. The induction of CYP2E1 in rats rendered diabetic by the use of Streptozotocin was found to be through the stabilization of the mRNA and protein and not through enhanced transcription (Song et al., 1987) while acetone and pyrazole induced CYP2E1 by means of only protein stabilization by

(Gonzalez, 2007). Because CYP2E1 gene expression in the heart was not altered by INH, c.f. protein, we can conclude that CYP2E1 down-regulation in the heart was the result of decreasing CYP2E1 mRNA translational activity and/or protein stability.

CYP2E1 has narrow regioselectivity towards AA hydroxylation to produce mainly 18- and 19-HETEs (Laethem et al., 1993), but the reaction precedes with lower activity compared with other CYPs (El-Sherbeni and El-Kadi, 2014b). Therefore, at constitutive levels, CYP2E1 contribution to the formation of 19-HETE has been merely reported after the induction of CYP2E1 by chemical agents (Poloyac et al., 2004, Laethem et al., 1993, Capdevila et al., 2000). Accordingly, down-regulating CYP2E1 in the heart by INH was not expected to decrease 19-HETE formation, since CYP4As is believed to dominate the constitutive AA hydroxylation in the heart (El-Sherbeni et al., 2013). Our results showed that AA metabolism mediated by heart microsomes of INH-treated rats was not different from control rats. However, altering CYP expression is only one mechanism through which the potential effects of INH on the levels of CYP-derived AA metabolites in heart tissue can be exerted. The other mechanism is through the reported direct effect of INH on the activity of some CYPs, namely CYP2Cs and CYP3As (Desta et al., 2001). It has been reported that the clinically relevant concentration of INH is about 50 μM (Desta et al., 2001, Zhang et al., 1992). Incubating control heart microsomes with INH led to significant alterations in AA metabolism. Our results showed a significant decrease in 20-HETE formation that is in line with previous reports (Poloyac et al., 2004). AA is metabolized by CYP in normal heart to mainly EETs and 20-HETE (El-Sherbeni and El-Kadi, 2014b). Therefore, normal hearts contain many-fold lower amounts of 19-HETE than EETs and 20-HETE (El-Sherbeni and El-Kadi, 2014a). Our data showed that INH blocked the formation of the main CYP-derived AA metabolites, EETs and 20-HETE, and accordingly, more AA was

available to be transformed to 19-HETE. This led to the observed increase in the cardiac level of 19-HETE by the 2-week treatment by INH (Figure 3.3.A).

Alterations in CYP levels and its associated AA metabolites have been reported during cardiac hypertrophy, regardless of animal model used, which include Ang II, isoproterenol and pressure overload (Zordoky et al., 2008, Althurwi et al., 2013, El-Sherbeni and El-Kadi, 2014a, Ai et al., 2009). Moreover, a strong correlation between CYP-mediated AA metabolites and the pathogenesis of cardiac hypertrophy has been established (Zordoky et al., 2008). Also, it was proposed that CYP enzymes are not only involved in the disease processes leading to heart failure, but they also play a role in heart failure progression (Elbekai and El-Kadi, 2006). In the current study, we induced cardiac hypertrophy in rats by 2-week Ang II treatment, which is a major component of the mechanisms regulating cardiovascular homeostasis by maintaining vascular tone salt and water balance (Jennings et al., 2010). In agreement with previous reports, we found a decrease in the cardiac EETs, and an increase in the cardiac 20-HETE and AA levels during Ang II-induced cardiac hypertrophy. It has been previously reported that Ang II activates cytosolic phospholipase A2 and release AA from phospholipids (Jennings et al., 2010). In addition to the indirect effect of AA through its metabolites, AA has a direct cardiotoxic effect by increasing ROS production (Cocco et al., 1999), and by reducing heart rate through altering the availability of intracellular calcium, suppressing membrane electrical excitability (Kang et al., 1995, Kang and Leaf, 1994). Under normal conditions AA is present in low amounts in the cardiac tissue (Van der Vusse et al., 1997).

In the current study, we examined whether counterbalancing these alterations can protect from cardiac hypertrophy. We examined INH, for the first time, to determine whether or not it can modify a serious heart pathology, cardiac hypertrophy, based on its effect on the cardiac

CYP-mediated AA metabolism. Interestingly, INH corrected the cardiac levels of the cardiotoxic AA and 20-HETE which had increased during Ang II-induced cardiac hypertrophy. Also, INH increased the cardiac levels of the cardioprotective 19-HETE, which has been reported to be the endogenous antagonist of 20-HETE (Figure 3.3.A). For example, Cheng et al, showed that endothelial cells treated with 20-HETE exhibit a 50% reduction in calcium ionophore-stimulated NO release and a significant increase in superoxide production; this effect of 20-HETE on NO and superoxide was reversed with 19-HETE (Cheng et al., 2008a). However, INH aggravated the decreasing effect of Ang II-induced cardiac hypertrophy on the cardiac levels of the cardioprotective 14,15-EET. Although INH was successful in alleviating several pathological parameters of Ang II-induced cardiac hypertrophy including heart weight to tibia length ratio, and the echocardiographic findings showed improved left ventricular internal dimension during systole and left ventricular posterior wall thickness during systole and diastole (Figure 3.10).

4.2. 2,3',4,5'-Tetramethoxystilbene protects against Ang II-induced cardiac hypertrophy

The effect of CYP1B1 inhibition through the use of TMS against Ang II-induced cardiac hypertrophy in rats was investigated. We then examined the effect of CYP1B1 inhibition on the cardiac levels of 5-, 12-, 15-, and 20-HETE. In order to study the mechanistic pathway by which TMS exerts its cardioprotective effect, human ventricular cardiomyocytes (RL-14) cells were treated with TMS and the involvement of ROS, MAPK and NF-κB studied.

CYP1B1 is the only member of the CYP1B subfamily and is present mainly in the extra-hepatic tissues, including the cardiovascular system. CYP1B1 metabolizes AA into mid-chain HETEs consisting primarily of 5-, 12- and 15-HETE, as well as generating 20-HETE (Choudhary et al., 2004). The formation of 20-HETE is mainly conducted through ω-hydroxylases, generally CYP4A and CYP4F subfamilies in addition to CYP1B1. However, CYP1B1 has been shown to be the second most abundantly expressed CYP gene in human hearts (Bieche et al., 2007).

The association between CYP1B1 and cardiac disease has been well documented. CYP1B1 was induced in the left ventricular tissue of spontaneously hypertensive rats (Thum and Borlak, 2002), as well as being significantly increased in isoproterenol-induced hypertrophied hearts, as compared with the control (Zordoky et al., 2008). CYP1B1 was also found to increase in H9C2 cells by both isoproterenol- and 20-HETE-induced cellular hypertrophy (Tse et al., 2013), implying a role for CYP1B1 in the progression of cardiac hypertrophy. Previous studies have in fact shown that Ang II-induced hypertension in mice is facilitated via CYP1B1 activity most likely through the production of 12- and 20-HETE (Jennings et al., 2012b), since it was found that Ang II infusion caused an increase in both 12- and 20-HETE levels in the kidneys of Cyp1b1+/+ but not Cyp1b1- /- mice. Furthermore, it was found that CYP1B1 inhibition, by TMS, had a protective role on DOCA-salt-induced hypertensive rats that highlights its possible role in the treatment of hypertension triggered by mineralocorticoid excess and salt (Sahan-Firat et al., 2010). Moreover, CYP1B1-mediated cardiotoxicity is believed to be through the action of its endogenous AA metabolites, in addition to the formation of DNA adducts and ROS generation (Korashy and El-Kadi, 2006). In agreement with our results it was found that CYP1B1 expression was not altered by TMS while there was an inhibition in its activity. Furthermore, we demonstrated that although the cardiac levels of CYP1B1 mRNA were not

altered by Ang II treatment, there was an increase in its protein level, concluding that CYP1B1 up-regulation in the heart might be due to increasing CYP1B1 protein stability (Sahan-Firat et al., 2010).

The cardioprotective effect of TMS in Ang II-induced cardiac hypertrophy was evident as seen by the ability of TMS to recover echocardiographic parameters including left ventricular internal diameter and left ventricular posterior wall thickness. In addition, TMS was able to reverse the change in heart weight to tibia length ratio. Highlighting the fact that heart weight to tibia length was measured as opposed to heart weight to body weight, as Ang II is found to decrease weight in part through an anorexigenic effect (Brink et al., 1996). Moreover, TMS was able to protect against Ang II-mediated induction of AA, mid-chain-, and 20-HETE. The release of AA from the phospholipid membrane is the rate-determining step in the generation of eicosanoids in myocardium (Jenkins et al., 2009). Ang II is known to activate cytosolic cPLA2, which in return increases the release of AA (Silfani and Freeman, 2002).

Further investigation was performed in order to study the cellular mechanism by which TMS exerts its cardioprotective effect. During heart failure and cardiac hypertrophy the gene expression of α-MHC is down-regulated, while β-MHC is up-regulated (Korashy et al., 2015, Lowes et al., 1997). Upon treating human ventricular cardiomyocyte RL-14 cells with TMS, we observed that TMS protected from Ang II-induced cellular hypertrophy, as indicated by the significant reduction in β/α-MHC mRNA expression (Figure 3.20). In addition, it was found for the first time that this is through an NF-κB-dependent mechanism in addition to its action on ERK1/2 and p38 pathways (Figure 3.22).

In the current study, the level of oxidative stress was determined by a fluorometric assay measuring the oxidation of 2′,7′-dichlorofluorescein. The ability of TMS to decrease the

induction in ROS production caused by Ang II was in agreement with other studies revealing that the inhibition of CYP1B1 enzymatic activity by incubation of TMS prevented this increase in renal oxidative stress in rats (Jennings et al., 2012a). ROS have also been implicated in the activation of p38 MAPK in vascular smooth muscle cells (VSMCs) (Touyz et al., 2003) and ERK1/2 in mesangial cells (Gorin et al., 2004).

To study the mechanistic pathway by which CYP1B1 contributes to Ang-II cardiac hypertrophy both MAPK and NF-κB pathways were examined. Several studies have described MAPK involvement in cardiac hypertrophy. MAPKs play a role in cardiac remodelling. In particular, ERK1/2 is involved in signal transduction pathways associated with cardiac hypertrophy (Zhang et al., 2003). We have previously demonstrated that the hypertrophic signaling pathway involved due to the direct addition of mid-chain HETE include the extracellular-signal-regulated kinases ERK1/2 but does not include p38 or Jun N-terminal kinase (JNK) (Maayah and El-Kadi, 2015). However, our results show the hypertrophic signaling pathway involved with Ang II-induced hypertrophy in RL14 cells involves ERK1/2 as well as p38 but does not seem to involve JNK (Figure 3.22.A).

NF-κB is found to be activated in patients with heart failure (Wong et al., 1998) The activation of mainly NF-κB p65, not p50, in heart failure aggravates cardiac remodelling in mice, in addition to its involvement in endoplasmic reticulum stress-mediated apoptosis in cardiomyocytes (Hamid et al., 2011). We found that TMS inhibited the stimulation of the NF-κB subunit p65 but not p50 and that Ang II is found to stimulate p65 subunit while not effecting p50 (Figure 3.22.B). This is in agreement with other studies that found that Ang II stimulates p65 nuclear translocation and transcriptional activity in addition to IκB degradation (Purcell et al., 2001). In addition, genetic inhibition of NF-κB diminishes Ang II-induced hypertrophy (Esposito

et al., 2002). Moreover, myocardial hypertrophy induced by aortic banding or chronic infusion of Ang II is found to be prevented by NF-κB blockade, suggesting an important role of NF-κB as a signaling pathway in the regulation of cardiac hypertrophy (Kawano et al., 2005).

NF-kB is a redox-sensitive transcription factor and has been found to be activated upon oxidative stress (Hirotani et al., 2002). Our results suggest the involvement NF-kB through an ROS-dependent mechanism. Previous studies have indicated that GPCR agonist–induced cardiac hypertrophy, including Ang II, is mediated through NF-κB activation via the generation of ROS and includes Apoptosis signal-regulating kinase 1 (ASK1) (Hirotani et al., 2002). In addition, ROS production is known to be stimulated by 20-HETE (Medhora et al., 2008). The effect of inhibiting CYP1B1 activity, using TMS, on cardiovascular function was evident both in vivo and in vitro. In SD rats, this was manifested by the normalization in the changes in echocardiographic parameters and heart weight to tibia length ratio seen with Ang II as well as reversing the rise in β/α-MHC mRNA expression. In addition, this was accompanied with decreased oxidative stress; reduced levels of cardiotoxic mid-chain HETEs and 20-HETE and deactivation of ERK1/2, p38 MAPK and p65 NF-κB signaling pathways.

General Conclusion

Cardiac hypertrophy is considered a major risk factor for several serious heart diseases, most importantly heart failure (Hawkins et al., 2007, Felix-Redondo et al., 2012). In addition, it is well known that left ventricular hypertrophy increases the incidence of myocardial infarction, arrhythmia and premature death (Schunkert et al., 1997). The term cardiac hypertrophy was coined to describe the distinctive alteration in heart wall thicknesses and heart chamber volumes in response to biomechanical stresses such as hypertension (Frey and Olson, 2003). Cardiac

hypertrophy has been studied extensively in order to identify new targets for its prevention and control. Thus our work has been focused on investigating the role of AA metabolites and how playing with CYP enzymes either by their induction or inhibition and consequently the resultant change in their metabolite levels may have a protective role in cardiac hypertrophy.

Our results demonstrate that the use of 19-HETE conferred cardioprotection against Ang II-induced cellular hypertrophy in human ventricular cells. Furthermore, INH caused substantial alterations in CYP-mediated AA metabolism in the heart, most notably an increase in the cardioprotective 19-HETE and a decrease in the cardiotoxic 20-HETE. These alterations were associated with protection against Ang II-induced cardiac hypertrophy, suggesting a potential therapeutic effect of INH and other cardiac 19-HETE pharmacological inducers on cardiac hypertrophy.

In an attempt to examine the protective effect of TMS against Ang II-induced cardiac hypertrophy, we were able to demonstrate that TMS had a cardioprotective role both at in vivo and in vitro levels. TMS significantly decreased the cardiac levels of mid-chain HETEs and 20-HETE as well as causing a decrease in oxidative stress and the deactivation of ERK1/2, p38 MAPK and p65 NF-κB signaling pathways.

Future directions

The results of the present work have highlighted the protective effect of 19-HETE and the role of AA metabolites in the pathogenesis of cardiac hypertrophy. However, more studies are needed to confirm the findings and further address the underlying molecular basis of cardiac hypertrophy.

1) To investigate the molecular mechanism by which 19-HETE, INH, and TMS confer

cardio protection.

2) To determine the combined effect of inhibiting mid-chain HETEs and inducing 19-HETE on cardiac hypertrophy in-vivo.
3) To determine the cardioprotective effect of 19-HETE, INH, and TMS in other models of cardiac hypertrophy such as pressure- or volume-overload induced cardiac hypertrophy.
4) To determine whether or not 19-HETE, INH, and TMS can reverse an established cardiac hypertrophy.

REFERENCES

ABOUTABL, M. E., ZORDOKY, B. N., HAMMOCK, B. D. & EL-KADI, A. O. 2011. Inhibition of soluble epoxide hydrolase confers cardioprotection and prevents cardiac cytochrome P450 induction by benzo(a)pyrene. *J Cardiovasc Pharmacol,* 57**,** 273-81.

AI, D., PANG, W., LI, N., XU, M., JONES, P. D., YANG, J., ZHANG, Y., CHIAMVIMONVAT, N., SHYY, J. Y., HAMMOCK, B. D. & ZHU, Y. 2009. Soluble epoxide hydrolase plays an essential role in angiotensin II-induced cardiac hypertrophy. *Proc Natl Acad Sci U S A,* 106**,** 564-9.

ALONSO-GALICIA, M., FALCK, J. R., REDDY, K. M. & ROMAN, R. J. 1999. 20-HETE agonists and antagonists in the renal circulation. *American Journal of Physiology,* 277**,** F790-6.

ALONSO-GALICIA, M., MAIER, K. G., GREENE, A. S., COWLEY, A. W., JR. & ROMAN, R. J. 2002. Role of 20-hydroxyeicosatetraenoic acid in the renal and vasoconstrictor actions of angiotensin II. *Am J Physiol Regul Integr Comp Physiol,* 283**,** R60-8.

ALSAAD, A. M., ZORDOKY, B. N., EL-SHERBENI, A. A. & EL-KADI, A. O. 2012. Chronic doxorubicin cardiotoxicity modulates cardiac cytochrome P450-mediated arachidonic acid metabolism in rats. *Drug Metab Dispos,* 40**,** 2126-35.

ALTHURWI, H. N., TSE, M. M., ABDELHAMID, G., ZORDOKY, B. N., HAMMOCK, B. D. & EL-KADI, A. O. 2013. Soluble epoxide hydrolase inhibitor, TUPS, protects against isoprenaline-induced cardiac hypertrophy. *Br J Pharmacol,* 168**,** 1794-807.

ANDREWS, N. C. & FALLER, D. V. 1991. A rapid micropreparation technique for extraction of DNA-binding proteins from limiting numbers of mammalian cells. *Nucleic Acids Res,* 19**,** 2499.

ANWAR-MOHAMED, A., EL-SHERBENI, A., KIM, S. H., ELSHENAWY, O. H., ALTHURWI, H. N., ZORDOKY, B. N. & EL-KADI, A. O. 2013. Acute arsenic treatment alters cytochrome P450 expression and arachidonic acid metabolism in lung, liver and kidney of C57Bl/6 mice. *Xenobiotica*.

ANWAR-MOHAMED, A., ZORDOKY, B. N., ABOUTABL, M. E. & EL-KADI, A. O. 2010. Alteration of cardiac cytochrome P450-mediated arachidonic acid metabolism in response to lipopolysaccharide-induced acute systemic inflammation. *Pharmacol Res,* 61**,** 410-8.

AUGER-MESSIER, M., ACCORNERO, F., GOONASEKERA, S. A., BUENO, O. F., LORENZ, J. N., VAN BERLO, J. H., WILLETTE, R. N. & MOLKENTIN, J. D. 2013. Unrestrained p38 MAPK activation in Dusp1/4 double-null mice induces cardiomyopathy. *Circ Res,* 112**,** 48-56.

BARAKAT, M. M., EL-KADI, A. O. & DU SOUICH, P. 2001. L-NAME prevents in vivo the inactivation but not the down-regulation of hepatic cytochrome P450 caused by an acute inflammatory reaction. *Life Sci,* 69**,** 1559-71.

BARANY, M. 1967. ATPase activity of myosin correlated with speed of muscle shortening. *J Gen Physiol,* 50**,** Suppl:197-218.

BARBIERI, A., BURSI, F., MANTOVANI, F., VALENTI, C., QUAGLIA, M., BERTI, E., MARINO, M. & MODENA, M. G. 2012. Left ventricular hypertrophy reclassification and death: application of the Recommendation of the American Society of Echocardiography/European Association of Echocardiography. *Eur Heart J Cardiovasc Imaging,* 13**,** 109-17.

BARYSHNIKOVA, O. K., LI, M. X. & SYKES, B. D. 2008. Modulation of cardiac troponin C function by the cardiac-specific N-terminus of troponin I: influence of PKA phosphorylation and involvement in cardiomyopathies. *J Mol Biol,* 375**,** 735-51.

BAUTISTA, R., SANCHEZ, A., HERNANDEZ, J., OYEKAN, A. & ESCALANTE, B. 2001. Angiotensin II type AT(2) receptor mRNA expression and renal vasodilatation are increased in renal failure. *Hypertension,* 38**,** 669-73.

BELLE, D. J. & SINGH, H. 2008. Genetic factors in drug metabolism. *Am Fam Physician,* 77**,** 1553-60.

BERS, D. M. 2002. Cardiac excitation-contraction coupling. *Nature,* 415**,** 198-205.

BERTRAND-THIEBAULT, C., FERRARI, L., BOUTHERIN-FALSON, O., KOCKX, M., DESQUAND-BILLIALD, S., FICHELLE, J. M., NOTTIN, R., RENAUD, J. F., BATT, A. M. & VISVIKIS, S. 2004. Cytochromes P450

are differently expressed in normal and varicose human saphenous veins: linkage with varicosis. *Clin Exp Pharmacol Physiol,* 31**,** 295-301.

BIECHE, I., NARJOZ, C., ASSELAH, T., VACHER, S., MARCELLIN, P., LIDEREAU, R., BEAUNE, P. & DE WAZIERS, I. 2007. Reverse transcriptase-PCR quantification of mRNA levels from cytochrome (CYP)1, CYP2 and CYP3 families in 22 different human tissues. *Pharmacogenet Genomics,* 17**,** 731-42.

BLEUMINK, G. S., KNETSCH, A. M., STURKENBOOM, M. C., STRAUS, S. M., HOFMAN, A., DECKERS, J. W., WITTEMAN, J. C. & STRICKER, B. H. 2004. Quantifying the heart failure epidemic: prevalence, incidence rate, lifetime risk and prognosis of heart failure The Rotterdam Study. *Eur Heart J,* 25**,** 1614-9.

BRINK, M., WELLEN, J. & DELAFONTAINE, P. 1996. Angiotensin II causes weight loss and decreases circulating insulin-like growth factor I in rats through a pressor-independent mechanism. *J Clin Invest,* 97**,** 2509-16.

BYRD, B. F., 3RD, ABRAHAM, T. P., BUXTON, D. B., COLETTA, A. V., COOPER, J. H., DOUGLAS, P. S., GILLAM, L. D., GOLDSTEIN, S. A., GRAF, T. R., HORTON, K. D., ISENBERG, A. A., KLEIN, A. L., KREEGER, J., MARTIN, R. P., NEDZA, S. M., NAVATHE, A., PELLIKKA, P. A., PICARD, M. H., PILOTTE, J. C., RYAN, T. J., RYCHIK, J., SENGUPTA, P. P., THOMAS, J. D., TUCKER, L., WALLACE, W., WARD, R. P., WEISSMAN, N. J., WIENER, D. H. & WOODRUFF, S. 2015. A Summary of the American Society of Echocardiography Foundation Value-Based Healthcare: Summit 2014: The Role of Cardiovascular Ultrasound in the New Paradigm. *J Am Soc Echocardiogr,* 28**,** 755-69.

CANTLEY, L. C. 2002. The phosphoinositide 3-kinase pathway. *Science,* 296**,** 1655-7.

CAPDEVILA, J., CHACOS, N., WERRINGLOER, J., PROUGH, R. A. & ESTABROOK, R. W. 1981. Liver microsomal cytochrome P-450 and the oxidative metabolism of arachidonic acid. *Proc Natl Acad Sci U S A,* 78**,** 5362-6.

CAPDEVILA, J. H., FALCK, J. R. & HARRIS, R. C. 2000. Cytochrome P450 and arachidonic acid bioactivation. Molecular and functional properties of the arachidonate monooxygenase. *J Lipid Res,* 41**,** 163-81.

CAVE, A., GRIEVE, D., JOHAR, S., ZHANG, M. & SHAH, A. M. 2005. NADPH oxidase-derived reactive oxygen species in cardiac pathophysiology. *Philos Trans R Soc Lond B Biol Sci,* 360**,** 2327-34.

CERTIKOVA CHABOVA, V., WALKOWSKA, A., KOMPANOWSKA-JEZIERSKA, E., SADOWSKI, J., KUJAL, P., VERNEROVA, Z., VANOURKOVA, Z., KOPKAN, L., KRAMER, H. J., FALCK, J. R., IMIG, J. D., HAMMOCK, B. D., VANECKOVA, I. & CERVENKA, L. 2010. Combined inhibition of 20-hydroxyeicosatetraenoic acid formation and of epoxyeicosatrienoic acids degradation attenuates hypertension and hypertension-induced end-organ damage in Ren-2 transgenic rats. *Clin Sci (Lond),* 118**,** 617-32.

CHENG, J., OU, J. S., SINGH, H., FALCK, J. R., NARSIMHASWAMY, D., PRITCHARD, K. A., JR. & SCHWARTZMAN, M. L. 2008a. 20-hydroxyeicosatetraenoic acid causes endothelial dysfunction via eNOS uncoupling. *Am J Physiol Heart Circ Physiol,* 294**,** H1018-26.

CHENG, J., OU, J. S., SINGH, H., FALCK, J. R., NARSIMHASWAMY, D., PRITCHARD, K. A., JR. & SCHWARTZMAN, M. L. 2008b. 20-hydroxyeicosatetraenoic acid causes endothelial dysfunction via eNOS uncoupling. *American Journal of Physiology - Heart & Circulatory Physiology,* 294**,** H1018-26.

CHIEN, J. Y., THUMMEL, K. E. & SLATTERY, J. T. 1997. Pharmacokinetic consequences of induction of CYP2E1 by ligand stabilization. *Drug Metab Dispos,* 25**,** 1165-75.

CHOUDHARY, D., JANSSON, I., STOILOV, I., SARFARAZI, M. & SCHENKMAN, J. B. 2004. Metabolism of retinoids and arachidonic acid by human and mouse cytochrome P450 1b1. *Drug Metab Dispos,* 32**,** 840-7.

CHU, Z. M., CROFT, K. D., KINGSBURY, D. A., FALCK, J. R., REDDY, K. M. & BEILIN, L. J. 2000. Cytochrome P450 metabolites of arachidonic acid may be important mediators in angiotensin II-induced vasoconstriction in the rat mesentery in vivo. *Clin Sci (Lond),* 98**,** 277-82.

COBB, M. H. 1999. MAP kinase pathways. *Prog Biophys Mol Biol,* 71**,** 479-500.

COCCO, T., DI PAOLA, M., PAPA, S. & LORUSSO, M. 1999. Arachidonic acid interaction with the mitochondrial electron transport chain promotes reactive oxygen species generation. *Free Radic Biol Med,* 27**,** 51-9.

CORONADO, R., MORRISSETTE, J., SUKHAREVA, M. & VAUGHAN, D. M. 1994. Structure and function of ryanodine receptors. *Am J Physiol,* 266**,** C1485-504.

CROWLEY, S. D., THARAUX, P. L., AUDOLY, L. P. & COFFMAN, T. M. 2004. Exploring type I angiotensin (AT1) receptor functions through gene targeting. *Acta Physiol Scand,* 181**,** 561-70.

DE WINDT, L. J., LIM, H. W., BUENO, O. F., LIANG, Q., DELLING, U., BRAZ, J. C., GLASCOCK, B. J., KIMBALL, T. F., DEL MONTE, F., HAJJAR, R. J. & MOLKENTIN, J. D. 2001. Targeted inhibition of calcineurin attenuates cardiac hypertrophy in vivo. *Proc Natl Acad Sci U S A,* 98**,** 3322-7.

DESTA, Z., SOUKHOVA, N. V. & FLOCKHART, D. A. 2001. Inhibition of cytochrome P450 (CYP450) isoforms by isoniazid: potent inhibition of CYP2C19 and CYP3A. *Antimicrob Agents Chemother,* 45**,** 382-92.

DING, X. & KAMINSKY, L. S. 2003. Human extrahepatic cytochromes P450: function in xenobiotic metabolism and tissue-selective chemical toxicity in the respiratory and gastrointestinal tracts. *Annu Rev Pharmacol Toxicol,* 43**,** 149-73.

DIVI, R. L., LUCH, A., VERMA, M. & MAHADEVAN, B. 2012. CYP1B1 detection. *Curr Protoc Toxicol,* Chapter 4**,** Unit 4 38.

EL-SHERBENI, A. A., ABOUTABL, M. E., ZORDOKY, B. N., ANWAR-MOHAMED, A. & EL-KADI, A. O. 2013. Determination of the dominant arachidonic acid cytochrome p450 monooxygenases in rat heart, lung, kidney, and liver: protein expression and metabolite kinetics. *AAPS J,* 15**,** 112-22.

EL-SHERBENI, A. A. & EL-KADI, A. O. 2013. Alterations in Cytochrome P450-derived arachidonic acid metabolism during pressure overload-induced Cardiac Hypertrophy. *Biochem Pharmacol*.

EL-SHERBENI, A. A. & EL-KADI, A. O. 2014a. Alterations in cytochrome P450-derived arachidonic acid metabolism during pressure overload-induced cardiac hypertrophy. *Biochem Pharmacol,* 87**,** 456-66.

EL-SHERBENI, A. A. & EL-KADI, A. O. 2014b. Characterization of arachidonic acid metabolism by rat cytochrome P450 enzymes: the involvement of CYP1As. *Drug Metab Dispos,* 42**,** 1498-507.

ELBEKAI, R. H. & EL-KADI, A. O. 2006. Cytochrome P450 enzymes: central players in cardiovascular health and disease. *Pharmacol Ther,* 112**,** 564-87.

ELSHENAWY, O. H., ANWAR-MOHAMED, A. & EL-KADI, A. O. 2013. 20-Hydroxyeicosatetraenoic acid is a potential therapeutic target in cardiovascular diseases. *Curr Drug Metab,* 14**,** 706-19.

ESCALANTE, B., SESSA, W. C., FALCK, J. R., YADAGIRI, P. & SCHWARTZMAN, M. L. 1990. Cytochrome P450-dependent arachidonic acid metabolites, 19- and 20-hydroxyeicosatetraenoic acids, enhance sodium-potassium ATPase activity in vascular smooth muscle. *J Cardiovasc Pharmacol,* 16**,** 438-43.

ESPOSITO, G., RAPACCIUOLO, A., NAGA PRASAD, S. V., TAKAOKA, H., THOMAS, S. A., KOCH, W. J. & ROCKMAN, H. A. 2002. Genetic alterations that inhibit in vivo pressure-overload hypertrophy prevent cardiac dysfunction despite increased wall stress. *Circulation,* 105**,** 85-92.

FELIX-REDONDO, F. J., FERNANDEZ-BERGES, D., CALDERON, A., CONSUEGRA-SANCHEZ, L., LOZANO, L. & BARRIOS, V. 2012. Prevalence of left-ventricular hypertrophy by multiple electrocardiographic criteria in general population: Hermex study. *J Hypertens,* 30**,** 1460-7.

FERGUSON, B. S., HARRISON, B. C., JEONG, M. Y., REID, B. G., WEMPE, M. F., WAGNER, F. F., HOLSON, E. B. & MCKINSEY, T. A. 2013. Signal-dependent repression of DUSP5 by class I HDACs controls nuclear ERK activity and cardiomyocyte hypertrophy. *Proc Natl Acad Sci U S A,* 110**,** 9806-11.

FREY, N. & OLSON, E. N. 2003. Cardiac hypertrophy: the good, the bad, and the ugly. *Annu Rev Physiol,* 65**,** 45-79.

FYHRQUIST, F., METSARINNE, K. & TIKKANEN, I. 1995. Role of angiotensin II in blood pressure regulation and in the pathophysiology of cardiovascular disorders. *J Hum Hypertens,* 9 Suppl 5**,** S19-24.

GERBAL-CHALOIN, S., PASCUSSI, J. M., PICHARD-GARCIA, L., DAUJAT, M., WAECHTER, F., FABRE, J. M., CARRERE, N. & MAUREL, P. 2001. Induction of CYP2C genes in human hepatocytes in primary culture. *Drug Metab Dispos,* 29**,** 242-51.

GHOSH, S., MAY, M. J. & KOPP, E. B. 1998. NF-kappa B and Rel proteins: evolutionarily conserved mediators of immune responses. *Annu Rev Immunol,* 16**,** 225-60.

GONZALEZ, F. J. 2007. The 2006 Bernard B. Brodie Award Lecture. Cyp2e1. *Drug Metab Dispos,* 35**,** 1-8.

GOODWIN, B., MOORE, L. B., STOLTZ, C. M., MCKEE, D. D. & KLIEWER, S. A. 2001. Regulation of the human CYP2B6 gene by the nuclear pregnane X receptor. *Mol Pharmacol,* 60**,** 427-31.

GORIN, Y., RICONO, J. M., WAGNER, B., KIM, N. H., BHANDARI, B., CHOUDHURY, G. G. & ABBOUD, H. E. 2004. Angiotensin II-induced ERK1/ERK2 activation and protein synthesis are redox-dependent in glomerular mesangial cells. *Biochem J,* 381**,** 231-9.

GRAHAM, M. M., KNUDTSON, M. L., O'NEILL, B. J., ROSS, D. B. & CANADIAN CARDIOVASCULAR SOCIETY ACCESS TO CARE WORKING, G. 2006. Treating the right patient at the right time: Access to cardiac catheterization, percutaneous coronary intervention and cardiac surgery. *Can J Cardiol,* 22**,** 679-83.

GRANVILLE, D. J., TASHAKKOR, B., TAKEUCHI, C., GUSTAFSSON, A. B., HUANG, C., SAYEN, M. R., WENTWORTH, P., JR., YEAGER, M. & GOTTLIEB, R. A. 2004. Reduction of ischemia and reperfusion-induced myocardial damage by cytochrome P450 inhibitors. *Proc Natl Acad Sci U S A,* 101**,** 1321-6.

GRIFFIN, S. A., BROWN, W. C., MACPHERSON, F., MCGRATH, J. C., WILSON, V. G., KORSGAARD, N., MULVANY, M. J. & LEVER, A. F. 1991. Angiotensin II causes vascular hypertrophy in part by a non-pressor mechanism. *Hypertension,* 17**,** 626-35.

GROSS, E. R., NITHIPATIKOM, K., HSU, A. K., PEART, J. N., FALCK, J. R., CAMPBELL, W. B. & GROSS, G. J. 2004. Cytochrome P450 omega-hydroxylase inhibition reduces infarct size during reperfusion via the sarcolemmal KATP channel. *J Mol Cell Cardiol,* 37**,** 1245-9.

HAMID, T., GUO, S. Z., KINGERY, J. R., XIANG, X., DAWN, B. & PRABHU, S. D. 2011. Cardiomyocyte NF-kappaB p65 promotes adverse remodelling, apoptosis, and endoplasmic reticulum stress in heart failure. *Cardiovasc Res,* 89**,** 129-38.

HANCOCK, J. T. 2010. *Cell signalling,* Oxford ; New York, Oxford University Press.

HAWKINS, N. M., WANG, D., MCMURRAY, J. J., PFEFFER, M. A., SWEDBERG, K., GRANGER, C. B., YUSUF, S., POCOCK, S. J., OSTERGREN, J., MICHELSON, E. L. & DUNN, F. G. 2007. Prevalence and prognostic implications of electrocardiographic left ventricular hypertrophy in heart failure: evidence from the CHARM programme. *Heart,* 93**,** 59-64.

HEINEKE, J. & MOLKENTIN, J. D. 2006. Regulation of cardiac hypertrophy by intracellular signalling pathways. *Nat Rev Mol Cell Biol,* 7**,** 589-600.

HIROTANI, S., OTSU, K., NISHIDA, K., HIGUCHI, Y., MORITA, T., NAKAYAMA, H., YAMAGUCHI, O., MANO, T., MATSUMURA, Y., UENO, H., TADA, M. & HORI, M. 2002. Involvement of nuclear factor-kappaB and apoptosis signal-regulating kinase 1 in G-protein-coupled receptor agonist-induced cardiomyocyte hypertrophy. *Circulation,* 105**,** 509-15.

ICHIHARA, S., SENBONMATSU, T., PRICE, E., JR., ICHIKI, T., GAFFNEY, F. A. & INAGAMI, T. 2001. Angiotensin II type 2 receptor is essential for left ventricular hypertrophy and cardiac fibrosis in chronic angiotensin II-induced hypertension. *Circulation,* 104**,** 346-51.

IMAOKA, S., HASHIZUME, T. & FUNAE, Y. 2005. Localization of rat cytochrome P450 in various tissues and comparison of arachidonic acid metabolism by rat P450 with that by human P450 orthologs. *Drug Metab Pharmacokinet,* 20**,** 478-84.

IOANNIDES, C. 2008. Cytochromes P450 role in the metabolism and toxicity of drugs and other xenobiotics. *Issues in toxicology.* Cambridge: RSC Pub.

ISHIHARA, Y., HAMAGUCHI, A., SEKINE, M., HIRAKAWA, A. & SHIMAMOTO, N. 2012. Accumulation of cytochrome P450 induced by proteasome inhibition during cardiac ischemia. *Arch Biochem Biophys,* 527**,** 16-22.

JENKINS, C. M., CEDARS, A. & GROSS, R. W. 2009. Eicosanoid signalling pathways in the heart. *Cardiovasc Res,* 82**,** 240-9.

JENNINGS, B. L., ANDERSON, L. J., ESTES, A. M., FANG, X. R., SONG, C. Y., CAMPBELL, W. B. & MALIK, K. U. 2012a. Involvement of cytochrome P-450 1B1 in renal dysfunction, injury, and inflammation associated with angiotensin II-induced hypertension in rats. *Am J Physiol Renal Physiol,* 302**,** F408-20.

JENNINGS, B. L., ANDERSON, L. J., ESTES, A. M., YAGHINI, F. A., FANG, X. R., PORTER, J., GONZALEZ, F. J., CAMPBELL, W. B. & MALIK, K. U. 2012b. Cytochrome P450 1B1 contributes to renal dysfunction and damage caused by angiotensin II in mice. *Hypertension,* 59**,** 348-54.

JENNINGS, B. L., SAHAN-FIRAT, S., ESTES, A. M., DAS, K., FARJANA, N., FANG, X. R., GONZALEZ, F. J. & MALIK, K. U. 2010. Cytochrome P450 1B1 contributes to angiotensin II-induced hypertension and associated pathophysiology. *Hypertension,* 56**,** 667-74.

KALOW, W., TANG, B. K. & ENDRENYI, L. 1998. Hypothesis: comparisons of inter- and intra-individual variations can substitute for twin studies in drug research. *Pharmacogenetics,* 8**,** 283-9.

KANG, J. X. & LEAF, A. 1994. Effects of long-chain polyunsaturated fatty acids on the contraction of neonatal rat cardiac myocytes. *Proc Natl Acad Sci U S A,* 91**,** 9886-90.

KANG, J. X., XIAO, Y. F. & LEAF, A. 1995. Free, long-chain, polyunsaturated fatty acids reduce membrane electrical excitability in neonatal rat cardiac myocytes. *Proc Natl Acad Sci U S A,* 92**,** 3997-4001.

KATZ, A. M. 2002. Maladaptive growth in the failing heart: the cardiomyopathy of overload. *Cardiovasc Drugs Ther,* 16**,** 245-9.

KAWANO, S., KUBOTA, T., MONDEN, Y., KAWAMURA, N., TSUTSUI, H., TAKESHITA, A. & SUNAGAWA, K. 2005. Blockade of NF-kappaB ameliorates myocardial hypertrophy in response to chronic infusion of angiotensin II. *Cardiovasc Res,* 67**,** 689-98.

KEHAT, I. & MOLKENTIN, J. D. 2010. Extracellular signal-regulated kinase 1/2 (ERK1/2) signaling in cardiac hypertrophy. *Ann N Y Acad Sci,* 1188**,** 96-102.

KERZEE, J. K. & RAMOS, K. S. 2001. Constitutive and inducible expression of Cyp1a1 and Cyp1b1 in vascular smooth muscle cells: role of the Ahr bHLH/PAS transcription factor. *Circ Res,* 89**,** 573-82.

KIM, S., KO, H., PARK, J. E., JUNG, S., LEE, S. K. & CHUN, Y. J. 2002. Design, synthesis, and discovery of novel trans-stilbene analogues as potent and selective human cytochrome P450 1B1 inhibitors. *J Med Chem,* 45**,** 160-4.

KIM, S. G., SHEHIN, S. E., STATES, J. C. & NOVAK, R. F. 1990. Evidence for increased translational efficiency in the induction of P450IIE1 by solvents: analysis of P450IIE1 mRNA polyribosomal distribution. *Biochem Biophys Res Commun,* 172**,** 767-74.

KOBAYASHI, K., URASHIMA, K., SHIMADA, N. & CHIBA, K. 2003. Selectivities of human cytochrome P450 inhibitors toward rat P450 isoforms: study with cDNA-expressed systems of the rat. *Drug Metab Dispos,* 31**,** 833-6.

KORASHY, H. M., AL-SUWAYEH, H. A., MAAYAH, Z. H., ANSARI, M. A., AHMAD, S. F. & BAKHEET, S. A. 2015. Mitogen-activated protein kinases pathways mediate the sunitinib-induced hypertrophy in rat cardiomyocyte H9c2 cells. *Cardiovasc Toxicol,* 15**,** 41-51.

KORASHY, H. M. & EL-KADI, A. O. 2006. The role of aryl hydrocarbon receptor in the pathogenesis of cardiovascular diseases. *Drug Metab Rev,* 38**,** 411-50.

KURATA, N., YOSHIDA, T., KUROIWA, Y., MASUKO, T. & HASHIMOTO, Y. 1989. Long-term effects of phenobarbital on rat liver microsomal drug-metabolizing enzymes and heme-metabolizing enzyme. *Res Commun Chem Pathol Pharmacol,* 65**,** 161-79.

LAETHEM, R. M., BALAZY, M., FALCK, J. R., LAETHEM, C. L. & KOOP, D. R. 1993. Formation of 19(S)-, 19(R)-, and 18(R)-hydroxyeicosatetraenoic acids by alcohol-inducible cytochrome P450 2E1. *J Biol Chem,* 268**,** 12912-8.

LEE, C. R., NORTH, K. E., BRAY, M. S., COUPER, D. J., HEISS, G. & ZELDIN, D. C. 2007. CYP2J2 and CYP2C8 polymorphisms and coronary heart disease risk: the Atherosclerosis Risk in Communities (ARIC) study. *Pharmacogenet Genomics,* 17**,** 349-58.

LEWIS, D. F. 2004. 57 varieties: the human cytochromes P450. *Pharmacogenomics,* 5**,** 305-18.

LIANG, Q., BUENO, O. F., WILKINS, B. J., KUAN, C. Y., XIA, Y. & MOLKENTIN, J. D. 2003. c-Jun N-terminal kinases (JNK) antagonize cardiac growth through cross-talk with calcineurin-NFAT signaling. *EMBO J,* 22**,** 5079-89.

LIN, H. S., CHOO, Q. Y. & HO, P. C. 2010. Quantification of oxyresveratrol analog trans-2,4,3',5'-tetramethoxystilbene in rat plasma by a rapid HPLC method: application in a pre-clinical pharmacokinetic study. *Biomed Chromatogr,* 24**,** 1373-8.

LIU, Q. & HOFMANN, P. A. 2004. Protein phosphatase 2A-mediated cross-talk between p38 MAPK and ERK in apoptosis of cardiac myocytes. *Am J Physiol Heart Circ Physiol,* 286**,** H2204-12.

LOMPRE, A. M., NADAL-GINARD, B. & MAHDAVI, V. 1984. Expression of the cardiac ventricular alpha- and beta-myosin heavy chain genes is developmentally and hormonally regulated. *J Biol Chem,* 259**,** 6437-46.

LOWES, B. D., MINOBE, W., ABRAHAM, W. T., RIZEQ, M. N., BOHLMEYER, T. J., QUAIFE, R. A., RODEN, R. L., DUTCHER, D. L., ROBERTSON, A. D., VOELKEL, N. F., BADESCH, D. B., GROVES, B. M., GILBERT, E. M. & BRISTOW, M. R. 1997. Changes in gene expression in the intact human heart. Downregulation of alpha-myosin heavy chain in hypertrophied, failing ventricular myocardium. *J Clin Invest,* 100**,** 2315-24.

LOWRY, O. H., ROSEBROUGH, N. J., FARR, A. L. & RANDALL, R. J. 1951. Protein measurement with the Folin phenol reagent. *J Biol Chem,* 193**,** 265-75.

LUND, A. K., GOENS, M. B., KANAGY, N. L. & WALKER, M. K. 2003. Cardiac hypertrophy in aryl hydrocarbon receptor null mice is correlated with elevated angiotensin II, endothelin-1, and mean arterial blood pressure. *Toxicol Appl Pharmacol,* 193**,** 177-87.

LUO, J. L., KAMATA, H. & KARIN, M. 2005. IKK/NF-kappaB signaling: balancing life and death--a new approach to cancer therapy. *J Clin Invest,* 115**,** 2625-32.

MA, Q. & LU, A. Y. 2007. CYP1A induction and human risk assessment: an evolving tale of in vitro and in vivo studies. *Drug Metab Dispos,* 35**,** 1009-16.

MAAYAH, Z. H. & EL-KADI, A. O. 2015. 5-, 12- and 15-Hydroxyeicosatetraenoic acids induce cellular hypertrophy in the human ventricular cardiomyocyte, RL-14 cell line, through MAPK- and NF-kappaB-dependent mechanism. *Arch Toxicol*.

MAAYAH, Z. H., ELSHENAWY, O. H., ALTHURWI, H. N., ABDELHAMID, G. & EL-KADI, A. O. 2015. Human fetal ventricular cardiomyocyte, RL-14 cell line, is a promising model to study drug metabolizing enzymes and their associated arachidonic acid metabolites. *J Pharmacol Toxicol Methods,* 71**,** 33-41.

MARBER, M. S., ROSE, B. & WANG, Y. 2011. The p38 mitogen-activated protein kinase pathway--a potential target for intervention in infarction, hypertrophy, and heart failure. *J Mol Cell Cardiol,* 51**,** 485-90.

MARCIANTE, K. D., TOTAH, R. A., HECKBERT, S. R., SMITH, N. L., LEMAITRE, R. N., LUMLEY, T., RICE, K. M., HINDORFF, L. A., BIS, J. C., HARTMAN, B. & PSATY, B. M. 2008. Common variation in cytochrome P450 epoxygenase genes and the risk of incident nonfatal myocardial infarction and ischemic stroke. *Pharmacogenet Genomics,* 18**,** 535-43.

MARTIGNONI, M., GROOTHUIS, G. M. & DE KANTER, R. 2006. Species differences between mouse, rat, dog, monkey and human CYP-mediated drug metabolism, inhibition and induction. *Expert Opin Drug Metab Toxicol,* 2**,** 875-94.

MARTINEZ-JIMENEZ, C. P., JOVER, R., DONATO, M. T., CASTELL, J. V. & GOMEZ-LECHON, M. J. 2007. Transcriptional regulation and expression of CYP3A4 in hepatocytes. *Curr Drug Metab,* 8**,** 185-94.

MCCOLLUM, L. T., GALLAGHER, P. E. & ANN TALLANT, E. 2012. Angiotensin-(1-7) attenuates angiotensin II-induced cardiac remodeling associated with upregulation of dual-specificity phosphatase 1. *Am J Physiol Heart Circ Physiol,* 302**,** H801-10.

MEDHORA, M., CHEN, Y., GRUENLOH, S., HARLAND, D., BODIGA, S., ZIELONKA, J., GEBREMEDHIN, D., GAO, Y., FALCK, J. R., ANJAIAH, S. & JACOBS, E. R. 2008. 20-HETE increases superoxide production and activates NAPDH oxidase in pulmonary artery endothelial cells. *Am J Physiol Lung Cell Mol Physiol,* 294**,** L902-11.

MICHAUD, V., FRAPPIER, M., DUMAS, M. C. & TURGEON, J. 2010. Metabolic activity and mRNA levels of human cardiac CYP450s involved in drug metabolism. *PLoS One,* 5**,** e15666.

MIHL, C., DASSEN, W. R. & KUIPERS, H. 2008. Cardiac remodelling: concentric versus eccentric hypertrophy in strength and endurance athletes. *Neth Heart J,* 16**,** 129-33.

MINAMIYAMA, Y., TAKEMURA, S., AKIYAMA, T., IMAOKA, S., INOUE, M., FUNAE, Y. & OKADA, S. 1999. Isoforms of cytochrome P450 on organic nitrate-derived nitric oxide release in human heart vessels. *FEBS Lett,* 452**,** 165-9.

MOLKENTIN, J. D., LU, J. R., ANTOS, C. L., MARKHAM, B., RICHARDSON, J., ROBBINS, J., GRANT, S. R. & OLSON, E. N. 1998. A calcineurin-dependent transcriptional pathway for cardiac hypertrophy. *Cell,* 93**,** 215-28.

MONOSTORY, K., PASCUSSI, J. M., KOBORI, L. & DVORAK, Z. 2009. Hormonal regulation of CYP1A expression. *Drug Metab Rev,* 41**,** 547-72.

MUKHERJEE, A. B., MIELE, L. & PATTABIRAMAN, N. 1994. Phospholipase A2 enzymes: regulation and physiological role. *Biochem Pharmacol,* 48**,** 1-10.

MUNSHI, A., SHARMA, V., KAUL, S., AL-HAZZANI, A., ALSHATWI, A. A., SHAFI, G., KOPPULA, R., MALLEMOGGALA, S. B. & JYOTHY, A. 2012. Association of 1347 G/A cytochrome P450 4F2 (CYP4F2) gene variant with hypertension and stroke. *Mol Biol Rep,* 39**,** 1677-82.

NADRUZ, W., JR., KOBARG, C. B., KOBARG, J. & FRANCHINI, K. G. 2004. c-Jun is regulated by combination of enhanced expression and phosphorylation in acute-overloaded rat heart. *Am J Physiol Heart Circ Physiol,* 286**,** H760-7.

NELSON, D. R. 2006. Cytochrome P450 nomenclature, 2004. *Methods Mol Biol,* 320**,** 1-10.

NITHIPATIKOM, K., GROSS, E. R., ENDSLEY, M. P., MOORE, J. M., ISBELL, M. A., FALCK, J. R., CAMPBELL, W. B. & GROSS, G. J. 2004. Inhibition of cytochrome P450omega-hydroxylase: a novel endogenous cardioprotective pathway. *Circ Res,* 95**,** e65-71.

OMATA, K., ABE, K., SHEU, H. L., YOSHIDA, K., TSUTSUMI, E., YOSHINAGA, K., ABRAHAM, N. G. & LANIADO-SCHWARTZMAN, M. 1992. Roles of renal cytochrome P450-dependent arachidonic acid metabolites in hypertension. *Tohoku J Exp Med,* 166**,** 93-106.

PARK, J. Y., KIM, K. A. & KIM, S. L. 2003. Chloramphenicol is a potent inhibitor of cytochrome P450 isoforms CYP2C19 and CYP3A4 in human liver microsomes. *Antimicrob Agents Chemother,* 47**,** 3464-9.

POLOYAC, S. M., TORTORICI, M. A., PRZYCHODZIN, D. I., REYNOLDS, R. B., XIE, W., FRYE, R. F. & ZEMAITIS, M. A. 2004. The effect of isoniazid on CYP2E1- and CYP4A-mediated hydroxylation of arachidonic acid in the rat liver and kidney. *Drug Metab Dispos,* 32**,** 727-33.

PURCELL, N. H., TANG, G., YU, C., MERCURIO, F., DIDONATO, J. A. & LIN, A. 2001. Activation of NF-kappa B is required for hypertrophic growth of primary rat neonatal ventricular cardiomyocytes. *Proc Natl Acad Sci U S A,* 98**,** 6668-73.

PURCELL, N. H., WILKINS, B. J., YORK, A., SABA-EL-LEIL, M. K., MELOCHE, S., ROBBINS, J. & MOLKENTIN, J. D. 2007. Genetic inhibition of cardiac ERK1/2 promotes stress-induced apoptosis and heart failure but has no effect on hypertrophy in vivo. *Proc Natl Acad Sci U S A,* 104**,** 14074-9.

QU, W., BRADBURY, J. A., TSAO, C. C., MARONPOT, R., HARRY, G. J., PARKER, C. E., DAVIS, L. S., BREYER, M. D., WAALKES, M. P., FALCK, J. R., CHEN, J., ROSENBERG, R. L. & ZELDIN, D. C. 2001. Cytochrome P450 CYP2J9, a new mouse arachidonic acid omega-1 hydroxylase predominantly expressed in brain. *J Biol Chem,* 276**,** 25467-79.

QUIGLEY, R., BAUM, M., REDDY, K. M., GRIENER, J. C. & FALCK, J. R. 2000. Effects of 20-HETE and 19(S)-HETE on rabbit proximal straight tubule volume transport. *Am J Physiol Renal Physiol,* 278**,** F949-53.

ROGER, V. L., GO, A. S., LLOYD-JONES, D. M., BENJAMIN, E. J., BERRY, J. D., BORDEN, W. B., BRAVATA, D. M., DAI, S., FORD, E. S., FOX, C. S., FULLERTON, H. J., GILLESPIE, C., HAILPERN, S. M., HEIT, J. A., HOWARD, V. J., KISSELA, B. M., KITTNER, S. J., LACKLAND, D. T., LICHTMAN, J. H., LISABETH, L. D., MAKUC, D. M., MARCUS, G. M., MARELLI, A., MATCHAR, D. B., MOY, C. S., MOZAFFARIAN, D., MUSSOLINO, M. E., NICHOL, G., PAYNTER, N. P., SOLIMAN, E. Z., SORLIE, P. D., SOTOODEHNIA, N., TURAN, T. N., VIRANI, S. S., WONG, N. D., WOO, D. & TURNER, M. B. 2012. Heart disease and stroke statistics--2012 update: a report from the American Heart Association. *Circulation,* 125**,** e2-e220.

ROMAN, R. J. 2002. P-450 metabolites of arachidonic acid in the control of cardiovascular function. *Physiol Rev,* 82**,** 131-85.

ROSE, B. A., FORCE, T. & WANG, Y. 2010. Mitogen-activated protein kinase signaling in the heart: angels versus demons in a heart-breaking tale. *Physiol Rev,* 90**,** 1507-46.

ROSENBAUGH, E. G., SAVALIA, K. K., MANICKAM, D. S. & ZIMMERMAN, M. C. 2013. Antioxidant-based therapies for angiotensin II-associated cardiovascular diseases. *Am J Physiol Regul Integr Comp Physiol,* 304**,** R917-28.

ROTHERMEL, B. A., MCKINSEY, T. A., VEGA, R. B., NICOL, R. L., MAMMEN, P., YANG, J., ANTOS, C. L., SHELTON, J. M., BASSEL-DUBY, R., OLSON, E. N. & WILLIAMS, R. S. 2001. Myocyte-enriched calcineurin-interacting protein, MCIP1, inhibits cardiac hypertrophy in vivo. *Proc Natl Acad Sci U S A,* 98**,** 3328-33.

SAHAN-FIRAT, S., JENNINGS, B. L., YAGHINI, F. A., SONG, C. Y., ESTES, A. M., FANG, X. R., FARJANA, N., KHAN, A. I. & MALIK, K. U. 2010. 2,3',4,5'-Tetramethoxystilbene prevents deoxycorticosterone-salt-induced hypertension: contribution of cytochrome P-450 1B1. *Am J Physiol Heart Circ Physiol,* 299**,** H1891-901.

SCHMITT, J. P., KAMISAGO, M., ASAHI, M., LI, G. H., AHMAD, F., MENDE, U., KRANIAS, E. G., MACLENNAN, D. H., SEIDMAN, J. G. & SEIDMAN, C. E. 2003. Dilated cardiomyopathy and heart failure caused by a mutation in phospholamban. *Science,* 299**,** 1410-3.

SCHUCK, R. N., THEKEN, K. N., EDIN, M. L., CAUGHEY, M., BASS, A., ELLIS, K., TRAN, B., STEELE, S., SIMMONS, B. P., LIH, F. B., TOMER, K. B., WU, M. C., HINDERLITER, A. L., STOUFFER, G. A.,

ZELDIN, D. C. & LEE, C. R. 2013. Cytochrome P450-derived eicosanoids and vascular dysfunction in coronary artery disease patients. *Atherosclerosis,* 227**,** 442-8.

SCHUNKERT, H., HENSE, H. W., MUSCHOLL, M., LUCHNER, A., KURZINGER, S., DANSER, A. H. & RIEGGER, G. A. 1997. Associations between circulating components of the renin-angiotensin-aldosterone system and left ventricular mass. *Heart,* 77**,** 24-31.

SCOOTE, M. & WILLIAMS, A. J. 2002. The cardiac ryanodine receptor (calcium release channel): emerging role in heart failure and arrhythmia pathogenesis. *Cardiovasc Res,* 56**,** 359-72.

SHIOI, T., KANG, P. M., DOUGLAS, P. S., HAMPE, J., YBALLE, C. M., LAWITTS, J., CANTLEY, L. C. & IZUMO, S. 2000. The conserved phosphoinositide 3-kinase pathway determines heart size in mice. *EMBO J,* 19**,** 2537-48.

SILFANI, T. N. & FREEMAN, E. J. 2002. Phosphatidylinositide 3-kinase regulates angiotensin II-induced cytosolic phospholipase A2 activity and growth in vascular smooth muscle cells. *Arch Biochem Biophys,* 402**,** 84-93.

SIM, S. C. & INGELMAN-SUNDBERG, M. 2006. The human cytochrome P450 Allele Nomenclature Committee Web site: submission criteria, procedures, and objectives. *Methods Mol Biol,* 320**,** 183-91.

SMUTNY, T., MANI, S. & PAVEK, P. 2013. Post-translational and post-transcriptional modifications of pregnane X receptor (PXR) in regulation of the cytochrome P450 superfamily. *Curr Drug Metab,* 14**,** 1059-69.

SOHASKEY, M. L. & FERRELL, J. E., JR. 1999. Distinct, constitutively active MAPK phosphatases function in Xenopus oocytes: implications for p42 MAPK regulation In vivo. *Mol Biol Cell,* 10**,** 3729-43.

SONG, B. J., MATSUNAGA, T., HARDWICK, J. P., PARK, S. S., VEECH, R. L., YANG, C. S., GELBOIN, H. V. & GONZALEZ, F. J. 1987. Stabilization of cytochrome P450j messenger ribonucleic acid in the diabetic rat. *Mol Endocrinol,* 1**,** 542-7.

SONG, B. J., VEECH, R. L., PARK, S. S., GELBOIN, H. V. & GONZALEZ, F. J. 1989. Induction of rat hepatic N-nitrosodimethylamine demethylase by acetone is due to protein stabilization. *J Biol Chem,* 264**,** 3568-72.

SPIECKER, M., DARIUS, H., HANKELN, T., SOUFI, M., SATTLER, A. M., SCHAEFER, J. R., NODE, K., BORGEL, J., MUGGE, A., LINDPAINTNER, K., HUESING, A., MAISCH, B., ZELDIN, D. C. & LIAO, J. K. 2004. Risk of coronary artery disease associated with polymorphism of the cytochrome P450 epoxygenase CYP2J2. *Circulation,* 110**,** 2132-6.

SYNOLD, T. W., DUSSAULT, I. & FORMAN, B. M. 2001. The orphan nuclear receptor SXR coordinately regulates drug metabolism and efflux. *Nat Med,* 7**,** 584-90.

TACCONELLI, S. & PATRIGNANI, P. 2014. Inside epoxyeicosatrienoic acids and cardiovascular disease. *Front Pharmacol,* 5**,** 239.

TALAVERA, K., STAES, M., JANSSENS, A., DROOGMANS, G. & NILIUS, B. 2004. Mechanism of arachidonic acid modulation of the T-type Ca2+ channel alpha1G. *J Gen Physiol,* 124**,** 225-38.

TAUBMAN, M. B. 2003. Angiotensin II: a vasoactive hormone with ever-increasing biological roles. *Circ Res,* 92**,** 9-11.

THACKABERRY, E. A., GABALDON, D. M., WALKER, M. K. & SMITH, S. M. 2002. Aryl hydrocarbon receptor null mice develop cardiac hypertrophy and increased hypoxia-inducible factor-1alpha in the absence of cardiac hypoxia. *Cardiovasc Toxicol,* 2**,** 263-74.

THUM, T. & BORLAK, J. 2000a. Cytochrome P450 mono-oxygenase gene expression and protein activity in cultures of adult cardiomyocytes of the rat. *Br J Pharmacol,* 130**,** 1745-52.

THUM, T. & BORLAK, J. 2000b. Gene expression in distinct regions of the heart. *Lancet,* 355**,** 979-83.

THUM, T. & BORLAK, J. 2002. Testosterone, cytochrome P450, and cardiac hypertrophy. *FASEB J,* 16**,** 1537-49.

TONKS, N. K. 2006. Protein tyrosine phosphatases: from genes, to function, to disease. *Nat Rev Mol Cell Biol,* 7**,** 833-46.

TOUYZ, R. M., CRUZADO, M., TABET, F., YAO, G., SALOMON, S. & SCHIFFRIN, E. L. 2003. Redox-dependent MAP kinase signaling by Ang II in vascular smooth muscle cells: role of receptor tyrosine kinase transactivation. *Can J Physiol Pharmacol,* 81**,** 159-67.

TSE, M. M., ABOUTABL, M. E., ALTHURWI, H. N., ELSHENAWY, O. H., ABDELHAMID, G. & EL-KADI, A. O. 2013. Cytochrome P450 epoxygenase metabolite, 14,15-EET, protects against isoproterenol-induced cellular hypertrophy in H9c2 rat cell line. *Vascul Pharmacol,* 58**,** 363-73.

UEDA, A., HAMADEH, H. K., WEBB, H. K., YAMAMOTO, Y., SUEYOSHI, T., AFSHARI, C. A., LEHMANN, J. M. & NEGISHI, M. 2002. Diverse roles of the nuclear orphan receptor CAR in regulating hepatic genes in response to phenobarbital. *Mol Pharmacol,* 61**,** 1-6.

UMENO, M., SONG, B. J., KOZAK, C., GELBOIN, H. V. & GONZALEZ, F. J. 1988. The rat P450IIE1 gene: complete intron and exon sequence, chromosome mapping, and correlation of developmental expression with specific 5' cytosine demethylation. *J Biol Chem,* 263**,** 4956-62.

VAN DER VUSSE, G. J., RENEMAN, R. S. & VAN BILSEN, M. 1997. Accumulation of arachidonic acid in ischemic/reperfused cardiac tissue: possible causes and consequences. *Prostaglandins Leukot Essent Fatty Acids,* 57**,** 85-93.

VANHAESEBROECK, B., LEEVERS, S. J., PANAYOTOU, G. & WATERFIELD, M. D. 1997. Phosphoinositide 3-kinases: a conserved family of signal transducers. *Trends Biochem Sci,* 22**,** 267-72.

VEGA, R. B., YANG, J., ROTHERMEL, B. A., BASSEL-DUBY, R. & WILLIAMS, R. S. 2002. Multiple domains of MCIP1 contribute to inhibition of calcineurin activity. *J Biol Chem,* 277**,** 30401-7.

WAKATSUKI, T., SCHLESSINGER, J. & ELSON, E. L. 2004. The biochemical response of the heart to hypertension and exercise. *Trends Biochem Sci,* 29**,** 609-17.

WANG, S., HAN, H. M., PAN, Z. W., HANG, P. Z., SUN, L. H., JIANG, Y. N., SONG, H. X., DU, Z. M. & LIU, Y. 2012. Choline inhibits angiotensin II-induced cardiac hypertrophy by intracellular calcium signal and p38 MAPK pathway. *Naunyn Schmiedebergs Arch Pharmacol,* 385**,** 823-31.

WANG, Y., HUANG, S., SAH, V. P., ROSS, J., JR., BROWN, J. H., HAN, J. & CHIEN, K. R. 1998. Cardiac muscle cell hypertrophy and apoptosis induced by distinct members of the p38 mitogen-activated protein kinase family. *J Biol Chem,* 273**,** 2161-8.

WEBER, K. T. & BRILLA, C. G. 1991. Pathological hypertrophy and cardiac interstitium. Fibrosis and renin-angiotensin-aldosterone system. *Circulation,* 83**,** 1849-65.

WILKINS, B. J. & MOLKENTIN, J. D. 2004. Calcium-calcineurin signaling in the regulation of cardiac hypertrophy. *Biochem Biophys Res Commun,* 322**,** 1178-91.

WONG, S. C., FUKUCHI, M., MELNYK, P., RODGER, I. & GIAID, A. 1998. Induction of cyclooxygenase-2 and activation of nuclear factor-kappaB in myocardium of patients with congestive heart failure. *Circulation,* 98**,** 100-3.

YU, C., YAN, Q., FU, C., SHI, W., WANG, H., ZENG, C. & WANG, X. 2014. CYP4F2 genetic polymorphisms are associated with coronary heart disease in a Chinese population. *Lipids Health Dis,* 13**,** 83.

ZAFARI, A. M., USHIO-FUKAI, M., MINIERI, C. A., AKERS, M., LASSEGUE, B. & GRIENDLING, K. K. 1999. Arachidonic acid metabolites mediate angiotensin II-induced NADH/NADPH oxidase activity and hypertrophy in vascular smooth muscle cells. *Antioxid Redox Signal,* 1**,** 167-79.

ZAND, R., NELSON, S. D., SLATTERY, J. T., THUMMEL, K. E., KALHORN, T. F., ADAMS, S. P. & WRIGHT, J. M. 1993. Inhibition and induction of cytochrome P4502E1-catalyzed oxidation by isoniazid in humans. *Clin Pharmacol Ther,* 54**,** 142-9.

ZELARAYAN, L., RENGER, A., NOACK, C., ZAFIRIOU, M. P., GEHRKE, C., VAN DER NAGEL, R., DIETZ, R., DE WINDT, L. & BERGMANN, M. W. 2009. NF-kappaB activation is required for adaptive cardiac hypertrophy. *Cardiovasc Res,* 84**,** 416-24.

ZHANG, F., DENG, H., KEMP, R., SINGH, H., GOPAL, V. R., FALCK, J. R., LANIADO-SCHWARTZMAN, M. & NASJLETTI, A. 2005. Decreased levels of cytochrome P450 2E1-derived eicosanoids sensitize renal arteries to constrictor agonists in spontaneously hypertensive rats. *Hypertension,* 45**,** 103-8.

ZHANG, R. L., WANG, Z. Y., LI, D. & CHENG, W. B. 1992. Effects of rifampicin on pharmacokinetics of isoniazid and its metabolite acetylhydrazine in rats. *Zhongguo Yao Li Xue Bao,* 13**,** 494-6.

ZHANG, W., ELIMBAN, V., NIJJAR, M. S., GUPTA, S. K. & DHALLA, N. S. 2003. Role of mitogen-activated protein kinase in cardiac hypertrophy and heart failure. *Exp Clin Cardiol,* 8**,** 173-83.

ZHANG, W. & LIU, H. T. 2002. MAPK signal pathways in the regulation of cell proliferation in mammalian cells. *Cell Res,* 12**,** 9-18.

ZHU, W., TRIVEDI, C. M., ZHOU, D., YUAN, L., LU, M. M. & EPSTEIN, J. A. 2009. Inpp5f is a polyphosphoinositide phosphatase that regulates cardiac hypertrophic responsiveness. *Circ Res,* 105**,** 1240-7.

ZORDOKY, B. N., ABOUTABL, M. E. & EL-KADI, A. O. 2008. Modulation of cytochrome P450 gene expression and arachidonic acid metabolism during isoproterenol-induced cardiac hypertrophy in rats. *Drug Metab Dispos,* 36**,** 2277-86.